Loading from Shallow Buried Blast Events and the Effect on Plate Deformations

Benjamin J. Fuller MEng

Thesis submitted to

The University of Sheffield
Department of Civil and Structural Engineering

for the degree of

Doctor of Philosophy

October 2018

Abstract

This thesis describes the design and construction of an experimental apparatus to enable the repeatable testing of appliqué protective systems against buried charges. This thesis highlights the difficulties in understanding and predicting buried blast loading, as well as why it is important to know the distribution of impulse as well as how quickly it is delivered.

A review of the literature investigating the phenomenology of buried charge testing is presented, along with previous work which has looked into the factors which can affect the output of a buried charge. Tests were conducted using the developed apparatus, with the detailed output of 21 tests against varying thicknesses of Armox 440T steel being presented within this thesis. The testing was conducted at 1/2 scale, with charge sizes between 400 and 1000 grams, and nominal plate thicknesses between 6 and 12 mm. For each test the full deformation profile was provided along with dynamic (peak) and residual deflections to enable numerical model validation. The preparation of the soil bed for the testing has been carefully controlled based on previous experience at the University of Sheffield. The test series used Leighton Buzzard 14/25 sand which is a silica based uniform soil with particle sizes between 0.6–1.18 mm. This was prepared to a moisture content of 5% and dry density of 1620 kg/m^3.

Analysis of the test series was done using the Nurick and Martin (1989) analysis method with modified correction factor based on the distribution of kinetic energy. This analysis has shown that for the appliqué systems tested, the normalised deflection can be predicted if the normalised total impulse as well as the distribution of impulse imparted to the system is known; this finding should be the basis of a fast running engineering model for plate deformation from shallow buried blast and other non-uniform impulsive loading.

Acknowledgements

Firstly, I would like to thank my supervisors Dr Sam Rigby and Prof. Andy Tyas for being a source of constant guidance and advice throughout the period of this research. The quality of the work owes much to their dedication and attention to detail. My thanks also go to Dr Sam Clarke for his guidance regarding the experimental methodology, as well as giving me the encouragement I needed at the right time to get me to this point. Supervisors that are friends are the best kind of supervisors.

Thanks to the technical staff at the Buxton Blast and Impact Laboratory for their support in the experimental work. Special thanks go to Andrew Barr, Kit Langran-Wheeler, Roy Mellor, Andrew Hibbert and Ash Burgess; as well as Paul Blackbourn from the Civil Engineering workshop for always helping me figure out how to build stuff.

Many thanks to Rachel for her help support and love, putting up with my sporadic working habits and stressful write-up period. Without her I could not have completed this thesis. I would also to thank all my family and friends. Special thanks to my church family at Christ Church Central for encouraging me in my faith and building me up along the way.

This research project was made possible through support from an EPSRC CASE scholarship which was provided by Dstl. My thanks go to Ian Elgy and Matt Gant who have supported me throughout my studies.

Contents

List of Figures xiii
List of Tables xv
List of Symbols xvii

1 Introduction **1**
1.1 Background 1
1.2 Scope and objectives 2
1.3 Thesis outline and details of intellectual ownership 3

2 Literature review **5**
2.1 Introduction 5
2.2 Early research into impulse distribution 6
2.3 Early experimental research focused on side-on pressures and total impulse 10
2.4 Experimental measurement of buried blast loading 13
2.5 Modelling of buried blast loading 17
2.6 Experimental measurement of target response to buried blast loading with numerical modelling 19
2.7 A review of Pickering et al. 2012 with integrated discussion . . . 21
2.8 Recent work by the University of Sheffield 28
2.9 Conclusions 33

3 Experimental Methodology **35**
3.1 Introduction 35
3.2 Previous testing apparatus 35
3.2.1 Pre-existing Setup 35

3.2.2 Difficulties . . . 37
3.3 Test design requirements . . . 38
3.3.1 Objectives . . . 38
3.3.2 Support conditions . . . 39
3.3.3 Ensuring consistent loading . . . 40
3.3.4 Portal frame modifications . . . 41
3.3.5 Soil bin and reaction base modifications . . . 41
3.4 Apparatus and test arrangement detailed design . . . 43
3.4.1 General apparatus arrangement and terminology . . . 43
3.4.2 Test layout details . . . 46
3.4.3 Picture frame, bushings and target interface plates details 48
3.4.4 Target hole layout . . . 50
3.5 Test protocol . . . 55
3.5.1 Overview . . . 55
3.5.2 Target preparation . . . 56
3.5.3 Soil bin preparation . . . 58
3.5.4 Photogrammetry method for residual deformations . . . 60
3.6 Chapter summary and test program . . . 62

4 Results and analysis **63**
4.1 Overview of results . . . 63
4.2 Introduction to analysis . . . 67
4.3 Loading . . . 67
4.4 Nurick Analysis . . . 73
4.5 Modifying and applying the Nurick Analysis . . . 74
4.6 Chapter summary . . . 84

5 Conclusions **87**

6 Synopsis by chapter and future work **89**
6.1 Future Work . . . 92

Bibliography **94**

A Deflection figures **101**

B MATLAB for random speckle pattern **123**

List of Figures

2.1 Semi-emperical Westine model, Westine et al. (1985) 8

2.2 Support Structure with impulse capture pendulum and side-on pressure gauge arrangement Ehrgott et al. (2011a) 17

2.3 Description of shallow buried blast event by Grujicic and Pandurangan (2008) 18

2.4 Test arrangement - Pickering et al. (2012) 21

2.5 Impulse vs depth of burial, 47 mm Stand-off, Various PE4 - Pickering et al. (2012) 22

2.6 Midpoint deflection vs. depth of burial, 47 mm Stand-off - Pickering et al. (2012) 23

2.7 Cross-sections of the 14 + 1 g PE4, 47 mm Stand-off, varied depth of burial target plate - Pickering et al. (2012) 24

2.8 Conceptual deflection types with loading conditions 24

2.9 Conceptual plate with lumped mass, non-uniform kinetic energy distribution results in a non-uniform strain distribution, $L_2 > L_1$ 26

2.10 Cross sectional view of plate deformation for 1.6 mm plates in order of increasing impulse from bottom - Jacob et al. (2004) . . 26

2.11 Thinning visible on a 2 mm thick square plate - Jacob et al. (2004) 27

2.12 Cross-sections of the 14 + 1 g PE4, 0 mm depth of burial, varied stand-off distances - Pickering et al. (2012) 28

2.13 Cross-sections of the 14 + 1 g PE4, 20 mm depth of burial, varied stand-off distancese - Pickering et al. (2012) 28

2.14 Impulse vs. stand-off distance, 14 + 1 g PE4 - Pickering et al. (2012) 28

2.15 Original apparatus - Front view, after Clarke et al. (2011) 29

2.16 Details of apparatus for measuring spacial reflected pressure distribution; Front view, Section view and Detail D, after Clarke et al. (2015a) 30
2.17 Details of apparatus for measuring spacial reflected pressure distribution; Isometric view, Bottom view and Detail F, after Clarke et al. (2015a) 31
2.18 Westine normalized data and model with data from the University of Sheffield (CoBL LB 2.5, CoBL LB Sat, and CoBL Stanag) . 32

3.1 Original apparatus - Front view 36
3.2 Original frame with original soil bin arrangement - Front view with section (mm) 38
3.3 Modified frame with improved soil bin arrangement - Front view with section (mm) 42
3.4 Improved steel base plate 42
3.5 Modified frame in new Appliqué rig arrangement - Isometric View Front 43
3.6 Improved steel bin and picture frame with bushings 44
3.7 Improved steel bin and picture frame with bushings 44
3.8 Appliqué Rig - Front View - (mm) 45
3.9 Appliqué Rig - Isometric View Back 45
3.10 Appliqué Rig - Section A-A - (mm) 46
3.11 Appliqué Rig - Detail B - (mm) 47
3.12 Bushing Mount Target Interface Plate Detail (mm) 50
3.13 Rigid Picture frame with interface plates and bushings (mm) . . 51
3.14 Example of target edge, the effect of hole size and spacing on three different failure modes; tension, bearing and shear 52
3.15 Hole layout details for targets 53
3.16 As built picture of Appliqué apparatus 54
3.17 As built picture of Appliqué apparatus mounting bushings 54
3.18 Flow chart of test protocol 55
3.19 Target speckle pattern generated in MATLAB 57
3.20 Example of 3D point cloud generated from 16 plate photographs - Barr and Fuller (2018) 61
3.21 Example of target with speckle pattern before firing 61

4.1 Example of target deformation on impact face after firing 63

4.2 Target thickness plotted against peak central residual deflection for different charge sizes 65

4.3 Target thickness plotted against peak central dynamic deflection for different charge sizes 65

4.4 Deformation profile for Test 1, target no. AM-06-004, plan view (top) and central section views (bottom) 66

4.5 Flow chart of load prediction and analysis using University of Sheffield test data in combination with Westine's normalized load prediction model 68

4.6 Westine normalized data and model with data from the University of Sheffield (CoBL LB 2.5, CoBL LB Sat, and CoBL Stanag; names of different soil conditions) 69

4.7 "Graph of displacement-thickness ratio versus non-dimensional impulse for the combined circular and quadrangular plate data, both pre-1989 and post 1989." Chung Kim Yuen et al. (2016) The "Dimensionless Number" used is the same as normalized impulse in this thesis 71

4.8 Example calculations demonstrating the difference in kinetic energy (KE) uptake, for impulsively loaded targets with different distributions of impulse; assuming discretely lumped masses (m) 72

4.9 Peak dynamic central deflection against total impulse for different target thickness and charge sizes 74

4.10 Normalized peak dynamic central deflection against total normalized impulse for different target thickness and charge sizes . 75

4.11 Normalized peak dynamic central deflection against total normalized impulse for different target thickness and charge sizes with line of best fit and Nurick line 77

4.12 Example deformation profile from Test 3, target number AM-06-002 78

4.13 Normalized deflection against total normalized impulse with kinetic energy modified data and Nurick Line 78

4.14 Diagram of theoretical upper-bound and lower-bound strain energy distribution response to the upper-bound kinetic energy uptake for a target loaded with a non-uniform impulse distribution 80

4.15 Details of kinetic energy correction factor 81

4.16 Cumulative integral of KE distribution explained 82

4.17 Normalized deflection against total normalized impulse data, normalised data with distribution based correction factor, normalised data with Nurick correction factor, and Nurick Line 83

4.18 Normalised data with distribution based correction factor vs Nurick Line 83

A.1 Deformation profile for Test 2, target no. AM-06-001, plan view (top) and central section views (bottom) 102

A.2 Deformation profile for Test 3, target no. AM-06-002, plan view (top) and central section views (bottom) 103

A.3 Deformation profile for Test 4, target no. AM-08-001, plan view (top) and central section views (bottom) 104

A.4 Deformation profile for Test 5, target no. AM-08-002, plan view (top) and central section views (bottom) 105

A.5 Deformation profile for Test 6, target no. AM-08-003, plan view (top) and central section views (bottom) 106

A.6 Deformation profile for Test 7, target no. AM-08-004, plan view (top) and central section views (bottom) 107

A.7 Deformation profile for Test 8, target no. AM-08-005, plan view (top) and central section views (bottom) 108

A.8 Deformation profile for Test 9, target no. AM-08-006, plan view (top) and central section views (bottom) 109

A.9 Deformation profile for Test 10, target no. AM-10-001, plan view (top) and central section views (bottom) 110

A.10 Deformation profile for Test 11, target no. AM-10-002, plan view (top) and central section views (bottom) 111

A.11 Deformation profile for Test 12, target no. AM-10-003, plan view (top) and central section views (bottom) 112

A.12 Deformation profile for Test 13, target no. AM-10-004, plan view (top) and central section views (bottom) 113

A.13 Deformation profile for Test 14, target no. AM-10-005, plan view (top) and central section views (bottom) 114

A.14 Deformation profile for Test 15, target no. AM-10-006, plan view (top) and central section views (bottom) 115

A.15 Deformation profile for Test 16, target no. AM-12-003, plan view (top) and central section views (bottom) 116

A.16 Deformation profile for Test 17, target no. AM-12-001, plan view (top) and central section views (bottom) 117

A.17 Deformation profile for Test 18, target no. AM-12-002, plan view (top) and central section views (bottom) 118
A.18 Deformation profile for Test 19, target no. AM-12-004, plan view (top) and central section views (bottom) 119
A.19 Deformation profile for Test 20, target no. AM-12-005, plan view (top) and central section views (bottom) 120
A.20 Deformation profile for Test 21, target no. AM-12-006, plan view (top) and central section views (bottom) 121

List of Tables

4.1 Test results matrix with average target thickness, charge weight, central peak dynamic deflection, and central peak residual deflection 64

4.2 Impulse values as calculated by adjusted Westine model with kinetic energy equivalent uniform impulse values 70

Nomenclature

I	Total impulse - newton seconds
I_N	Normalized impulse - unit-less
M_P	Mass of plate - kilograms
M_D	Mass of discrete area - kilograms
I_D	Discrete impulse applied to a specific area/mass - newton seconds
t_p	Plate thickness - meters
B_p	Plate breadth - meters
L_p	Plate length - meters
ρ	Material density - kilograms/meters^2
δ	Deflection - meters
δ_N	Normalized deflection - unit-less
ε	Strain - change in length/original length
σ	Material yield stress - newtons/meters^2
E_k	Kinetic energy - joules
E_{kd}	Kinetic energy of discrete mass - joules
m	Mass - kilograms

Chapter 1

Introduction

1.1 Background

The necessity of protective vehicle platforms is a reality of the world we live in. In many parts of the world, and for many different reasons, there are people who require the ability to travel in environments where hostile groups or individuals are actively trying to cause harm, by any means possible. Buried explosive attacks against such vehicles can cause severe injury or death when the protection level of the vehicle is over-matched by the threat.

Designers of such vehicles currently face many problems, mostly related to the increased uncertainty associated with buried threats. Some of the most significant problems are uncertainties regarding the:

- size and nature of the buried explosive device;
- conditions of burial of the explosive device;
- effect of burial conditions on the behaviour of the buried explosive device;
- how a change in behaviour of the event will impact the loading imparted to a vehicle under-carriage, and;
- exactly what information about the loading is required to accurately predict deformations for a vehicle under-carriage.

These knowledge gaps have prevented the development of well validated predictive methods for protection performance, be that high fidelity numerical modelling or semi-empirical tools.

Unfortunately, due to logistical, economical and tactical considerations it is not possible to simply over-design every vehicle protection system to account for ev-

ery imaginable threat level, especially when considering all the aforementioned uncertainties/unknowns.

For the planners of activities, in locations requiring these protective vehicle platforms, the uncertainty can be reduced by thorough research and route planning; however, the uncertainty will always remain and a risk-based approach should be used to assess the protection provided by the vehicles to the occupants for a given activity, in a given location. This presents yet another problem; for risk-based approaches to work well, a large number of scenarios and threats need to be analysed, but the prediction methods are currently neither fast nor well validated to fully accommodate the needs of planners and designers.

In summary, there are always unknowns but it is imperative that the problem is better understood across its vast parameter space. This understanding will enable the effect of any hypothetical scenario to be characterised with sufficient speed, accuracy and confidence to allow designers and planners to characterize, in a meaningful way, the protection level provided by a given vehicle platform to its occupants. If the physics of a buried blast events are not well characterised or understood for a wide range of the possible input parameters, the lack of predictive capability will continue.

1.2 Scope and objectives

The effect of buried blast loading on vehicles is a broad and complex topic, with many variations of soil conditions, target type, explosive configuration etc. being used when performing experiments and numerical modelling for buried blast. The literature review details what work has been published in the field and assesses how the work has added to the understanding of buried blast physics and the prediction capability for buried blast events. However, the literature review is intentionally scrutinized with respect to the short comings in the field, in an attempt to demonstrate what aspects of the problem are still poorly understood or poorly characterized. The intention is to produce a review which not only provides the detail of what has been done already, but also provides the reader with information about the quality and relevance of the work in light of all the work that has been done to date. As such, the literature review contains significant sections of the authors original work in the form of explanations to support the critique of existing work. Whilst the literature review does present a thorough overview of the gaps in the field, the original experimental work and analysis presented in this thesis is focused on a small sub-section of the problem.

This thesis has four objectives:

1. To highlight where there are gaps in the current understanding of buried blast physics.

2. To detail the development of a new experimental arrangement for assessing the performance of protective materials and systems, in plate/panel form, against buried blast threats. That is, to expound on how the test arrangement was developed by consolidating the knowledge from previous work in the field to inform the soil preparation and design of the testing apparatus.

3. To demonstrate that an understanding of the spatial and temporal distribution of loading is essential to understand and predict plate response.

4. To investigate whether knowledge of the distribution of impulse from a buried blast event can be used to predict target deformation without any numerical modelling of the target or the blast event. This will be attempted for different target spans, thickness, materials and total impulse values.

1.3 Thesis outline and details of intellectual ownership

Chapter 2 - Literature review and critique

This chapter focuses upon presenting the existing body of work that informs the current understanding of buried blast, as well as critiquing the assumptions, conclusions and methodologies of previous work. Section 2.7 uses the discussion around one piece of literature to begin building a line of reasoning expounded on in the analysis in Chapter 5. The section titled "Recent work by the University of Sheffield" explains previous and ongoing work at the University of Sheffield that has informed the investigation in this thesis. The work being described is referenced and is not the intellectual property of the author of this thesis. The application of understanding and information gained through an analysis of the previous work is the intellectual property of the author and is used as an integral part of the analysis chapter.

Chapter 3 - Methodology for performance assessment of protective systems

This chapter is concerned with describing the detailed design and experimental methodology employed in this study; as well as describing the thought processes behind some of the design decisions. Everything in this chapter is the intellectual property of the author unless directly referenced. The photogrammetry processed used for characterizing residual deformations was developed in partnership with Dr. Andrew Barr. Dr. Andrew Barr setup the Matlab scripts for processing the photogrammetry data and the author designed the speckle pattern and target preparation method.

Chapter 4 - Example experimental results and analysis

The results are partially presented here; the full set of results can be found in the appendices. The information regarding loading distribution which is available in the literature, is used here to characterise the loading experienced by the targets in the testing. This information is used to predict target deformations by modifying an existing approach which was developed for free-air blast. It is a unique combination and modification of several preexisting approaches with data from the literature to demonstrate a methodology for interpreting the experimental data and predicting deformation.

Chapter 5 - Summary and conclusions

This section summarizes the work presented in the thesis and gives details of future work that is needed in the field.

Chapter 2

Literature review

2.1 Introduction

Research initiatives to quantify the loading delivered to a target from a buried blast event have been ongoing since the early 60's such as Kincheloe (1962). Not than no buried blast work was done before that time; but, it wasn't until the early 70's that experimental measurement of loading distribution was attempted. Previous work simply tested the effect of a particular blast scenario on a particular target to demonstrate the level of protection that would be provided. Since the 70's many experimental and numerical studies have been undertaken to try and characterise the total impulse delivered to an entire target, the distribution of impulse across a target, and the pressure-time history at any location across a target. As computational power has increased exponentially over the last 4–5 decades, the drive to be able to model buried blast events has also increased. Increasing demand for validated modelling approaches, driven by significant armed conflicts in recent years, has consolidated the requirement for high quality experimental data. This data is needed to validate modelling approaches; but it is also needed to develop a better understanding of the physical mechanisms that develop during a shallow buried blast event. There have been many numerical studies that have tried to use the output from un-validated numerical models to learn something about the physical mechanisms, this is the wrong way around. The experimental investigation should inform the physics underpinning the models. However, it is true that numerical modelling approaches can be used in preparation for experimental work to try and understand as much about the problem before designing the experimental set-up. It is possible to see a phenomena in a numerical model that wouldn't have been an obvious aspect to accommodate in the experiment without the modelling. At every juncture of investigation, understanding as much as possible about all the tools and techniques available to answer the question

is imperative. The first aim of this literature review is to cover the body of work that deals with experimental measurement of shallow buried blast events; for different soils, conditions and arrangements. Secondly, this literature review will cover a selection of work that aims at numerically modelling these blast events directly or predicting the loading in some way. Lastly, some attention will be given to literature concerned with characterising the effect of specific well controlled buried blast events on well characterised targets.

It is worth re-iterating at this point that the context and objective of this study is the protection of vehicles from buried blast events. As such, several references are made to the Allied Engineering Publication, AEP-55, Volume 2, "Procedures for evaluating the protection level of logistic and light armoured vehicles" and the STANAG 4569 threat levels defined therein. These threat levels detail the specifications for surrogate TNT mines used to evaluate the performance of vehicle platforms against such threats (NATO 2006).

In some instances the criticism of previous studies put forward by the author is blunt. This is not an attempt to discredit previous work, nor does is it intended to suggest that the author's own work is any less worthy of criticism. It is intended to highlight problematic aspects of previous work with the benefit of hindsight which has been developed since publication.

2.2 Early research into impulse distribution

In 1972 Wenzel and Esparza published a technical report for the U.S. Army Mobility Equipment Research and Development Centre (Wenzel and Esparza 1972). This report detailed a series of both free-air and buried blast experiments measuring the impulse distributed across the face of a target using "impulse plugs". This is the first piece of work that begins to quantify the magnitude and distribution of loading across a target. Impulse plugs are usually cylindrical plugs resting in corresponding holes in a rigid target plate such that when the target plate is subjected to a blast load the plugs are free to travel out of the holes away from the plate as a result of the impulse that has been imparted by the loading. By tracking the speed of the plugs and determining the initial velocity with some instrumentation scheme the specific impulse imparted to each plug can be determined. Therein characterising the impulse from the blast at discrete point across the target plate where the impulse plugs were employed. The geometric arrangement of the experimental elements were varied to try and characterise the effect of different parameters on the observed loading;

parameters such as burial depth, charge size, and stand-off of the target from the soil surface.

As early as 1972, when Westine published "The Impulse Imparted to Targets by the Detonation of Land Mines", he provided detailed descriptions of the development of a buried blast event and how it differed from a free-air event (Westine 1972). Westine hypothesised that the buried blast would be comparable to blast events in a vacuum where most of the loading was caused by the detonation products impacting the target as opposed to an air shock. In 1985 Westine expanded his description of buried blast events and said that the loading is "the inertial effects only" of the soil impacting the target (Westine et al. 1985). Westine claimed that the impulse imparted to a target would simply be the sum of mass times velocity of all the soil particles impacting the target. As such, Westine claimed that the only important factor for the soil was the mass. Whilst Westine's hypothesis about the fundamental mechanisms of buried blast loading is appropriate in some scenarios, it is inadequate in others. Westine premised his description of a buried blast event in 1972 by saying that it involved a far more complicated set of processes than the free-air blast loading scenario; in this he was absolutely correct. The reason why Westine was not able to provide an accurate description of buried blast loading mechanisms is two fold.

First, Westine did not control and fully explore the parameter space sufficiently, to be able see the variety of loading mechanisms which exist. High-speed video, flash X-ray, and reflected pressure measurements have shown that the geotechnical conditions of the soil have significant effect on the development of a buried blast event.; specific details such as the particle size relative to the charge size and burial depth, the particle size distribution, the moisture content, and in some cases even the chemical composition of the granular material effects the behaviour of the rapid expansion of detonation products, Milne et al. (2014). These parameters also become more or less dominating as a function of other parameters Westine did control, such as stand-off. Some of the tests Westine describes were commensurate with buried blast loading on vehicle tracks; the stand-off in those tests was zero. However, when Westine developed his conceptual model of buried blast loading he did not consider that the difference in results between zero stand-off and larger non-zero stand-off might be because the developing mechanisms of loading are fundamentally different for the two extremes. Westine compiled all his data into one normalised set, regardless of stand-off extremes, for which he developed an empirical equation based on his understanding of blast loading mechanisms. The final version of Westine's equation almost describes all the data if it is divided and multiplied by 1.8 to

giving the upper and lower boundaries. As shown in Figure 2.1 the experimental spread is significant because the number of variables intentionally varied or simply uncontrolled is large, and it is highly likely that Westine's data spans at least two different regimes of behaviour because of including zero stand-off results with larger stand-off tests. Moreover, there were very few repeats, making it difficult to draw conclusive trends from what was tested.

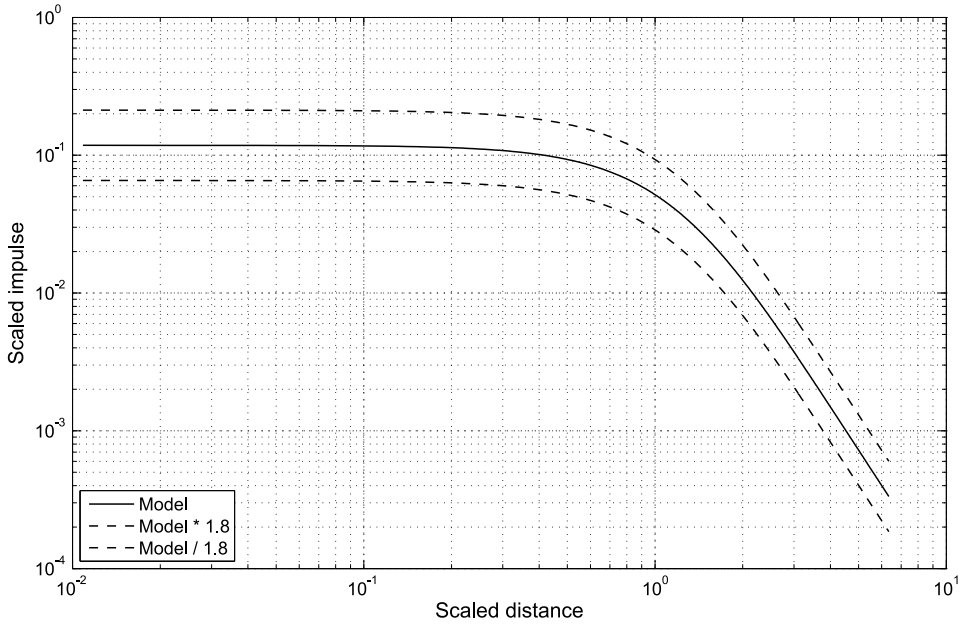

Figure 2.1: Semi-emperical Westine model, Westine et al. (1985)

Secondly, Westine did not have enough diagnostic fidelity to be able to correlate differences in loading with changes in the way the blast event developed. Because Westine was only considering the final result of loading on a target, the impulse imparted to plugs, even if he had systematically varied all the specific details discussed above it may not have improved his understanding of buried blast events. The impulse delivered to a plug in a steel plate is the culmination of a complex series of interconnected physical processes; it is difficult to say exactly what mechanisms have led to the imparted momentum. The distribution of impulse may be all that is required to characterise the loading of a single event, but it is not all that is required to be able to predict the loading for a wide range of events with certainty. Because, what Westine did not know at the time, is that the soil conditions can change not just the magnitude of loading from a buried blast event but also the behaviour of the detonation products themselves. Westine stated, "Detonation of the explosive sent earth and debris into the air which impulsively loaded the plugs", despite the fact that he had

not measured the duration of the reflected loading experimentally and had no hard data to prove that the loading would indeed be impulsive.

It is true that in real world scenarios of buried blast such as land mines acting on vehicles, there is no way to know exactly what soil conditions will be present for any given event. In this way, buried blast events will be inherently variable. However, being able to understand what initial conditions give rise to these variations, and why, is crucial to developing an understanding of buried blast events that will allow the variability to be accounted for rigorously. Certain combinations of parameters have proven to be very repeatable, where as other combinations have demonstrated considerable variability. More work needs to be done to fully understand the underpinning physical reasons for the variety of behaviour and resulting variety in loading magnitude and distribution. Buried blast events are not inherently variable, there are simply a great number of factors that must be intentionally controlled to facilitate repeatable experiments. A conceptual model of blast events that accommodates all the possible combinations of parameters and how those parameters change the event and the effect on a target would allow for a robust assessment of risk, and worse-case scenarios; which would lead to well informed design safety factors. A better understanding of the problem would increase potential for innovative solutions to protect again buried blast. Furthermore, numerical modelling techniques are unlikely to be a robust resource for predicting buried blast loading on targets across the full range of scenarios until the physics that needs to be represented in the modelling is actual understood in practice.

The works and analysis done by Wenzel, Esparza and Westine are important because they were the first bodies of work that really began to quantify the loading delivered to a target from a buried explosive detonation. Moreover, the ideas that Westine put forward regarding the development of a blast event from detonation to the end of target loading seeded future work in the field with a certain preconceived model of what happens in a buried blast event and what causes the loading experienced by the target. Westine admitted that the factors surrounding the development of a buried blast would result in a complex interaction of all the constituents of the event; but as will be seen in the next section, there are other authors who have a different idea of what that complex interaction looks like and what causes target loading.

2.3 Early experimental research focused on side-on pressures and total impulse

The fundamental difference between the conceptual models for buried blast events of Westine and Bergeron hinges around the contribution of air shock and the detonation products to the loading. Bergeron claims that the detonation products and air shock can have a significant contribution to the loading (Bergeron and Tremblay 2000); whereas Westine claims that their contribution will be negligible. Also, Westine claimed that most of the loading would be generated by the momentum of the soil particles (Westine et al. 1985), whereas Bergeron claims that this may be the case in some scenarios, but that it would depend on other parameters such and depth of burial and local soil conditions (Bergeron and Tremblay 2000). Bergeron highlighted the fact that much work needed to be done to understand the effects of many parameters such as particle size, density, saturation level and cohesion as well as how these factors may combine with others such as depth of burial to influence the propagation of the event from detonation onwards.

In 1998, Bergeron published a report for the Canadian Defence Research Establishment Suffield which detailed a series of 20 tests using 100 gram C4 charges buried at various depths in silca sand (Bergeron et al. 1998). The purpose of the series was to understand more about the physics of shallow buried blast events and to propagate a data set to use for numerical model validation. The plan was to use flash X-ray to interrogate the early stages of the event and high speed video (HSV) for the latter stages of detonation product expansion and the travel of the soil surrounding the charge. These two diagnostics in conjunction with side-on over pressure gauges in the soil bed and in the air were the sources of data intended to inform the conceptual model and provide the validation data for the computer codes. The post-test crater profile was also intended as code validation data.

The sand used in these tests had almost zero moisture content and was prepared to a consistent dry density; however, the charge and detonator conditions were not suitable to produce repeatable results at this small scale. The spread of results was between 20% and 80%. Recent work at the University of Sheffield has shown the for this size of charge the arrangement of charge case, detonator orientation, and the consistent placement of those components is crucial for repeatable results (Clarke et al. 2014, 2015b). Bergeron was top-detonating the charges, and the charges were in cases with a substantial cap and detonator holding lug. Bergeron found that the results were more repeatable when the

smaller RP-2 (30 mg PETN) detonators were used instead of the RP-83 (86 mg PETN, 123 mg RDX, 908 mg HMX). Especially for the tests where the burial depth was only 30 mm, having a thick charge cap, and a large detonator would displace such a large portion of the sand over the small 100 gram charge that it would certainly effect the way in the soil cap expands and breaks up. Moreover, using a detonator from the top that contains over 1000 mg of HE will pre-disturb the soil overburden with it own expansion, as the expansion of the detonation products from the main charge is beginning; which will certainly add early instabilities to the processes taking place. Using un-capped, bottom detonated charges with nothing disrupting a homogeneous overburden, in direct contact with the explosive material is a much more appropriate way to produce repeatable results, assuming the other parameters are well controlled. Much more repeatable results for similar conditions have been demonstrated by the University of Sheffield (Clarke et al. 2015b, 2017). For larger tests with an over-burden of 100 mm and a charge size of 5 kg, it is much less likely that a top detonated, capped charge, using a large detonator would have significant effects on the repeatability; because the majority of the soil cap would be undisrupted by the relatively small space taken up by the detonator and cap.

Given the fact that Bergeron claimed the proportion of loading associated with soil particle momentum transfer could vary wildly based on test parameters such as depth of burial, soil type, saturation and others it is surprising that the only form of diagnostic he employed to measure the loading a target would receive was side-one pressure gauges. This ensured that there would be no way to determine the true reflected specific impulse at the centre of a target. Moreover, the side-one pressure gauges were only placed on the axis of the cylindrical charge, meaning no data showing the decay of pressure and specific impulse moving away from the axis was recorded. Bergeron planned to used the pressure data from the soil air gauges in combination with the position-time information on the soil and detonation products provided by the X-ray and HSV as validation data for CFD models. Although Bergeron's work is very good overall and makes good use of what was available, the problem with his suggested validation approach is that it requires too many assumptions about the behaviour of the event to give confidence in the validation. First, it assumes that if the axial side-on pressures captured in the model match the experimental data that the distribution and magnitude of reflected impulse will also be correct. Second, it assumes that if the final crater size in the model matches the data that there will be a corresponding level of accuracy for the reflected pressure. Lastly, it does not seem possible from the resolution of the X-ray and HSV stills in the report to really interpret an accurate position and/or local density of the soil

and detonation products. When computational methods are developed and are "calibrated" to a certain scenario where the validation data is not the output aim of the computational model, how can there be any confidence that the model is representing the event in a meaningful way with respect to the output of interest? In some areas of blast such as far field free air, that are very well understood and characterised, it would be entirely appropriate to use side-on pressures to calibrate a CFD model because the relationship between side-on pressure and reflected pressure is well documented. In a scenario such as shallow buried blast where it is not even certain if continuum modelling is appropriate and where there is no consensus regarding the contribution of different phenomena to the final reflected impulse, it is not appropriate to use axillary parameters such as crater size, side-on pressure or displacement time history of the overburden front to validate a model intended to predict the loading delivered to a target. This tendency to validate models intended to predict target loading with data other than target loading data is important to comment on here because as will be demonstrated in subsequent sections, this approach has been widely adopted in the decades that followed Bergeron. It would seem that in the same way that the conceptual models of shallow buried blast physics of Westine and Bergeron affected the assumptions of future studies, the approach which Bergeron took with model validation would also be replicated in future work by other contributors to buried blast research.

Bergeron and Tremblay (2000) published a paper detailing a study aimed at capturing the total impulse imparted to a target under different moisture contents and burial depths. Whilst this study is useful in terms of its contribution to the understanding of total impulse delivery as a function of moisture content and depth of burial for a particular soil type, prairie soil; it does not actually inform anything about the different contributions of air shock and detonation products vs soil impact, nor does it offer any correlation information between side on pressure and reflected pressure. Bergeron claimed that the testing was done because more needed to be known about the contribution of the soil to the loading than could be interpreted by the previous work measuring side-on pressures. But, the test used a different soil type, different charge sizes, different burial depths and only captured total impulse imparted to a target with no measurement of central reflected or side on pressure. It is the opinion of the author that no meaningful information about the relative contribution of one parameter over another to the loading experienced by a target could be drawn out the two test series that Bergeron published in 1998 and 2000.

2.4 Experimental measurement of buried blast loading

The work done by Hlady (2004) described a series of shallow buried blast tests measuring total impulse imparted to a target using a vertically translating pendulum (Hlady 2004). The work was at a small scale (25 gram charges) and uses two soil types, one fine grained silty clay called prairie soil and one sand called CFAS (a fine concrete aggregate sand). In the trial, moisture content, burial depth, and stand-off were varied. Results showing a significant increase in impulse when the soil is near saturation was matched well by later work at the University of Sheffield (Clarke et al. 2017). Hlady makes note of the different behaviour of the event for the two soil types as observed in the HSV; where the silty clay comes off in chunks at high velocity compared to the evenly dispersed sand throw. This change in behaviour is cited as the reason which increasing stand-off for the silty clay has little effect on the imparted energy because the lumps of flying clay impart similar energy even at greater distances. The variability of the results in this series of test is significant with some results changing by as much as 50% for nominally identical tests. It is the opinion of the author that the control of the geotechnical parameters was not rigours and precise enough to produce repeatable results.

The work done by Fourney et al. (2005) consisted of air-blast and shallow buried blast tests measuring the impulse imparted to rigid plates. The scale was small with charge sizes of approximately 3 grams. Tests were conducted for variety of soil conditions with the free air case as a baseline. Most of the conclusions drawn regarding soil parameter effects were commensurate with other work in the field in a qualitative sense; such as, impulse increasing with saturation level. However, the test series involved very few repeats giving very little confidence in any of the quantitative conclusions. Moreover, the testing did not carefully control all the geotechnical conditions in a systematic way ensuring the effect of certain parameters could be studied in isolation. Finally, definitive claims were made regarding the relative contributions of air blast and soil ejecta to target loading; which for a series of tests that were only measuring total impulse it is scientifically unsatisfactory. Performing tests for free-air, and two different burial arrangements and measuring the total momentum imparted to a target does not tell anything about what mechanisms of loading contributed in the buried blast case. The only thing such testing can inform is the difference between a pure free air blast and an event where some combination of particle barrage and air-blast causes the loading, the contributions are still unknown.

Taylor et al. (2010) produced work on buried blast loading measurements on a rigid target and Leiste et al. (2013) published work using the same test apparatus.

The main diagnostic equipment used by Taylor and Leiste was Hopkinson pressure bars (HPBs), which as a complete aside are incorrectly named by Taylor and Leiste as Kolsky bars. Kolsky bars refer to the split bar arrangement developed by Kolsky for material testing. There is a common misconception within the field of pressure bars that Hopkinson had anything to do with the split bar arrangement developed by Kolsky. The split bar arrangement is often referred to as a split Hopkinson pressure bar; it is the opinion of the author that split bar arrangements should be called Kolsky bars. Hopkinson used single pressure bars as a force transducers (how Taylor and Leiste used them), never in the split arrangement.

The work is broadly commensurate with similar work done at a later date by the University of Sheffield which will be discussed in Section 2.8. However, the scale of this work is small, 4.4 gram charges and 10 mm burial depth; compared to the 100 gram charges and 25 mm burial depth used by the University of Sheffield. With respect to STANAG 4569 Threat Level (NATO 2006), the work at the University of Sheffield measuring total impulse from buried blast is one-half length scale and the work measuring reflected pressures at discrete locations is one-quarter length scale. The work published by Talor and Leiste is less than one-eighth length scale, and it shows a high degree of variation. This is likely because at such a small scale, the effects of any inaccuracies in the test layout and geometry are more significant, in terms of percentage error. Also, no mention is made of how the scale of the soil particles might effect the results and whether any consideration was made for those effects. The only information about the sand that was provided was which store it was bought from. Soil particles of 3 mm diameter at Taylor and Leiste scale would be the equivalent to 24 mm diameter particles at full scale.

The results presented by Leiste show that saturated soils result in the highest impulse measurements compare with other moisture contents and that decreasing the stand-off increases the peak pressures experienced as well as the non-uniformity of pressure across the target (central concentration). Although the work by Taylor and Leiste does provide some information regarding the ways in which loading is affected by various conditions of burial and saturation, there is still much uncertainty about the behavior of the experimental constituents. The explosive, the sand, the water and the air all need to be considered in a shallow buried blast event development in terms of how their differences result in and

change in behavior and loading. Also, at such a small scale without explicit control of the soil particle size to match the test scale, any in-depth study of the physics using further diagnostic approaches such as X-ray would be dubious.

Anderson et al. (2011) performed a series of 18 tests using 625 gram charges buried at 50 mm depth in "common sand". The aim of the work was to build a data set that had three repeats for each test condition. The impulse delivered to the target was the main output for the tests. This was done by measuring jump height with a cable-pull potentiometer and with an accelerometer on the target. The justification for the size of sand bin used to represent an infinite bed was based on an initial computer modelling analysis using CTH. The repeatability of the total impulse at moisture contents of 7% and 14% is high, but for the total impulse at moisture a content of 22% the furthest result is 17% from the mean. No information was provided regarding the preparation method for the soil beds, it is highly likely the lack of repeatability is due to inconsistent moisture content through the depth of the soil bin. The cardboard Sonotube with a plywood base used to contain the soil for testing may not have provided a sufficiently waterproof container to consistently control the moisture content of the soil at high levels. For most sands it is normally impossible to achieve any moisture content between approximately 10% and saturation because the water drops out of the soil structure and begins pooling at the base of the container it is contained in. The only consistent moisture content above this level that can be accurately achieved in practise is full saturation. In order to achieve accurate full saturation the soil bed must be compacted to the desired dry density and then saturated from the bottom of the container up, using a pre-installed water delivery system (Clarke et al. 2012, 2015b).

The trend in the data showing an increase in impulse transfer with increasing moisture content is attributed to the increase in density as a result of adding water to space in between the sand particles. This conclusion is made in the absence of a rigorous investigation of the parameter space and without any other diagnostic sources to understand the behaviour of the event. Subsequent work by Clarke et al. (2017) has shown that the increase in impulse is due the soil being close to its saturation level, which fundamentally changes the soil overburden behaviour during the expansion of the detonation products. Fully saturated soils prevent early breakout of the detonation products preventing lateral expansion and confining the detonation products to the centre of the target for longer, increasing the imparted impulse. Anderson's work is well presented, but as will be demonstrated in subsequent discussions, the data does not provide sufficient information for numerical simulation validation as Anderson claims. The distribution of impulse across the target is a very important pa-

rameter; therefore, validating back to a global parameter such as total impulse will not provide sufficient confidence in the ability of the numerical method to represent buried blast events in an accurate way.

In 2011, Ehrgott published two papers investigating buried blast events. One paper detailed the experimental setup and design (Ehrgott et al. 2011a) and the other discussed some of the results as well as the influence of soil parameters on impulse delivery and air-blast overpressure (Ehrgott et al. 2011b). The test regime incorporated a vertical translating pendulum for impulse capture and side-on baffle gauges for over-pressure. Separate tests were performed for capturing total impulse or side-on pressures. In the paper describing the experimental arrangement pressure gauges mounted in the impulse capture target face are detailed; however, no results from these gauges were published outside of Ehrgott's thesis, this is because the gauges did not survive the soil particle impacts and the results were inconsistent. Because the soil beds were prepared in-situ and compacted with a vibration compaction plate being ran over the test bed, it is unlikely that the density of the test bed was homogeneous and accurate. Also, no repeat tests were performed for any of the soil conditions, which doesn't give great confidence in any emerging trends.

Figure 2.2 shows the experimental layout for the side-on pressure gauge arrangement and the impulse capture arrangement. A comparison of the two arrangements shows that, only three side on pressure gauges map onto the target face of the impulse capture mass. The central gauge and two gauges that are positioned at the very edge of the impulse capture target face. Because the reflected pressure gauges in the target face were not reliable, and there is only one side on pressure gauge at the central location with no repeats, it is very difficult to draw any substantiated conclusions about the distribution of side-on pressure from the central axis radially outwards, and even more so with respect to specific impulse distribution. The work concluded that for buried charges the soil type and conditions can affect the break-out behaviour of the detonation products. If the soil surrounding the charge has high-air-voids and is permeable dry sand material then the air blast breaks out early reducing the impulse delivered to the target by soil impact and air blast. Whereas, if the the soil overburden maintains its integrity for longer (more fines and less air voids) then the soil focuses the detonation products onto the target face and increases the delivered impulse. This finding is consistent with other work in the field such as Pickering et al. (2012).

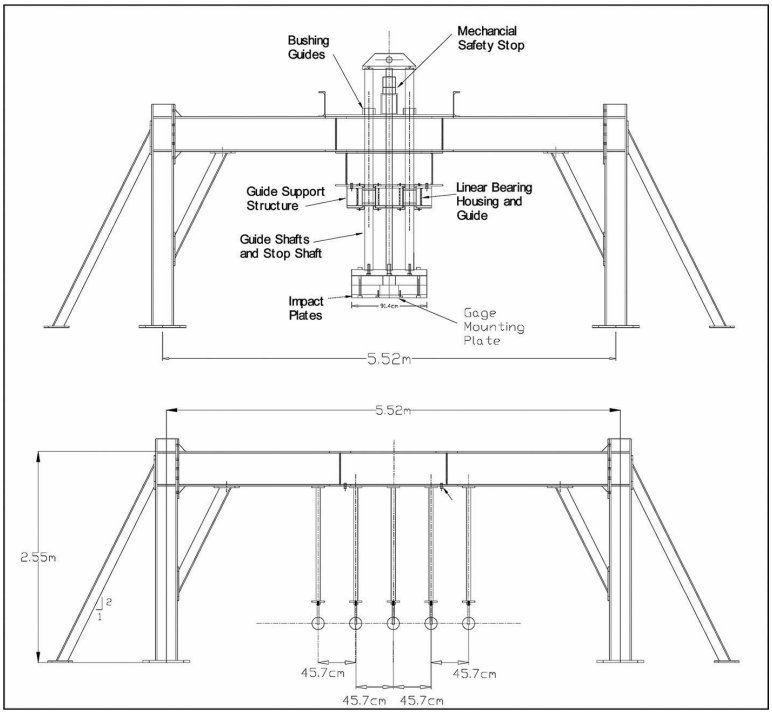

Figure 2.2: Support Structure with impulse capture pendulum and side-on pressure gauge arrangement Ehrgott et al. (2011a)

2.5 Modelling of buried blast loading

Grujicic has produced a significant amount of numerical modelling work in the field of shallow buried blast (Grujicic et al. 2006a,b, 2007a,b, Grujicic and Pandurangan 2008, Grujicic et al. 2008, 2011). Investigating various modelling approaches such as discrete particle methods and continuum models using multiple proprietary codes and in house codes. The modelling work is thorough with convergence studies and validations. However, all of the validation has been against soil-bubble expansion, total impulse, side-on pressures or crater size. None of the validation has been against distributions of pressure-time across a target or distribution of impulse across a target. Data such as Westine et al. (1985) exists in the literature and the modelling should have been compared to distributed reflected impulse measurements; which are what led to target deformation and predicting these deformations should be the ultimate goal. If the goal was to predict crater size or soil bubble expansion with time validate against those metrics. But if the goal is to predict the distributed loading across the face of a target, validate against that. Furthermore, Grujicic has preconceived ideas about the physics of a shallow buried blast event which simplify

the problem to a point that validating against a parameter such as side-on pressure is valid. Figure 2.3 is a diagram of Grujicic's idea of how a shallow buried blast event develops. The problem is that whilst this may indeed be an accurate description of a buried blast event for some scenarios, not near enough is known about the effect of grain size, saturation ratio, burial depth, charge shape, stand-off from target etc. to be able to run this model out across all buried blast events. Grujicic has done some very interesting work but it would be more convincing to see his work validated against some reflected pressure-time histories at discrete locations on a target such as (Clarke et al. 2015a, Rigby et al. 2015, 2018).

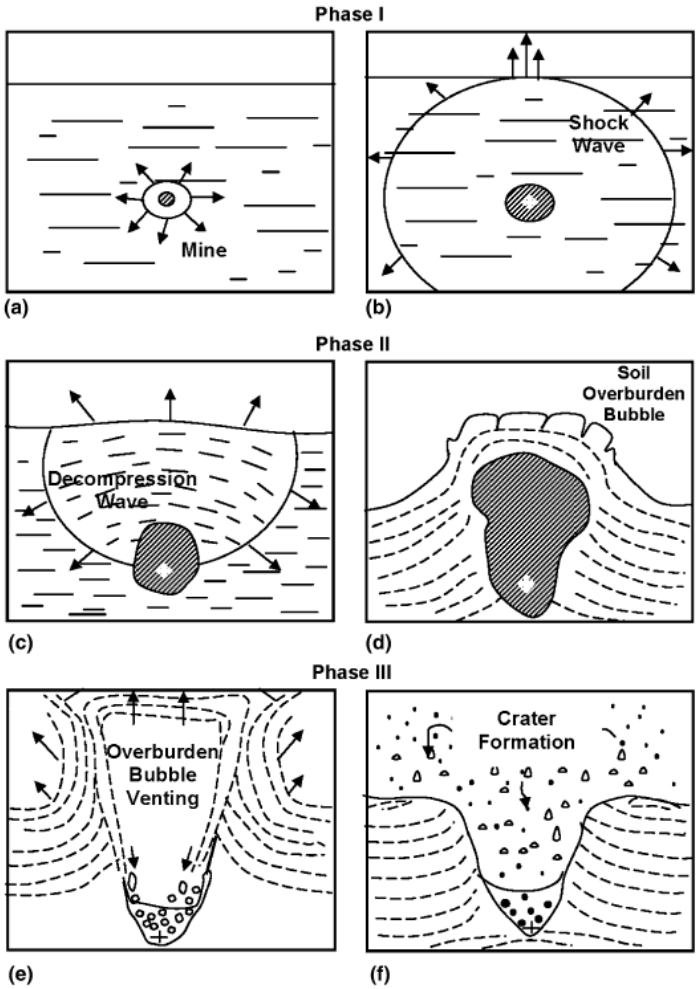

Figure 2.3: Description of shallow buried blast event by Grujicic and Pandurangan (2008)

Heider and Klomfass (2005) performed shallow buried blast tests measuring the jump height of a plate (total impulse) and compared these tests to a numerical model with good agreement. No comparison of the distribution of impulse was made between the modelling and the experiments, as plate jump experimental approaches do not provide any information other than total imparted impulse.

Fox et al. (2011) and Fox et al. (2014) also performed shallow buried blast tests measuring the jump height of a plate (total impulse) and compared these tests to a numerical model with good agreement. No comparison to the distribution of impulse was made between the modelling and the experiments as plate jump experimental approaches do not provide any information other than total imparted impulse. Fox performed the tests and modelling for several different soil types and water contents.

2.6 Experimental measurement of target response to buried blast loading with numerical modelling

Neuberger et al. (2007) used a coupled model in LS-DYNA to predict the deflection of a plate subjected to a blast from a flush buried sphere of TNT. The soil model parameters where changed until the deflection of the plate matched the results of the first test. The other tests were identically set up, but at different scales. Reducing a significant amount of complex physical processes down to one final parameter such as plate deflection, calibrating to this parameter, and then describing the modelling technique as accurately predicting other tests (which are scaled versions) could be considered misleading. Moreover, a flush buried spherical charge will not produce the same type of behaviour of the detonation products or soil over burden as a buried 3:1 diameter:height cylindrical charge fully buried. Flush buried spherical charges are not indicative of any IED or land mine arrangement and therefore are of little interest in predicting IED or land mine loading. However, that is not to say that using an idealized geometry to investigate the fundamental behaviour of material is not useful in some circumstances. Much useful work has been done with spherical charges surrounded by shells of material, but this work has been focused on understanding the fundamental behaviour of different materials subjected to 1D blast effects.

Deshpande developed a constitutive model for high-rate deformation of an aggregate (Deshpande et al. 2009). The sand model was incorporated into a coupled Eulerian/Lagrangian modelling approach to replicate some experiments where C4 spheres surrounded with a shell of dry sand, wet sand or bare were

detonated above a clamped stainless steel target plate. The sand used was a manufactured spherical glass micro sphere sand. The modelling is used to interrogate the behaviour of the explosive and sand seen in the HSV from the testing. The assumption is that the modelling is representing the physics present in the test such that "looking inside" the event using information from the model is valid. However, the only validation of the model was done by comparing the final deformed profile of the plate to the prediction of the model. The problem with this piece of work was not with the work itself, it is with what problem the work claims to be solving. The work is aimed at developing a modelling technique for shallow buried blast events. The loading event that a target above an IED sized and shaped charge, buried in a real in-situ soil, will experience is not necessarily commensurate with a perfect spherical charge surrounded by a spherical shell of manufactured sand that is suspended above the target plate. No information is provided regarding how these two scenarios might be different and how the mechanism of loading might not be the same. Moreover, with no measurement of the loading, and no displacement-time history for the plate, validating the model back to final plate deflections condenses all the forgone physics into one single parameter.

Borvik et al. (2011) used the discrete particle modelling method in a fully coupled approach to investigate the response of the stainless steel clamped plates described by Deshpande et al. (2009). The loading from the detonation products, the air shock and the sand are determined by the discrete particle method and a finite element model is used for the plate deformation. Borvik includes an intial model validation/calibration step before commencing with the charge-sand-plate model. Borvik used a copper cylinder expansion test and the radial displacement-time data normally used to calibrate an EOS to calibrate the corpuscular constants for C4 in his discrete particle approach. However, the models which incorporated the dry sand and the wet sand still needed to be calibrated in terms of the soil parameters in order to match the plate deflections from the test. As in Deshpande's work, all the physics that takes place in the blast event, which is meant to be represented in the modelling, is validated back to one final global condition, plate deflection. In order to fully validate this approach it needs to be checked against other experimental results such as distribution of specific impulse over the target, pressure-time history across the target, flash X-ray data showing the position of the sand with time or some other metric that gives an indication that the modelling approach actually represents the physics taking place.

2.7 A review of Pickering et al. 2012 with integrated discussion

Pickering et al. (2012) performed three series of tests using small PE4 charges from 7 grams to 21 grams buried in dry sand at burial depths between zero and 70 mm, see Figure 2.4 for the test arrangement. The sand used was generic construction sand, but it was sifted to ensure no particles larger than 0.6 mm were present. More work needs to be done regarding particle size scaling, but it was obvious that preventing any uncharacteristically large particles from being used in the burial medium will improve the repeatability of the experiments and should improve the likelihood that the experiments will be accurately representing the full scale event. The targets used were fully clamped steel square targets with a deformable area of 300 mm × 300 mm. Impulse was measured using a vertical pendulum and tracing pens.

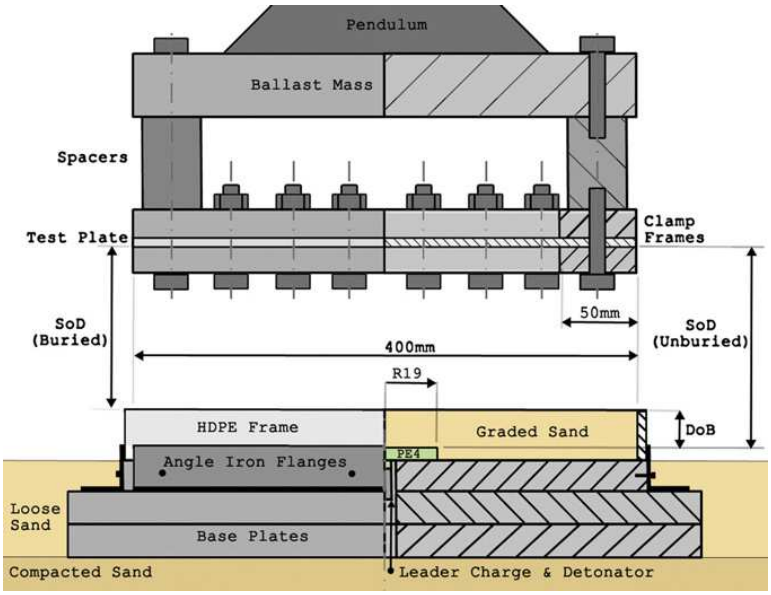

Figure 2.4: Test arrangement - Pickering et al. (2012)

The experimental apparatus incorporated a solid steel base from the base of the charge downwards, meaning the charge is only surrounded by the sand on the sides and the top. This approach was sensible from a pragmatic experimental setup perspective; that is, no complicated compaction of sand into a soil bin, which may have been a source of variability in previous studies. However, it would have been a more rigorous and validated experimental approach if a

small number of tests had been done to demonstrate how a test with a charge buried in an "infinite bed" compared to this arrangement.

The first series of the tests varied the mass of the explosive while maintaining the stand-off and using 3 different depths of burial. The second series of tests varied the depth of burial, whilst maintaining a constant stand-off using three different charge masses. The third series of tests varied the stand-off and kept the same mass of explosive for two burial depths (0 mm and 20 mm). The extensive investigation of the parameter space in these three series of tests allows conclusions to be drawn about buried blast event behaviour without overlooking the "big picture".

Pickering concludes that the reason why impulse increases with burial depth (to a point) is because the sand acts as an inertial barrier to the detonation products keeping them in contact with the target for longer (Figure 2.5). This conclusion was supported by the modelling presented in the paper, and is also supported by findings in recent work at the University of Sheffield Rigby et al. (2018) where the loading from such events is measured across the face of the target.

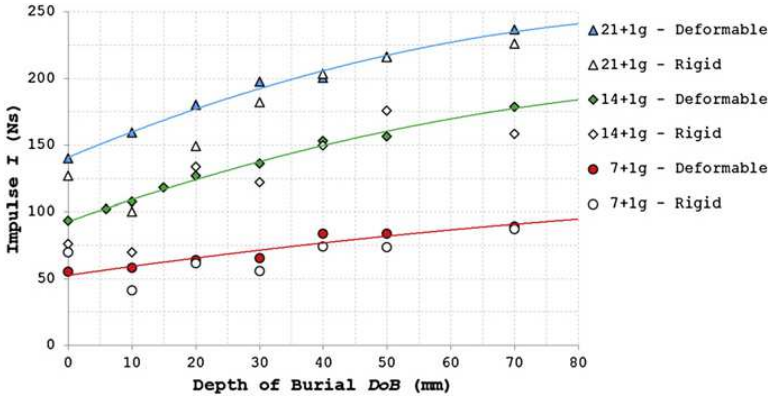

Figure 2.5: Impulse vs depth of burial, 47 mm Stand-off, Various PE4 - Pickering et al. (2012)

Pickering comments on the depth of burial increasing the inertia of the sand over the charge, which in turn has significant effects on the time of arrival of the loading. What Pickering did not comment on was what the effect of this increased inertia would have on the time scale of the impulse delivery. Because the loading was not being measured with respect to time, the effect of sand inertia on the time scale of impulse delivery could not be determined in these experiments. Recent work at the University of Sheffield (Clarke et al. 2018), has shown that increasing the depth of burial will increase the duration of the

loading. Time is a very significant factor in the case of these tests, as will be demonstrated later in this section. Another item which Pickering does not comment on is the difference in the distribution of impulse across the face of the target for different test parameters. There is a discussion regarding the focusing of the detonation products by the sand and therein an optimum depth of burial to focus the detonation products without releasing too much work to the plastic deformation of the sand. However, this "focusing" of the detonation products is considered to be responsible for the increase in total impulse, which is true, but the "focusing" also concentrates the distribution of impulse over the centre of the target, resulting in a more non-uniform load not just a larger total impulse.

Figures 2.5 and 2.6 show that for a given charge size on these graphs, impulse increases with increasing burial depth. Whereas, deflection decreases with increasing burial depth. There are many analysis approaches which use total impulse to predict plate deformations, none of them would predict decreasing deformation for increasing impulse. There are two parameters which contribute to this apparent discrepancy. The first is the duration of loading and the second is the distribution of loading. Figure 2.7 shows the deformation profiles of the plates (section through the centre) subjected to blasts from different burial depths with the same stand-off and charge size.

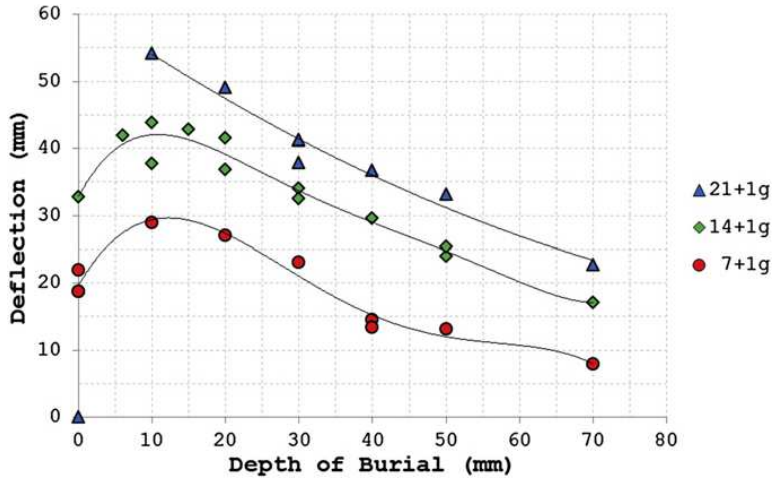

Figure 2.6: Midpoint deflection vs. depth of burial, 47 mm Stand-off - Pickering et al. (2012)

The profile of the target subjected to the blast buried at 70 mm is a different shape to the profile of the targets subjected to blasts buried at 6 mm, 10 mm, 15 mm, 20 mm and 30 mm; in that there is a definite plastic hinge zone in the centre of the target for the more shallow burial depths. Example 1 in Figure

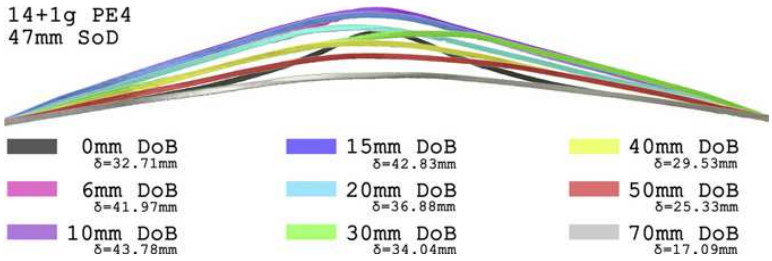

Figure 2.7: Cross-sections of the 14 + 1 g PE4, 47 mm Stand-off, varied depth of burial target plate - Pickering et al. (2012)

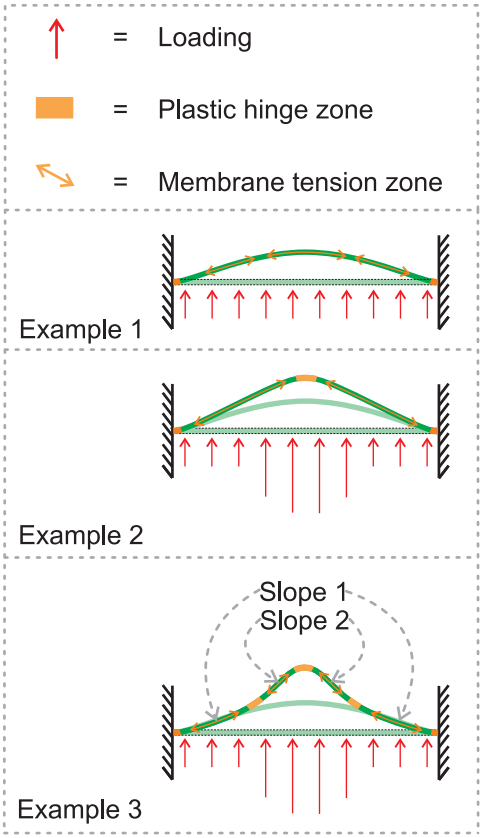

Figure 2.8: Conceptual deflection types with loading conditions

2.8 shows one type of deflected shape that can be produced in ductile targets; hinges will form at the supports first, even if the loading is impulsive. However, the shape in Example 1 can only be produced if the loading is distributed evenly. Considering that the total impulse decreases with decreasing burial depth for the deformation profiles in Figure 2.7, the only way that the shape could change to something similar to Example 2 in Figure 2.8 with decreasing depth of burial,

is if the concentration of the loading changed, whether or not the loading is impulsive, or dynamic. Example 2 in Figure 2.8 could in theory by produced by uniform load or a non-uniform load depending on the magnitude. However, to move from Example 1 to Example 2 under a lower impulse could only be achieved by a concentrated load. Impulsive loading being defined as loading in which the duration is significantly shorter than the natural period of the target, such that the target has not responded globally in any significant way until after the loading is complete. Dynamic loading being defined as loading in which the target has time to respond globally while the loading is still being applied. By responding during the application of the loading the target will reduce the velocity at which any discrete section of the target is travelling when the loading is finished; i.e. a reduction in the kinetic energy imparted to the deforming parts of the target. The difference between the deformed profile of the target for 0 mm burial depth and all the others is time (duration of the loading). Clarke et al. (2018) showed that the duration of loading applied to a rigid target when no overburden in present compared to a charge covered by an overburden of 25 mm is eight times shorter. Consider the difference between Example 2 and Example 3 in Figure 2.8; the only way to produce the additional change in slope in Example 3 is by a non-uniform distribution of kinetic energy. In any scenario where there is time for stresses to equilibrate across the plate the result would not be the upwards curvature in Example 3. Apart from inertial restraint, there are no other forces that could restrain the section denoted as Slope 1 in Example 3, allowing the section denoted as Slope 2 to rotate around a moving plastic hinge zone. An inertial constraint of Slope 1 would only occur if there was difference in initial velocity imparted across the plate; that is, the centre of the plate travelling with more kinetic energy than the edges. In all the work presented by Nurick where the loading is from uniform free air blast, not one of the deformation profiles presented exhibits the deflection type in Example 3; despite the short duration of the loading, there is no resulting non-uniform initial velocity profile across the plate because the impulse is uniform across the plate. Figure 2.9 shows how for a target with a distribution of kinetic energy across its face, the area of maximum strain will be near the area with the greatest slope in the kinetic energy distribution curve.

It is worth noting that for very concentrated loads of very short duration relative to plate response, a plastic hinge forms as the centre of the target moves away from material around the edges that has picked up lower initial velocities. This plastic hinge travels towards the supports, as the centre of the target moves away from the material at the edges.

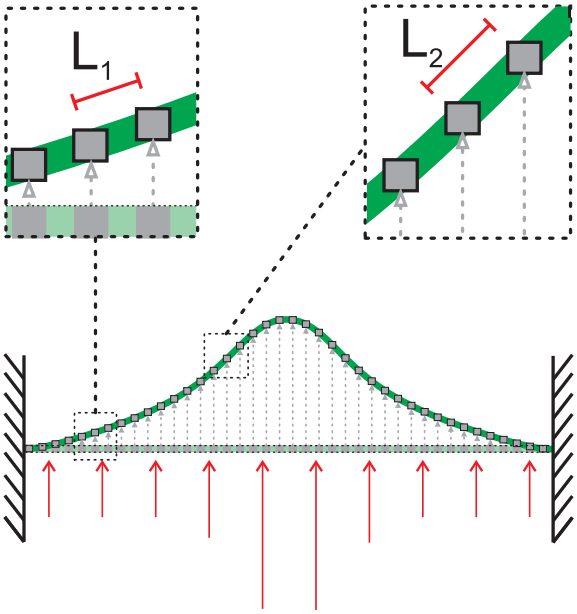

Figure 2.9: Conceptual plate with lumped mass, non-uniform kinetic energy distribution results in a non-uniform strain distribution, $L_2 > L_1$

Figures 2.10 and 2.11 from work done by Jacob et al. (2004) show deformed profiles for different impulses, all with concentrated loading of very short durations (near field free air blast).

Figure 2.10: Cross sectional view of plate deformation for 1.6 mm plates in order of increasing impulse from bottom - Jacob et al. (2004)

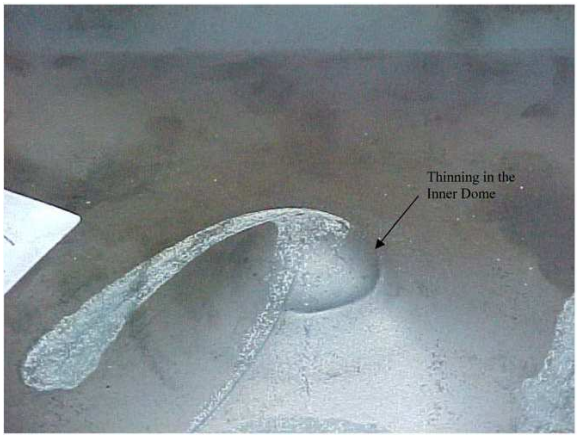

Figure 2.11: Thinning visible on a 2 mm thick square plate - Jacob et al. (2004)

“ The targets have the same shape because the relative distribution of impulse and time scale of the loading was very similar in each test. Because the charge size was increasing the total impulse was increasing and thus the total deformation increased, whilst maintaining the same shape.

Eventually failure occurs when the local stress exceeds the material ultimate tensile stress, which in Jacob et al. (2004) is always at the location on the cross-section of the target with the greatest slope. It is the theory of the author that this location of maximum slope on the target will correspond to the location of maximum slope on the kinetic energy distribution across the target.

Figures 2.12 and 2.13 show that for each burial depth, 0 mm and 20 mm respectively, the deformation increases with decreasing stand-off, but that the overall shape of deformation is maintained across different stand-off distances. Also, all the profiles of the tests with 0 mm burial depth have shape that is generated by a non-uniform distribution of kinetic energy as detailed in Figure 2.8, whereas the profiles from 20 mm burial depth do not. Lastly, for the 0 mm burial depth targets there is a disproportional increase in deflection for the small increase in impulse (Figure 2.14); whilst for the 20 mm burial depth the increases in deflection are broadly proportional to the increase in impulse. Given that kinetic energy (Equation 4.4) imparted to a specific area will be proportional to the square of the specific impulse imparted to the area if the loading is truly impulsive, it makes sense to see a more rapid increase in deflection with increasing impulse for the 0 mm burial tests; given that it is the most likely to be producing truly impulsive loading.

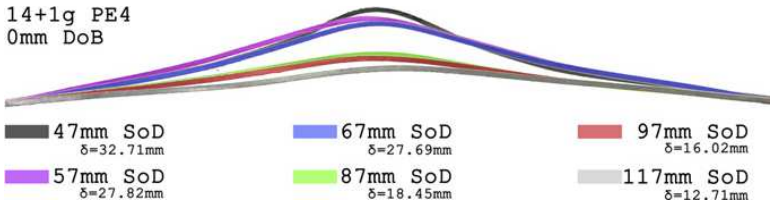

Figure 2.12: Cross-sections of the 14 + 1 g PE4, 0 mm depth of burial, varied stand-off distances - Pickering et al. (2012)

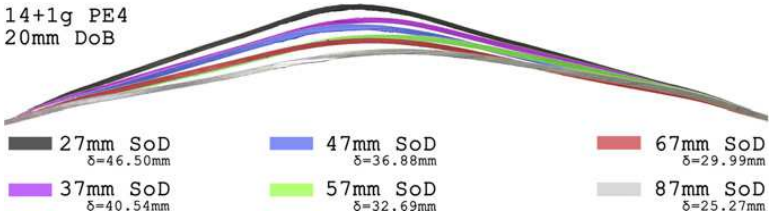

Figure 2.13: Cross-sections of the 14 + 1 g PE4, 20 mm depth of burial, varied stand-off distancese - Pickering et al. (2012)

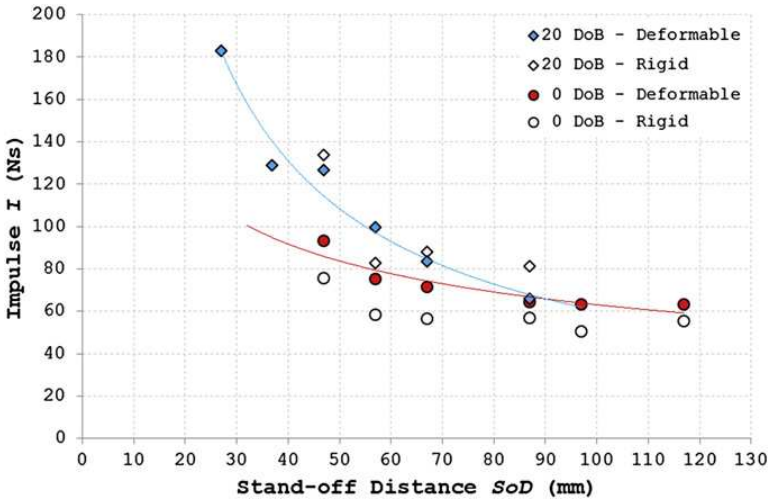

Figure 2.14: Impulse vs. stand-off distance, 14 + 1 g PE4 - Pickering et al. (2012)

2.8 Recent work by the University of Sheffield

Since 2010 the University of Sheffield has conducted approximately 250 buried blast tests (Clarke et al. 2011, 2012, 2014, 2015a,b, 2017, 2018, Rigby et al. 2014, 2016, 2018). Most of the testing has been performed using one of two different experimental approaches. The first is an experimental arrangement designed to measure total impulse delivered to a target using a vertical pen-

dulum, Figure 2.15 (Clarke et al. 2015b). This test arrangement was used to investigate the effect of geotechnical parameters on the output from buried blast events. The tests were performed at 1/2 Stanag 4569 NATO (2006) scale, using 50 mm burial depth and 625 gram PE4 charges. One hundred and fifty tests have been done with this test arrangement, this large body of tests facilitated the development of suitable techniques for preparing buried blast experiments that produce repeatable results. An accurate study of the effects of geotechnical conditions such as particle size, moisture content, and density can only be done if the results are sufficiently repeatable to be able to distinguish differences. This body of tests also showed which soil conditions yielded the most repeatable results. The knowledge and experience required to accurately control the geotechnical conditions was applied to the second experimental arrangement used by the University of Sheffield to study buried blast events.

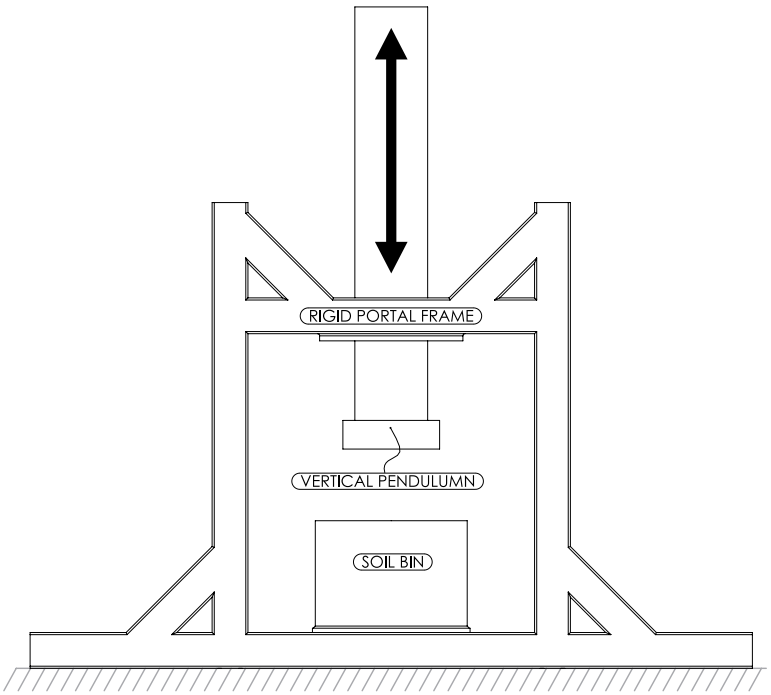

Figure 2.15: Original apparatus - Front view, after Clarke et al. (2011)

One hundred tests have been performed using the test arrangement shown in Figures 2.16 and 2.17. Pressure-time histories can be recorded at discrete locations across the face of the reflecting target using the Hopkinson pressure bars in this test apparatus. The experiments done with this arrangement are commensurate with the work done by Fourney et al. (2010), but as already mentioned, the testing at the University of Sheffield was conducted at a larger scale (1/4

STANAG 4569) with a much better understanding of the geotechnical parameters; meaning the repeatability was better. The test results for different soil conditions can be plotted on the normalized impulse distribution plot produced by Westine, as shown in Figure 2.18. The figure also shows that although Westine had suitable model for predicting the distribution of impulse, the spread of his data set was large. The spread was large because the geotechnical conditions were not well controlled and considered as separate parameters. The

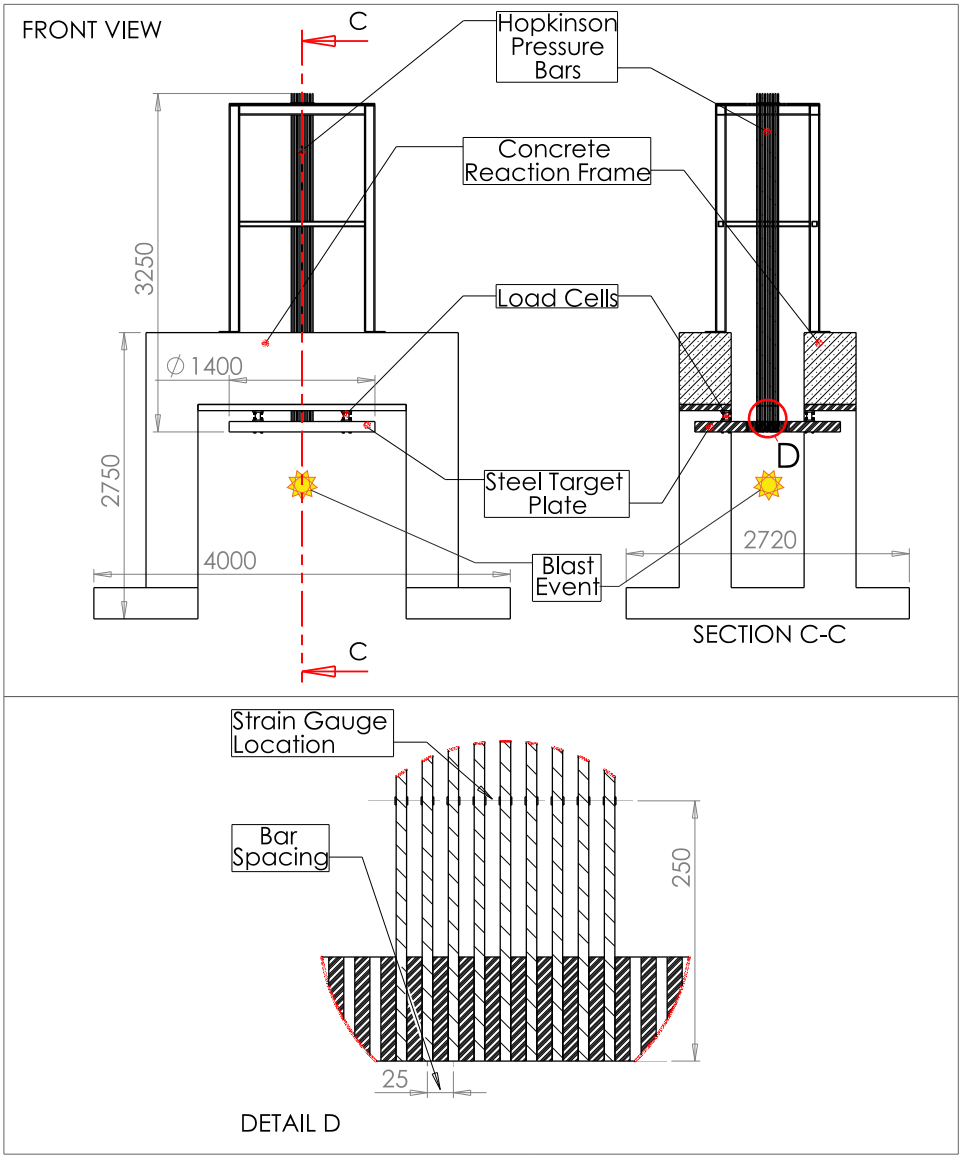

Figure 2.16: Details of apparatus for measuring spacial reflected pressure distribution; Front view, Section view and Detail D, after Clarke et al. (2015a)

results of each of the soil conditions from the University of Sheffield testing reside on what is effectively their own line. As shown by the "CoBl LB Sat" data points and the "Model Mod" line in Figure 2.18, Westine's model can be calibrated to a specific soil condition. "CoBl LB Sat" is the test data from one specific soil condition.

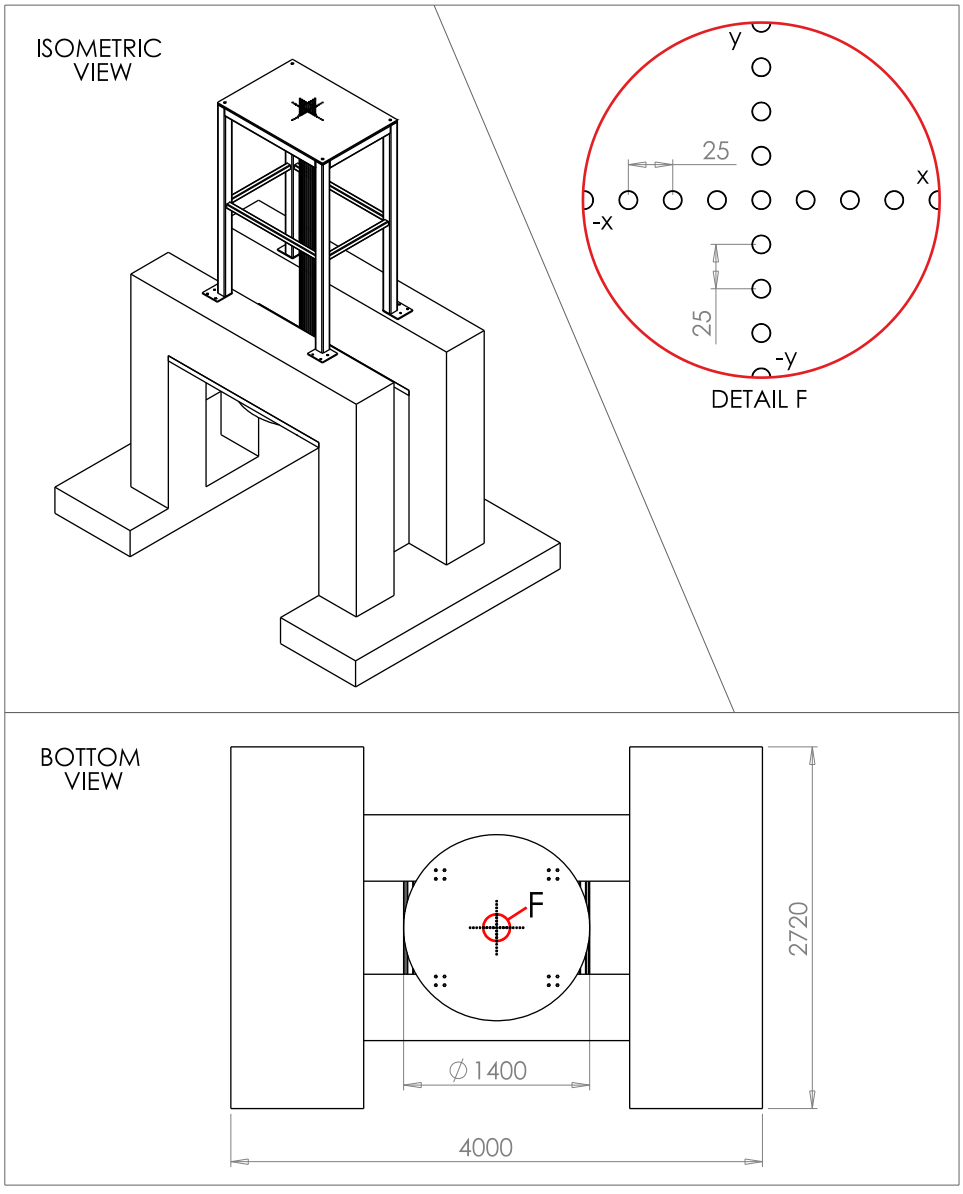

Figure 2.17: Details of apparatus for measuring spacial reflected pressure distribution; Isometric view, Bottom view and Detail F, after Clarke et al. (2015a)

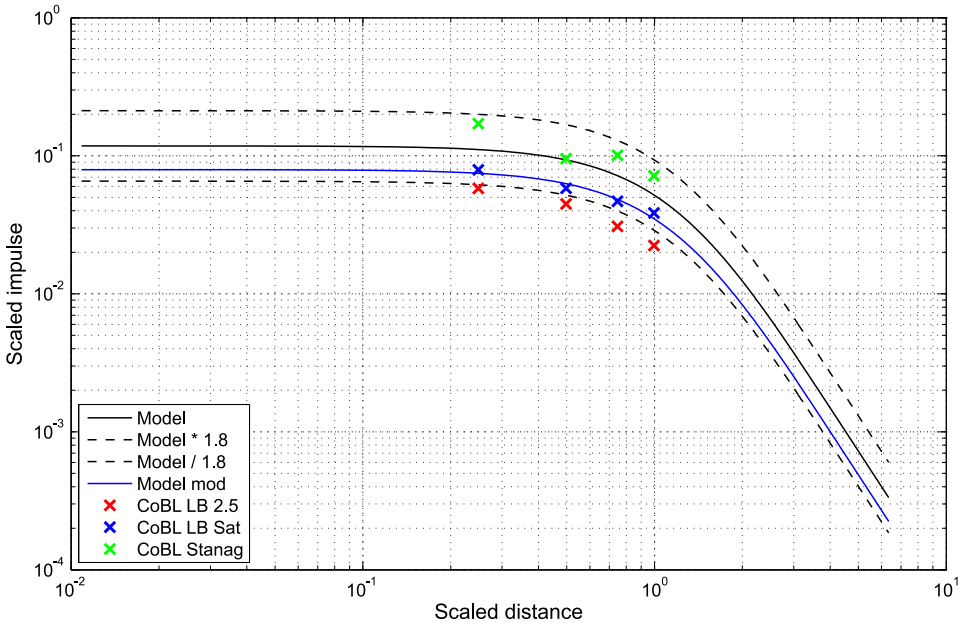

Figure 2.18: Westine normalized data and model with data from the University of Sheffield (CoBL LB 2.5, CoBL LB Sat, and CoBL Stanag)

The particle sizes of the soils used at 1/2 were not adjusted for the 1/4 scale tests. It is unlikely that the effect of particle size will be significant for the fine grained soils. However, with respect to the sandy gravel in particular, where the particle size can be as large as 20 mm, the effect could be significant. Considering the burial depth for the 1/4 scale tests (28 mm), where the entire burial depth could be spanned by just two particles in contact. At such extreme scales the soil above the charge could behave very differently from the full scale tests with a burial depth of 103 mm, where the soil may still behave as a continuum and be subjected to a compaction process by the expanding detonation products. With just a few particles of depth in the soil bed above the charge, the confinement offered by the soil bed is likely to be very different from the full scale event. More work is required to measure reflected pressures at larger scales to fully understand the effects of scale and develop a validated approach to scaling the soil particle size and knowing when it is required.

The high speed video employed in the 1/4 scale tests by the University of Sheffield in combination with the Hopkinson pressure bar readings are able to shed some light on the physical mechanisms taking place between detonation and the end of the loading on a target. However, in terms of quality experimental evidence this area of the physics is still mostly unknown.

2.9 Conclusions

Westine investigated the distribution of impulse across a target loaded by a buried blast event in the 70's and 80's. However, Westine did not control the geotechnical parameters effectively, making it difficult to see differences between specific trends from the results. Since Westine, the work done by the University of Sheffield is the some of the only work to investigate the distribution of impulse and the only work which includes the temporal resolution. Other work measures or is validated back to total impulse or plate deformation without direct consideration of the distribution of loading. As such, there is very little experimental data that provides information regarding the distribution of impulse across a target and even less that includes any temporal resolution of the loading duration.

A large number of papers have been produced on the topic of modelling buried blast events using some numerical approach; however, most of it is not validated against data with fidelity in loading duration or spacial distribution of impulse. All of the studies validated their modelling against total impulse, crater size, maximum central plate deflection, or some other parameter that has no direct link to the distributed load which the target will experience, and for only one or two soil conditions. Thus, there is no way to distinguish whether the distribution of impulse or time-base of the loading is correct in the modelling. There has been very little work aimed at producing fast running models or prediction methods for the simple deflection of protection materials and systems.

Importantly, as was demonstrated by the analysis of the work presented by Pickering et al. (2012), an understanding of the distribution and the duration of the loading is essential for an accurate prediction of target performance; total impulse alone is simply insufficient information to predict behaviour with confidence. A review of the literature has highlighted the need for a focussed, systematic, multi-diagnostic experimental study to gain a better insight into the mechanisms governing target deformation due to buried explosive events. Such information will also be invaluable for future numerical modelling studies as it will provide high-fidelity, temporal and spatially resolved data. Experimental work to gain an understanding of the detonation of the explosive with the expanding detonation products and how this process interacts with the soil overburden and air gap, before eventually loading a target, is crucial to improving prediction and modelling capability. Particularly if a full spectrum of soil conditions and geometric parameters are considered. The physics of any

scenario must be well understood before any judgement about the assumptions of a modelling approach can be made.

There is much about buried blast that is not well characterised and requires additional examination. The aim of the study presented in the following chapters is to demonstrate that:

a) The knowledge from the existing literature can be used to inform a methodology for well controlled and well characterised testing of buried blast protection materials and systems.

b) Knowledge of the distribution of impulse from a buried blast event can be used to predict target deformation without any FE modelling of the target or any numerical modelling of the blast event. For different target strengths, spans, thickness, materials and total impulse values.

The experimental arrangement detailed in this study was chosen explicitly because the distribution of impulse across the face of the target can be calculated, as will be demonstrated. As discussed already in this chapter, almost no other work in the field is currently measuring the distribution of loading from shallow buried blast. With respect to numerical modelling of buried blast events, almost no studies have validated the modelling back to the distributed impulse.

Chapter 3

Experimental Methodology

3.1 Introduction

This section explains how existing knowledge in the field and previous buried blast experimental programs at the University of Sheffield informed the development of a new apparatus and experimental approach presented here.

This testing was done under contract for Dstl as part of an ongoing theme of work. The objectives for the testing, as far as the customer (Dstl) was concerned, are detailed in Section 3.3.1.

This section also provides in-depth detail of the final test arrangement and protocol.

3.2 Previous testing apparatus

3.2.1 Pre-existing Setup

A long standing track record of buried blast experimental work by the University of Sheffield and Dstl was the underpinning basis for the new experimental arrangement employed by this investigation as detailed in Clarke et al. (2011, 2015b). The HITSss rig, an existing large frame testing apparatus (Figure 3.1) from this previous work was re-purposed and modified to suit the new experimental requirements.

This previous testing frame was used to house a large free flying reaction mass (≈1500 kg). Below the large free flying mass a 1000 mm diameter steel bin was used to hold the soil for the buried explosives testing. The large free flying mass was used to capture the impulse delivered to a target for a given geotechnical

and explosive arrangement; it was effectively used as a vertical pendulum. The general test procedure was to attach a deformable steel target to the underside of the vertical pendulum, place a prepared soil bin with buried charge on the base of the apparatus, adjust the soil height/bin height to give the correct stand-off to the target, detonate the explosives and then record the vertical travel of the pendulum with high speed video (HSV) to be able to calculate initial velocity and thus impulse (mass × initial velocity).

As discussed in the literature review this test arrangement is capable of delivering very consistent total impulse when the geotechnical parameters are well controlled. This test approach needed further refinement in terms the equipment. Some parts of the test were very difficult to align and some pieces of equipment were breaking after only a few tests, making it difficult to be efficient with range time.

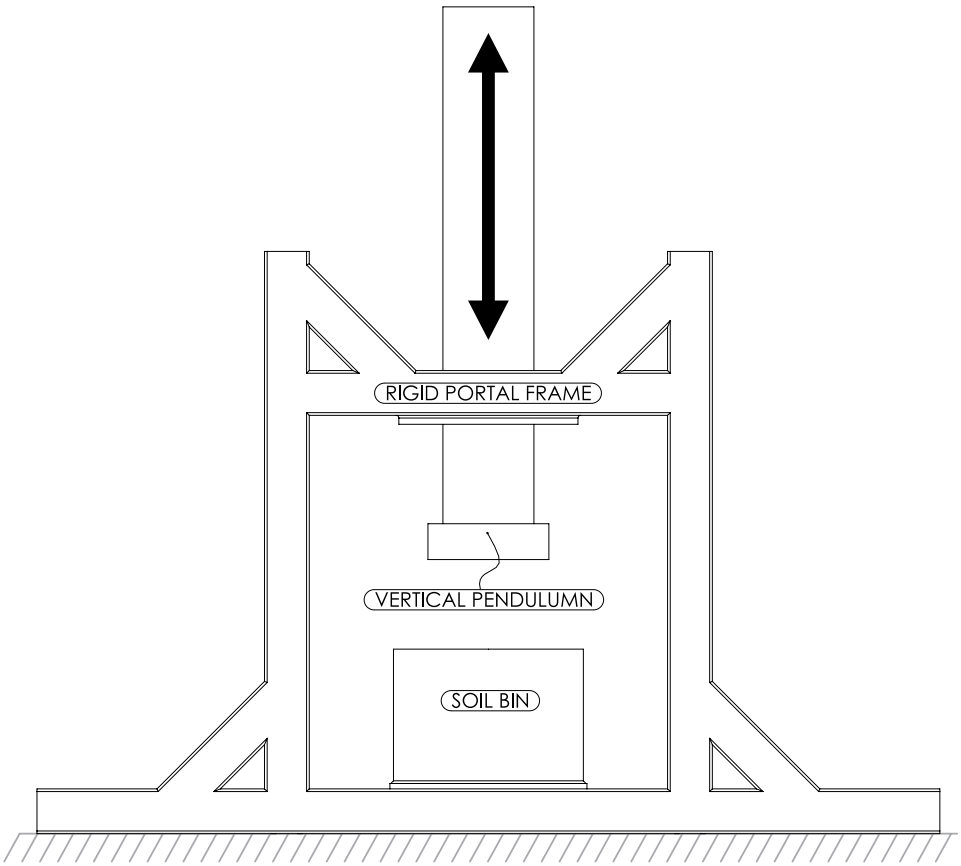

Figure 3.1: Original apparatus - Front view

3.2.2 Difficulties

Figure 3.2 shows a section detail of the base of the HITSss apparatus and the soil bin as it was originally set out. This arrangement resulted in excessive damage to the base of the bins after only a few shots. The thickness of the steel bins (30 mm) in combination with the layer of hardcore underneath the bin was not sufficiently resistant to permanent bending deformation of the soil bin bases. The permanent deformation on the base of the bins meant that the bins did not sit flat on the hardcore base nor did they sit at the same height relative to the target for each test. The bin resting at a different height after every test led to every test setup involving tedious packing and measuring to ensure the correct stand-off and parallel alignment between the target and soil surface.

The other problem with the test arrangement was the axial alignment of the soil bins with the centre of the target. The circular hollow sections of the bins were welded to square plates which were all slightly different sizes in plan. Therefore, every bin had to be individually measured into position on plan; which is difficult to do accurately with a 2200 kg soil bin.

The crucial implication of a difficult test setup is not the effect on test turn around time; it is the effect on consistency and accuracy. The more labour intensive the test setup the higher the likelihood of human error effecting the accuracy and consistency of the test. In short, if a person holding a tape measure has to align the in-plan location, the stand-off distance and the parallel planar alignment of the soil surface to the target surface for every test it will not be the same every time. Not to mention the fact that if the soil surface is adjusted relative to the rim of the bin after charge placement the charge has to be adjusted as well to maintain the correct burial depth/alignment. Particularly if the bin is a different size and shape after every test.

Moreover, a rigid reaction surface instead of the free flying mass was needed for the experimental approach employed in this study. As such, a number of modifications were made to the rig itself and the soil bin arrangement.

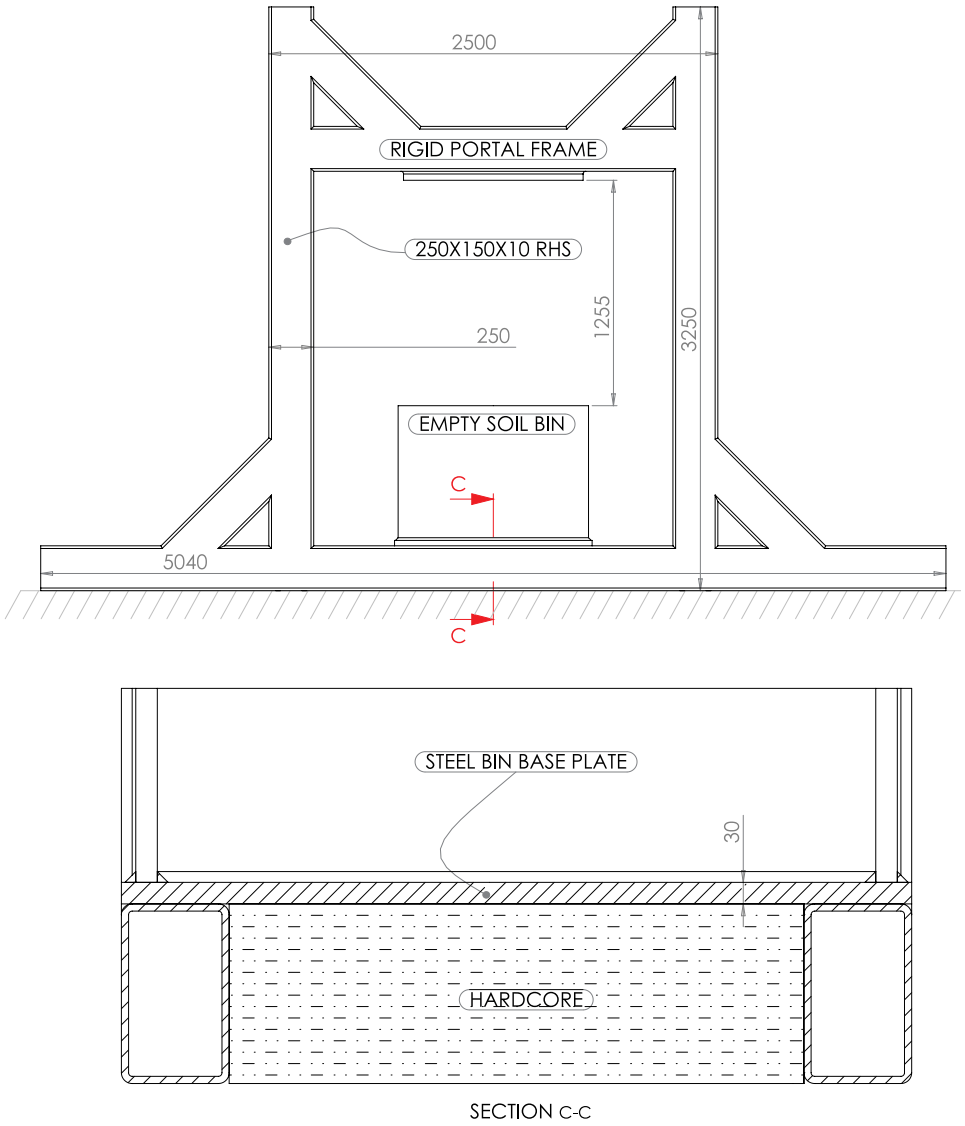

Figure 3.2: Original frame with original soil bin arrangement - Front view with section (mm)

3.3 Test design requirements

3.3.1 Objectives

Before modifications could be made to the test apparatus addressing the difficulties of the previous methodology, the requirements of the new approach

needed to be understood so as to incorporate all the changes in a holistic way into the new test arrangement and equipment.

The main deliverable for the testing was performance data for Armox steel plates and other materials subjected to buried blast loading. The requirement was for a benchmark data set of various plate performances against which any future plate/systems could be compared. The test arrangement was required to be able to accommodate plates of varying thickness as well as multi layered systems. The intention was to test square target plates which were 1000 × 1000 mm on plan and where the unsupported span for deformation was at least 650 mm. The output data required was peak dynamic deflection in the centre of the target and the final residual deformation across the entire plate. The spacial resolution for the residual measurements needed to be at least a 75 mm grid.

3.3.2 Support conditions

The original plan was to have a "clamped" holding arrangement for the plate. This approach has several problems. First, in practice, appliqué type protection plates for underbelly vehicle protection (main driving application of this project) are almost never installed in a true "clamped" arrangement. Second, actually achieving a fully clamped arrangement even in an abstract test setup is difficult for blast loading scenarios. It normally involves excessive bolt torques which results in high fastener attrition and a time consuming installation for every target. Thirdly, given the difference in coefficients of friction between plates of different materials, which influences the degree of clamped constraint for each material; this does not produce a fair comparison of performance. A different approach to target support was required.

A simply supported target is practically easy to arrange and consistent between materials of different types. However, a simply supported plate is an idealized support condition that is never seen in practice on underbelly vehicle protection.

A more comparable support condition would be bearing support with fasteners in shear to retard the inward translation of the plate under general membrane action; where the fasteners are only torqued to a minimum level sufficient to hold the target in place against the bearing surface. Such an arrangement would also provide some rotation resistance at the supports. This kind of system is much closer to how the plates might actually be used in practice on the underside of a vehicle. Unfortunately, previous similar work done at the University of Sheffield had shown that in this arrangement the fasteners themselves often undergo excessive plastic deformation under the combination of axial and shear

loading, often damaging the threads. This resulted in difficulty removing the panel from the apparatus after every test.

The complications detailed above regarding various constraint approaches led to the development of a new approach to target restraint which aims to balance the need to test the targets in a comparable constraint regime to actual under vehicle protection; whilst also reducing excessive fastener deformations. The details of the final arrangement are given in Section 3.4.3.

3.3.3 Ensuring consistent loading

The original plan for the test arrangement, with respect to ensuring that the total impulse delivered to the target was consistent every test, was to maintain the vertical pendulum system and measure the imparted impulse for every test. This approach proved to have some unnecessary difficulties. First, the target size of one metre square was much larger than the targets from the previous setup. Second, the strength and thickness of the targets to be tested was much higher than the previous work meaning the total impulse required to produce significant deformations would be much higher; resulting in large vertical travel of the reaction mass beyond its maximum travel. Third, the time and expense of running the high speed video required to capture the vertical travel of the pendulum was prohibitive to the budget of the project.

The extensive set of data collected by the University of Sheffield as in Clarke et al. (2015b) shows that it is not necessary to measure the total impulse of every test to ensure consistent loading. The previous work shows that it is possible to perform buried explosive tests with a test to test total impulse variation of less than ± 3% from the average. The specific sand type, dry density and moisture content chosen was based on an analysis of the data from this previous work; ensuring that the most repeatable combination of properties was used for the tests in this project.

3.3.4 Portal frame modifications

The previous experimental campaign, which used this rigid portal frame arrangement, did not deliver all the impulse to the horizontal beam. The impulse was delivered to the reaction mass which would travel vertically arrested by gravity. Only when the imparted impulse was sufficient to translate the vertical pendulum to its maximum travel would the horizontal beam provide a downwards reaction force to arrest the reaction mass before it reached the zenith of its trajectory. The test arrangement required for this project would deliver all of the impulse to the horizontal beam. Additionally, the charge sizes were not fixed at 625 grams as in the previous work meaning that the total impulse could be higher with charges up to 1000 grams. As such, the horizontal beam was reinforced with a web-stiffened I-beam (Figure 3.3). This also had the added benefit of bringing the soffit of the horizontal member closer to the rim of the soil bin as in Figure 3.3; reducing the amount of packing needed to bring the "picture frame" down to the correct distance from the bin (Figure 3.5) (details of "picture frame" terminology found in Section 3.4.1). Using less packing plates to stand the "picture frame" down from the beam increases the stiffness and stability of the system. Detailed in Section 3.5, this stiffness and repeatable distance between the "picture frame" and the rim of the soil bin is crucial for the ease of repeatable testing.

3.3.5 Soil bin and reaction base modifications

As discussed already the attrition rates of the soil bin bases was high in the previous work. Part of the problem was the hardcore infill between the ground beams and the fact that it was not a stiff enough reaction base (Figure 3.2). Concrete could have replaced the hardcore to produce a stiffer reaction base. However, there was an ongoing requirement to be able to move the apparatus around the site where it was located and adding a non-removable concrete base would have made the rig prohibitively heavy. Also, the time scale for completion of rig modifications was not sufficient for full concrete cure.

Instead the hardcore remained a feature of the reaction base and a 100 mm thick steel plate was installed. Also, the base thickness of the soil bins was increased from 30 mm to 50 mm as can be seen in Figure 3.3 and Figure 3.4. With 150 mm of steel in total thickness below the soil in the bins, this arrangement proved to be sufficient in preventing any permanent deformation of the soil bin bases.

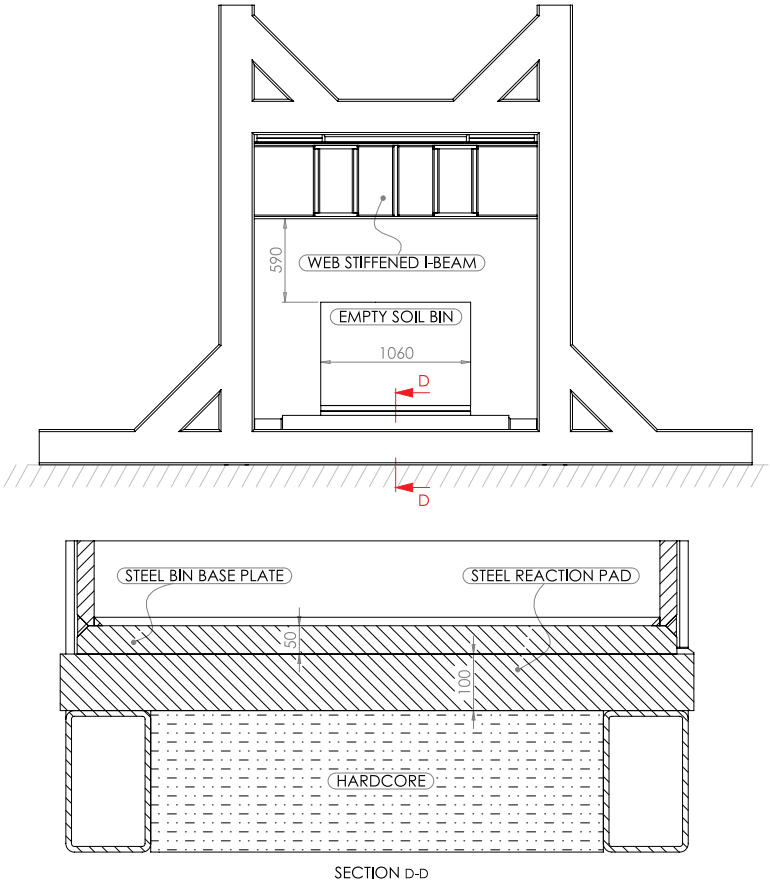

Figure 3.3: Modified frame with improved soil bin arrangement - Front view with section (mm)

Figure 3.4: Improved steel base plate

3.4 Apparatus and test arrangement detailed design

3.4.1 General apparatus arrangement and terminology

The essential modification of the HITSss apparatus from its original form was to remove the free flying mass and replace it with a stiff "picture frame" type reaction body, bearing directly against the portal frames re-purposed from the original setup as can be seen in Figures 3.5 - 3.9. The arrangement of the actual interface and fastening system between the picture frame and targets is fully detailed in Section 3.4.3. Figure 3.5 and Figure 3.8 show the location of the target interface plates in the apparatus. The target interface plates provide the reaction surface for the targets and house the fastening scheme. The interface plates are bolted to the picture frame. The picture frame is packed down from the web-stiffened I-beam section on solid steel plates and bolted through onto the bottom flange of the I-beam as can be seen in Figure 3.6 and Figure 3.7. In short, there is a stiff direct load transfer path from the reaction face of the targets to the horizontal member of the portal frame. Another important change to the soil bin arrangement was the locating stops shown in Figure 3.9.

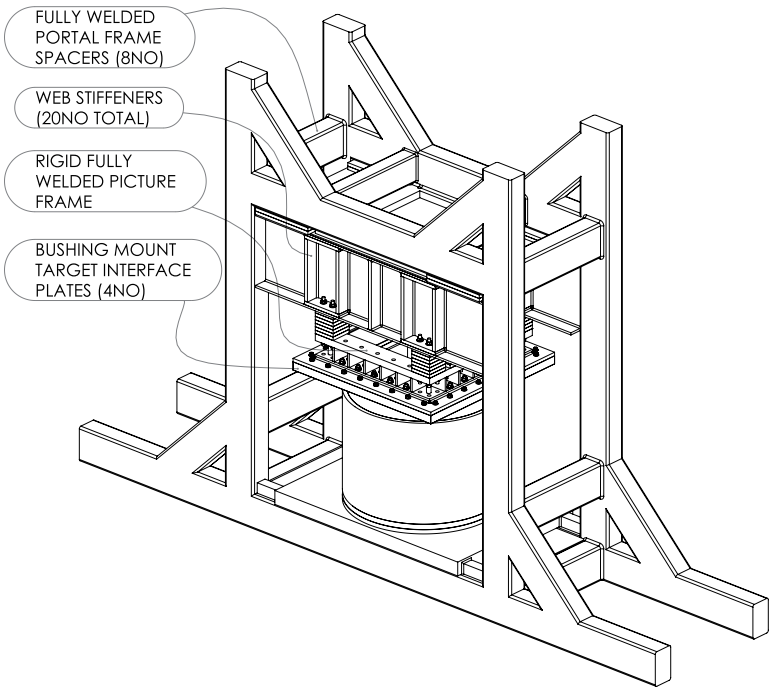

Figure 3.5: Modified frame in new Appliqué rig arrangement - Isometric View Front

Figure 3.6: Improved steel bin and picture frame with bushings

Figure 3.7: Improved steel bin and picture frame with bushings

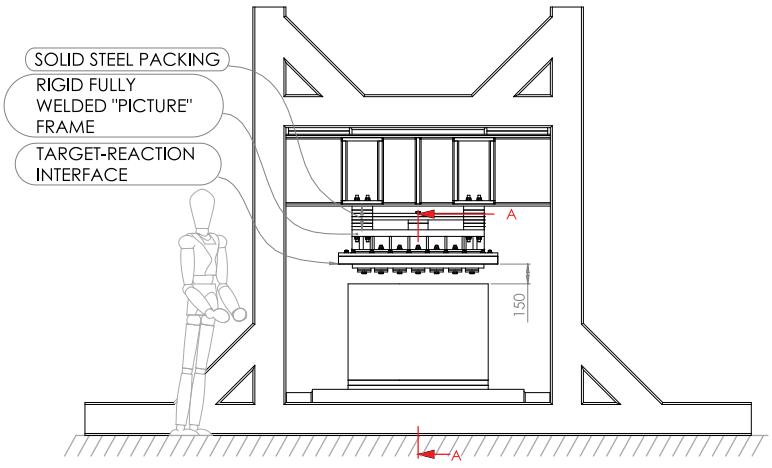

Figure 3.8: Appliqué Rig - Front View - (mm)

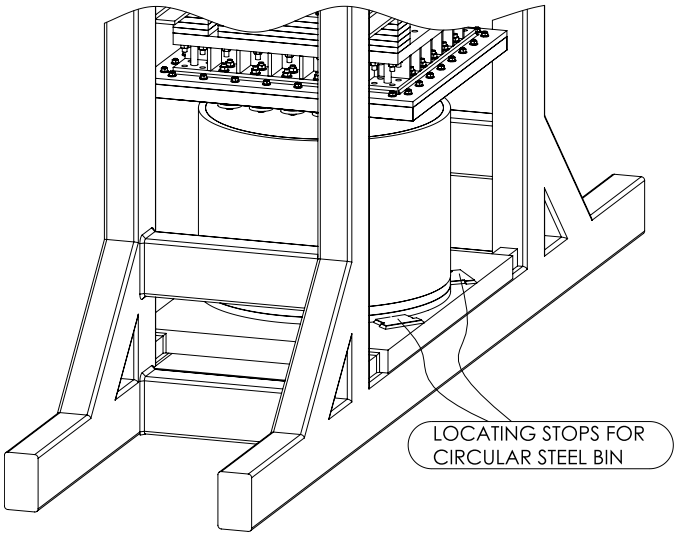

Figure 3.9: Appliqué Rig - Isometric View Back

Because the new soil bins incorporated round base plates of the same diameter as the circular hollow section they were made from, and because there was now a fixed datum of the 100mm thick steel base plate, two calibrated stops welded to the steel base could be used to quickly centre the soil bin under the target. Using a forklift the bins could be slid across the steel base until coming to rest against both stops. The addition of the locating stops eliminated the test to test possibility of human error with regards to the central location of the soil bins. Figure 3.8 shows the overall test arrangement as viewed from the front as well as the location of the section line A-A, which is shown in Figure 3.10.

3.4.2 Test layout details

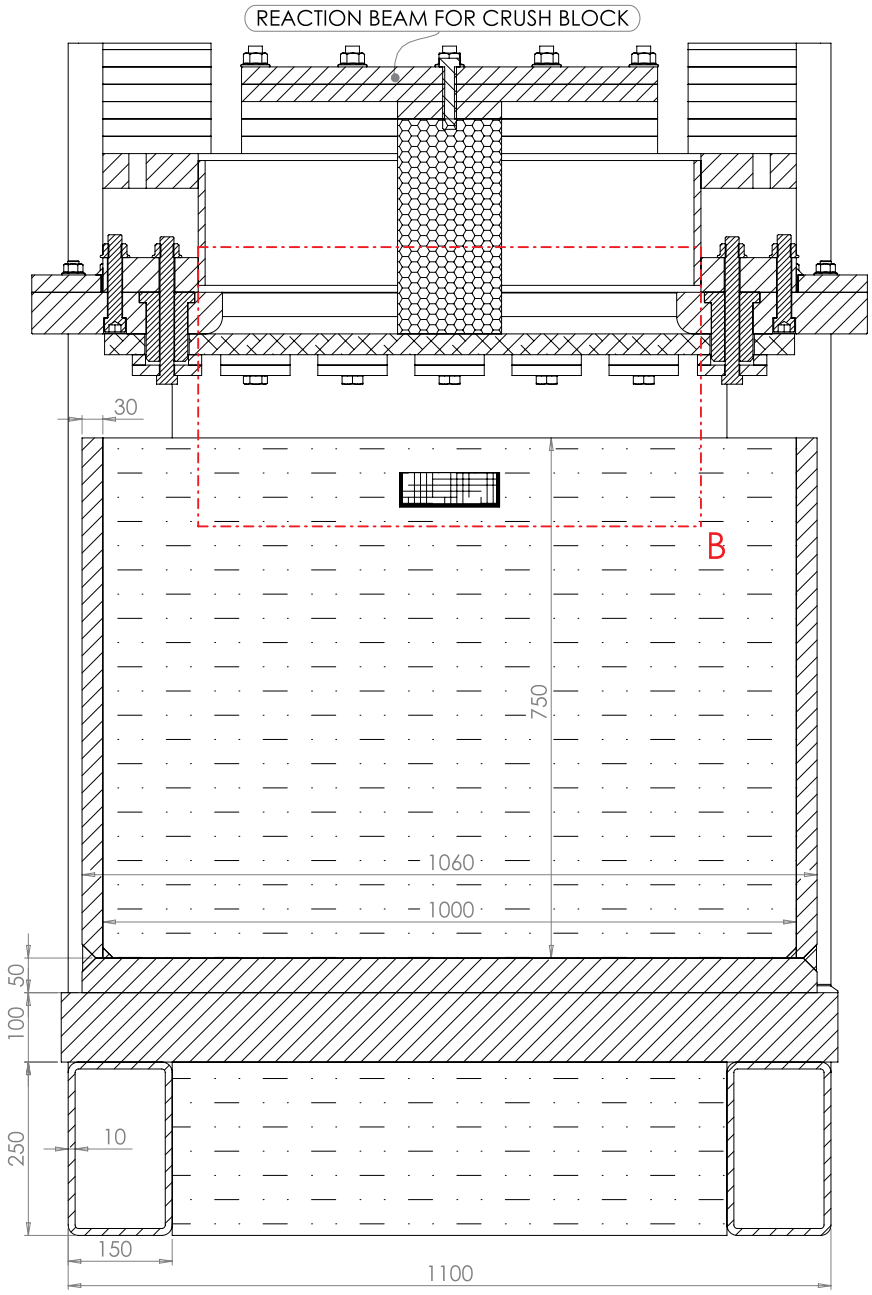

Figure 3.10: Appliqué Rig - Section A-A - (mm)

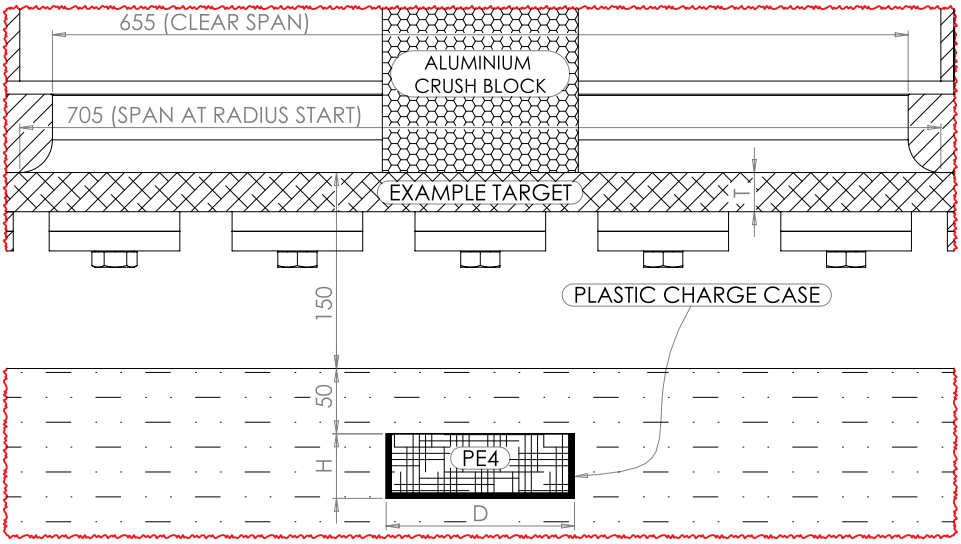

Figure 3.11: Appliqué Rig - Detail B - (mm)

The overall arrangement of the testing approach is illustrated in Figure 3.10 and Figure 3.11. Figure 3.10 shows that the targets bear against the stiff reaction surface of the interface plates and that the soil bins sit directly on the rigid datum of the 100 mm steel base. After the soil bins (6no.) were fabricated the top rim of each bin was machined parallel to the base surface also ensuring that all the bins were the same height (± 0.2 mm). When the picture frame and interface plates were installed the steel packing system down from the I-beam provided a facility to adjust the interface plates to the required distance from the rim of the steel bins (± 0.5 mm). This system of fixed steel base datum, accurate bin heights and accurate interface plate offset ensured a consistent and simple setup procedure for stand-off and charge placement. The sand in the bins could be screeded off flush with the rim of the bin and the charge could be centred and buried relative to the rim of the bin. Using the locating stops already mentioned the bin could simply be slid into place automatically aligning the charge, sand, bin and target central axis; as well ensuring the correct stand-off and parallel alignment of the sand surface and interface plates.

Figure 3.10 and Figure 3.11 show the aluminium crush block situated directly behind the target as well as the reaction beam above the crush block. This system was used to measure the peak dynamic deflection of rear face (opposite face to the blast loaded face) of the target. The maximum deflection of the target displaces the crush block which does not rebound after the test. The distance from the deformed crush block surface from original location of the

rear target face can be measured by holding a straight-edge across the interface plate and measuring between the crush block and straight edge.

The clear span of the area over which the target could deform was 655 mm (Figure 3.11). However the edge of the interface plates was radiused to avoid high sheer stress at the edge of the support leading to early failure of target.

For the purposes of this test approach it was decided that the stand-off should be measured from the rear face of the target/protection system to the surface of the sand, where the charge was always buried the same depth from the surface (Figure 3.11). The reason for this definition of stand-off was to avoid inappropriate benefit to materials/system which were less dense. If the stand-off was measured from the front face (loaded face) of the target, the rear face of less dense targets would sit further away from the charge, that is "T" would be greater for less dense materials (Figure 3.11). For systems with a sacrificial layer on the front the structural layer would be further from the charge. Furthermore, an important reason to define stand-off in this way is related to vehicle ride height. Using a less dense appliqué system would actually decrease the distance from the underside of the vehicle to the ground, unless the overall ride height was raised. Raising the ride height of an armoured military vehicle is not advisable from the perspective of the signals corps as they want the vehicle to have as low of a profile as possible. The stand-off was fixed at 150 mm from the rear face of the target to the surface of the sand.

PE4 charges were used in this test arrangement. The charges were 3:1 cylinders (3D:1H, see Figure 3.11), in open-topped 3D printed plastic cases 4 mm thick. The charges ranged in size from 600 grams to 1000 grams. The charge size was adjusted as the testing progressed to ensure appreciable deformation of the targets without causing break-through or block failure. The charges were top detonated using non-electric detonators. The burial depth for all tests was 50 mm from the sand surface to the top surface of the charge as in Figure 3.11.

3.4.3 Picture frame, bushings and target interface plates details

Figure 3.12 and Figure 3.13 show the integration of the picture frame and the interface plates which also incorporate the fastening system for the targets. As mentioned in Section 3.3.2 the intended regime for support was simple bearing of the target against the reaction face with some provision of fastening to act in shear and prevent the inwards translation of the target and provide some resistance against rotation. Figure 3.12 shows the EN24V bushings with shoulders used to provide the the lateral support (5no. on each side, 20no. in total).

These bushing were press-fit into counter bored holes in the back of the interface plates with the bushing shoulders bearing against the rim of the counter bored holes (Figure 3.12 Section F-F). Figure 3.10 shows how bolts through the bushings and washers over the bushings were used to hold the target plate against the interface plates. The M20 bolts were tightened to 35Nm, enough to ensure the target was touching the interface plate but not clamping the target against the interface plate. Section F-F shows that the end of the bushings were machined to sit slightly proud of the back of the interface plates ensuring constant pressure of the bushing shoulder against the rim of the counter bored hole when the shoulder bolts (Section E-E) and standard cap head bolts (Section F-F) attaching the interface plates to the picture frame were tightened. Shims were placed between the picture frame and interface plates the the shoulder bolt locations to ensure the interface plates would sit flat against the picture frame given the proud bushings. A Lumsden grinder was used to flatten the face of the picture frame before installing the mitred 60 mm thick S355 interface plates to ensure a planar surface for the plates to mate against. The mitred interface plate were positioned and clamped down to the picture frame using standard cap head bolts. Then, the holes for the shoulder bolts were drilled and reamed passing through the interface plates and picture frame in one operation. This ensured a slip-free connection between the interface plates and the the picture frame. All of the shear load on the bushings from the target pulling inwards under load is transferred into the interface plates. The mitred ends and the zero tolerance shoulder bolts ensured a rigid and robust housing for the bushings. The essential rationale for the bushings was a system of fixed bearing studs that would take all the shear loading without any plastic deformation and the actual bolts used would only have to resist the axial loads required to prevent target rotation (lifting off the bushings). This system has worked well with no attrition of the bushings or interface plates after dozens of tests. Depending on the thickness of the targets more or less washers were used to protrude above the bushing and allow the targets to be held against the interface plates.

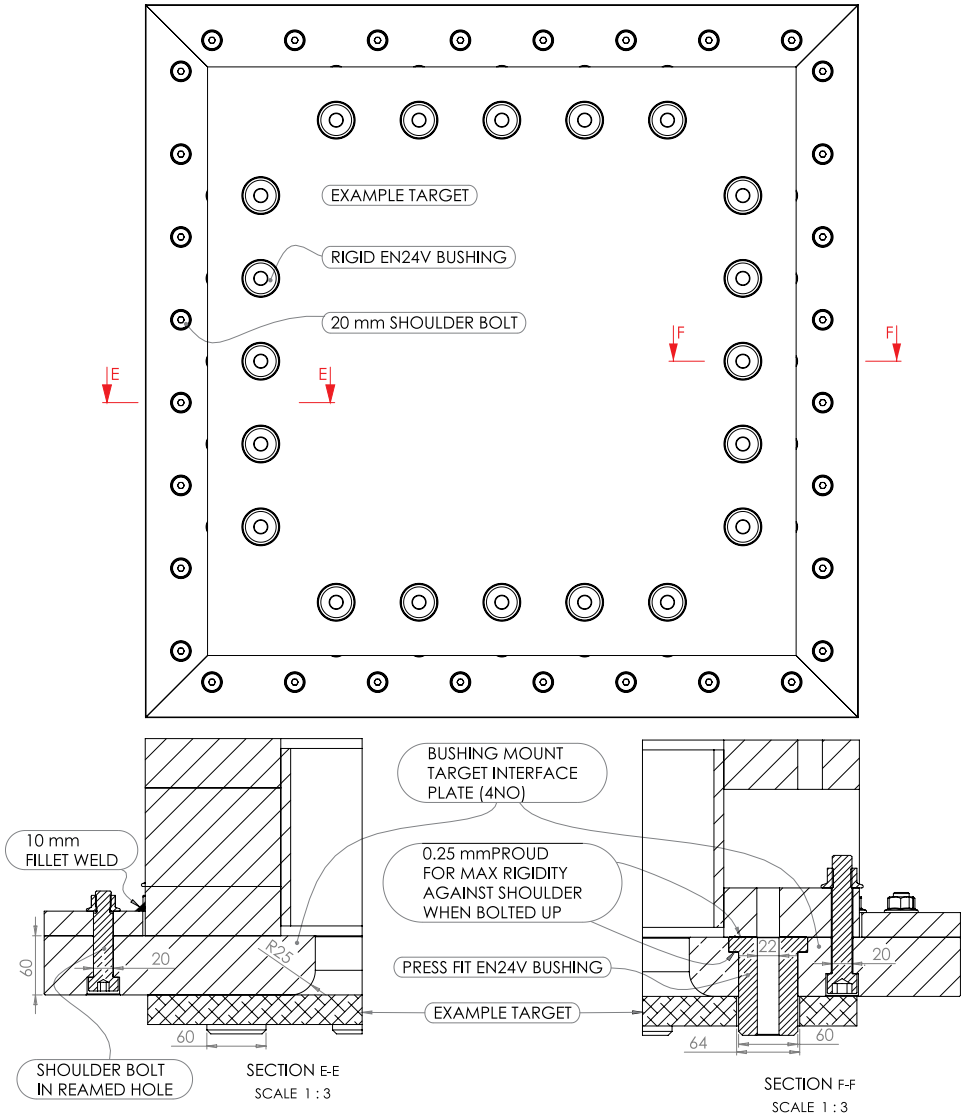

Figure 3.12: Bushing Mount Target Interface Plate Detail (mm)

3.4.4 Target hole layout

Figure 3.13 rigid picture frame layout and the bushing arrangement. When choosing the size, number and location of the bushings/holes there were several factors to consider. The diameter of the bushings was 60 mm and the diameter of the holes in the targets was 64 mm. Oversized holes in the targets was simply a pragmatic approach to ensure easy insertion of the targets onto the rigid bushings.

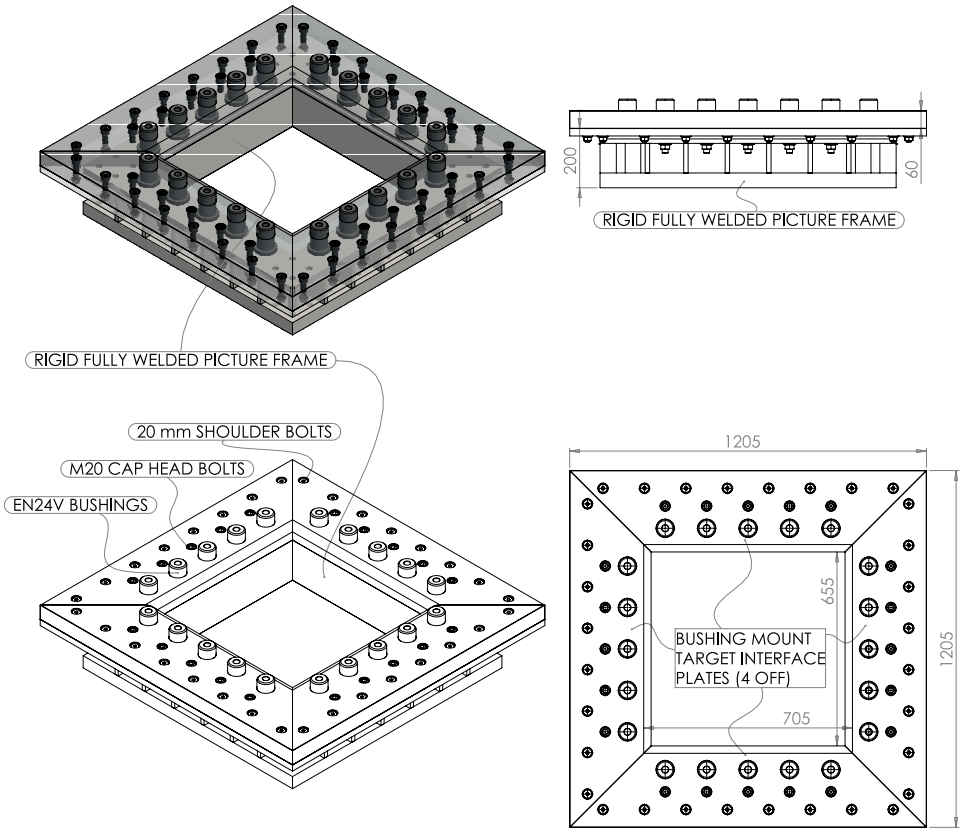

Figure 3.13: Rigid Picture frame with interface plates and bushings (mm)

Figure 3.14 illustrates the three failure modes of the target that were considered as well as how the capacity of the target against these failure modes would change by moving, re-sizing or increasing the number of bushings.

First, reducing the total amount of material between the fasteners reduces the total tension capacity of that side of the target (Figure 3.14, tension failure).

Second, increasing the size of a bushing would increase the bearing capacity of that bushing, but given the fixed span requirement, it would also reduce the distance to the edge and the cross sectional area left between the bushings. Increasing the number of bushings would not reduce the distance to the edge of the target but would reduce the cross sectional area left between the bushings (Figure 3.14, bearing failure).

Third, the bushings needed to be robustly mounted in the interface plates, whilst being as far from the edge as possible to prevent block shear failure (Figure 3.14, shear failure). Increasing the bushing distance from the edge increases the shear

capacity of the target for that bushing. The minimum span requirement of 650 mm was the controlling factor for any bushing size in terms of the distance from the edge of the target (they could only be moved in so far).

SCI Simple joints to Eurocode 3 was used as a simplified static analysis approach to calculating the shear, bearing and tension capacity for one side of a target (Assuming S355 steel as the material). The size, number and spacing of the bushings was adjusted to balance the calculated capacities of shear, bearing and tension capacity. The basic objective was to prevent one particular failure mode (associated with the fixing arrangement) from dominating and causing premature failure of the target or excessive deformations not indicative of the material, but of the fixing arrangement. As will be shown in the results section this approach proved to be very effective; with no targets of any material failing at the supports. Although after testing some targets did show signs of plastic shear and bearing deformation around the bushing holes.

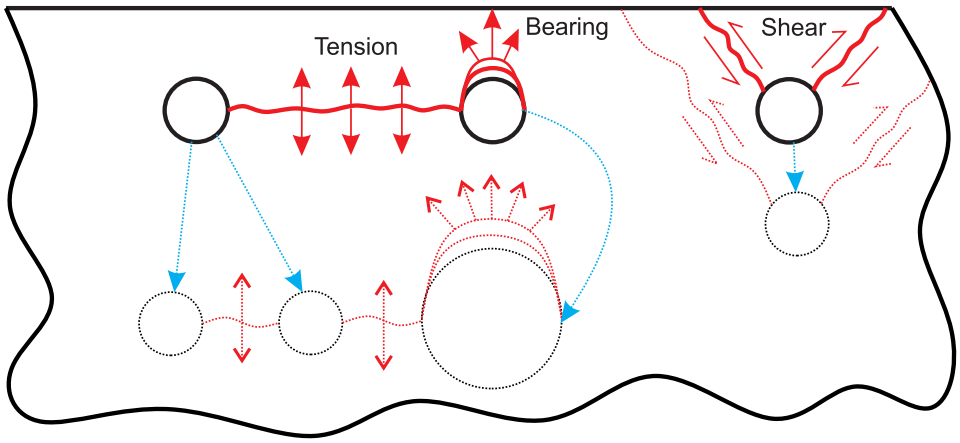

Figure 3.14: Example of target edge, the effect of hole size and spacing on three different failure modes; tension, bearing and shear

Figure 3.15 shows the final target size and hole layout corresponding to the bushing locations. Figures 3.16 and 3.17 are picture of the full as built Appliqué apparatus in use.

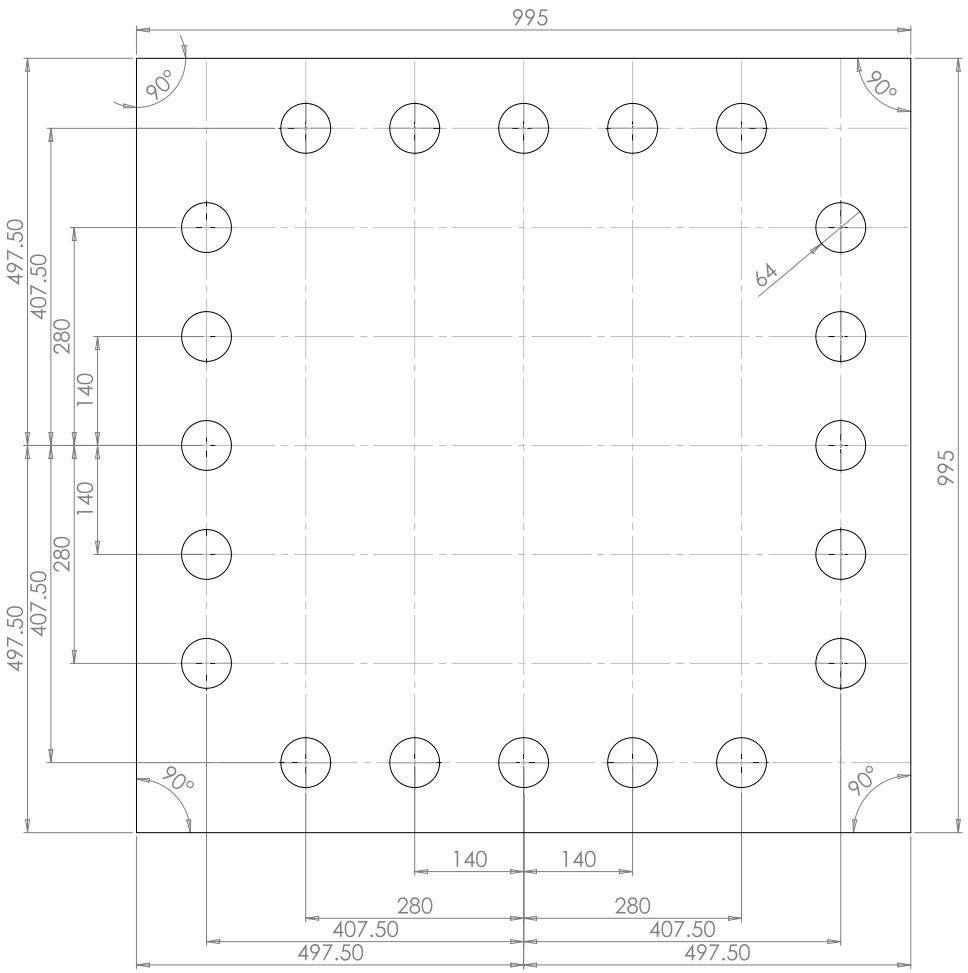

Figure 3.15: Hole layout details for targets

Figure 3.16: As built picture of Appliqué apparatus

Figure 3.17: As built picture of Appliqué apparatus mounting bushings

3.5 Test protocol

3.5.1 Overview

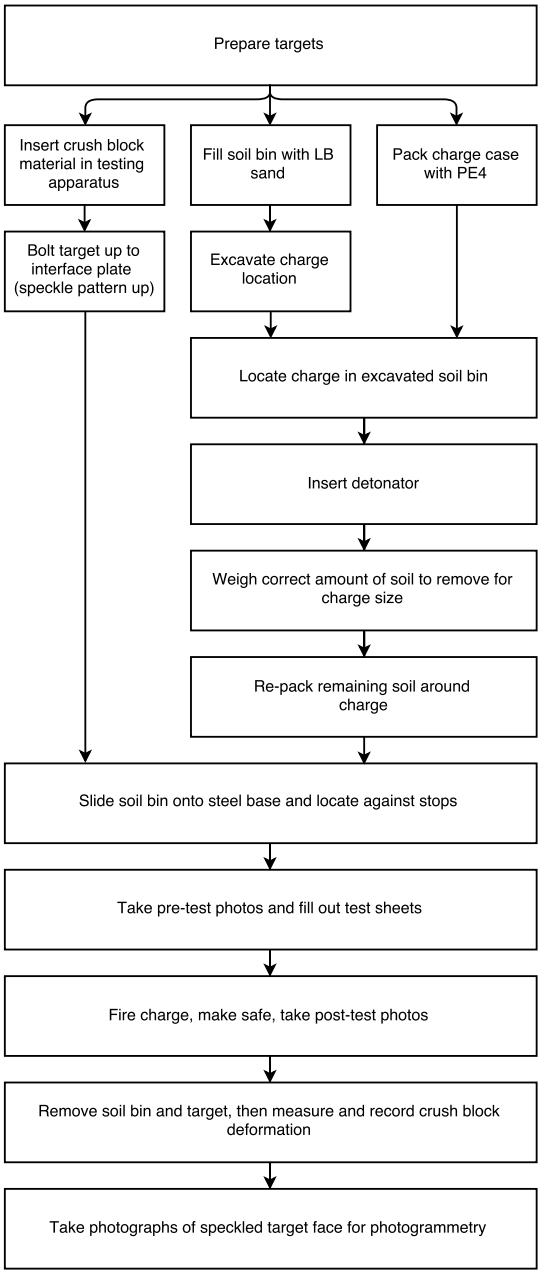

Figure 3.18: Flow chart of test protocol

As with the design of the testing apparatus the test protocol draws on previous work, discarding and retaining the different aspects as appropriate given the new test requirements and the opportunity to learn from past mistakes. Figure 3.18 details the overall order of operations for the test procedure. (Figure 3.18 does not provide every detailed step and does not include all the safety protocols needed for safe experimentation with explosives)

3.5.2 Target preparation

Various materials were allocated by Dstl for testing, including but not limited to various grades of steel, aluminium and titanium. Some grades of steel and titanium can be very difficult to drill/machine, increasing the cost to produce the targets from plate stock. Water jet cutting is a cost effective and suitably accurate method to cut the target plates to size and cut the holes in one operation. Also, using a water jet cutting machine as opposed to a laser cutting machine ensures that the material properties of the targets will not suffer from heat affected changes near the cut/hole locations.

After water jet cutting the targets were painted white on one side in preparation for a black speckle pattern. Etch primer was used to paint the targets white as well as the black speckle pattern. Etch primer adheres well to a wide range of materials, dries quickly, and can be applied very thinly. Thin paint layers with good adhesion prevent excessive paint spalling that can occur when blast testing.

The speckle pattern stencilled onto the targets was used to improve the effectiveness and accuracy of the photogrammetry technique employed for the purposes of residual plate deformation measurement. Photogrammetry is the technique of using photos of an object or environment in an algorithm which determines unique points that appear in more than one image as well as determining the location in space relative to the images that the camera must have been positioned. From this information a point cloud is generated mapping the surfaces in the pictures. A surface with very little contrast and detail will not provide the algorithm with a sufficient number of such unique points. MATLAB was used to generate a random pattern of markers consisting of an even distribution of triangles, squares, circles and diamonds. The location and size of any marker was random (Figure 3.19). This speckle pattern was scaled to 995 × 995 mm and laser cut from thin steel sheet to used as the stencil for the black pattern on every target. Using a stencil and a HVLP sprayer is a much quicker way of producing consistent patterns for increased detail and high contrast than other

methods which rely on manually speckling the target with paint. The MATLAB script used for the speckle pattern is provided in Appendix B.

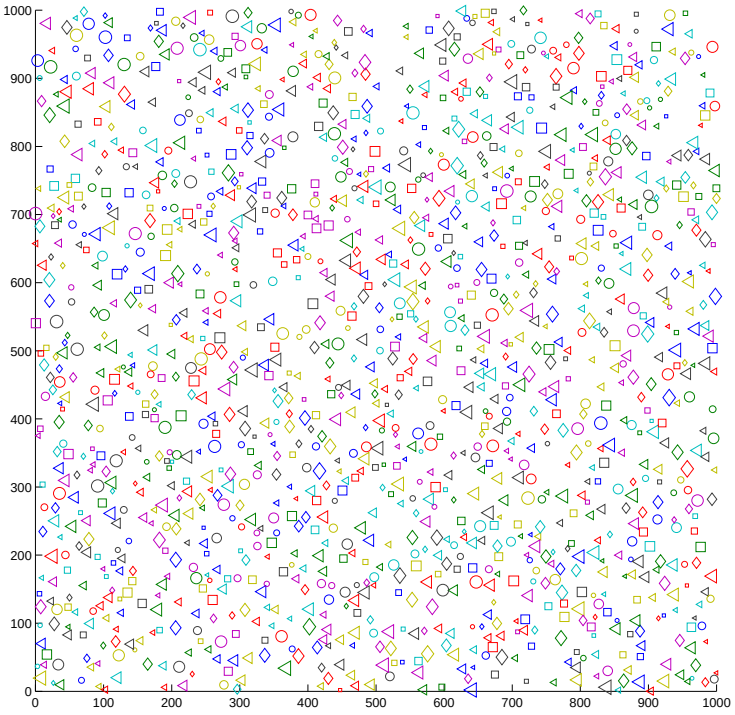

Figure 3.19: Target speckle pattern generated in MATLAB

3.5.3 Soil bin preparation

The methodology for bin preparation and the control of geotechnical conditions was largely informed by previous testing done by the University of Sheffield for buried explosives, such as in the work by Clarke et al. (2011).

There is one deviation from Clarke et al. (2011) for the soil bin preparation in this test approach that is important to mention; the addition of a cardboard based energy dissipating material in the base of the soil bin. Three layers of 18 mm thick Dufaylite Ultra Board were cut to size and placed in the base of the soil bin and then covered with plastic sheet to protect the cardboard from moisture. The reason for this addition was to further protect the base of the soil bin from plastic deformation. This addition in combination with the redesigned reaction base and soil bin has been completely effective in preventing any permanent deformation of the 6 soil bins after more than 60 tests in total. Soil bin base deformation was a significant difficultly in previous testing as highlighted in Section 3.2.2. Once the ultra board was placed in the bin the soil filling process could begin. Adding this layer of energy dissipating material to the base of the bins would of course effect the way shock waves in the soil are reflected in the base of the bin. However, because the soil bins are 750 mm deep and the stand-off to the target surface it always less than 150 mm, by the time any reflected shock has travelled back up to the surface of the soil the rest of the loading would be over; as such, it is not considered to have any significant effect on target deformation. Whatever effect the ultra board might possibly have on target loading would be the same for every target, still ensuring consistent test to test loading. Protecting the soil bins from plastic deformation ensures consistent stand-off test to test; which is far more important than whether the softer reflection in the base of the bin has a small effect on late time target loading.

If possible in future testing, and if total impulse is being measured, it would be interesting to test several bins without the ultra board and several with the ultra board to determine if total imparted impulse is effected by the ultra board in the base of the bin. Also, it would be useful to fire one bin with several shots (not at a target) without the board to see if the bins remain un-deformed without any board in the base; perhaps it is an unnecessary precaution.

In order to produce repeatable loading on the target plates the dry density and moisture content of the Leighton Buzzard 14/25 sand used had to be consistent test to test and uniformly distributed through the entire soil bed for every test. The design moisture content for the soil bins was chosen such that none of the

sand from the supplier would already be at a moisture content higher than the design moisture content. Drying sand is expensive and time consuming, it is much more practical to simply add more water to bring it up specification. This of course assumes that the target moisture content is actually possible to achieve without water settling in the soil bin base over time. For this test procedure a moisture content of 5% by mass was used.

The other consideration for soil conditions is the dry density. If the design dry density of the soil in the bin is too low, any movement of the bin will cause the soil to further self compact after controlled preparation. If the design dry density is too high the process of compacting the soil in the bin becomes necessarily laborious. For this test procedure a design dry density of 1620 kg/m^3 was chosen.

The procedure for soil control and placement is detailed below:

1. Calculate the total volume of the soil bin minus the ultra board
2. Calculate the mass of sand required to fill this volume with sand of required dry density and moisture content
3. Fill mixer with a known mass of sand and mix till all moisture is uniformly distributed (the mixer used in this test procedure help approximately 1/3 of the total mass needed to fill the bin)
4. Check the moisture content of the sand in the mixer and calculate how much more water is needed to bring the moisture content up to the target percentage
5. Add the correct water volume to the sand and re-mix to ensure the water is evenly distributed
6. Place homogenized sand of the required moisture content and mass into the soil bin (for the bin size in this testing, the soil was placed in 3 lifts to ensure uniform compaction through the depth)
7. Level the sand and measure the height in naturally occupies in the bin
8. Calculate how far the soil needs to compress downwards from its position to achieve the target bulk density
9. Use a stiff, heavy, flat, circular, steel load spreader which just fits inside the soil bin and compact the soil downwards by hitting the load spreader with a sledge hammer until the correct soil height is achieved. The soil

must be level at the start of the process and the hammer blows must be evenly distributed to ensure level compaction of the bin. Additionally, measurements are taken from several locations and then averaged when checking the height of the soil to account for any none level compaction that does occur.

10. Repeat sand mixing, moisture content control, weighing and placement two more times (steps 3-8)

11. On the last lift when the sand is compacted to the correct bulk density the surface of the sand will be flush with the rim of the bin

12. Use a straight edge to ensure the surface of the sand is perfectly flat across the rim

13. Immediately seal the soil bin with plastic to ensure the moisture content conditions does not change before testing (remove just before charge placement and firing)

3.5.4 Photogrammetry method for residual deformations

From Barr and Fuller (2018), "Full-field residual deflection measurements were taken over the top surface of the tested plates by generating a 3D model using a photogrammetric technique. For each plate 16 photographs were processed into a point cloud using VisualSFM, as shown in Figure 3.20. This point cloud was then scaled to real world units in MeshLab using the length of the plate edge, and aligned to a Cartesian coordinate system so that:

a) the floor was parallel to the $x - y$ plane;

b) the original top surface of the plate was centred on the origin; and

c) deflections occurred in the positive z direction.

In plates where the edges were also significantly deformed, the corners of the top surface of the plate were used as the datum for the z axis: this is noted where appropriate. MATLAB was used to mesh the point cloud to a 10 mm grid, which is represented through plans and sections in Chapter 4.

In the source photographs the average pixel represents a length of approximately 2.5 mm, and the plate edge can be identified in the point cloud within

approximately 5 mm: on a 995 mm plate this corresponds to a scaling error of ±1.5% on the deflection measurements.

Peak deflection measurements were taken at the centre of each plate using the deformation of aluminium crush blocks."

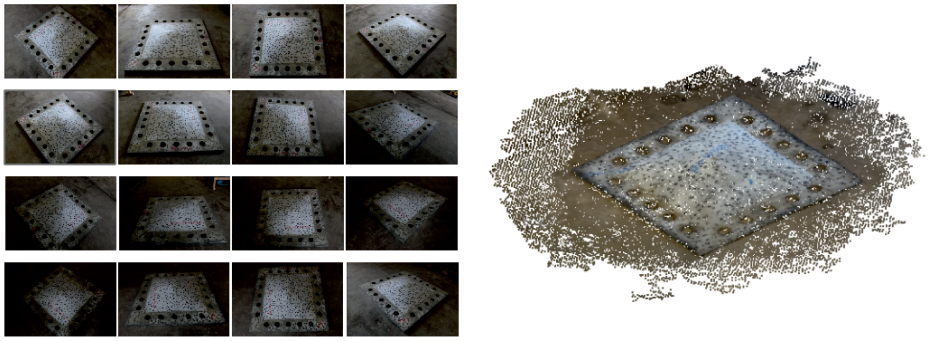

Figure 3.20: Example of 3D point cloud generated from 16 plate photographs - Barr and Fuller (2018)

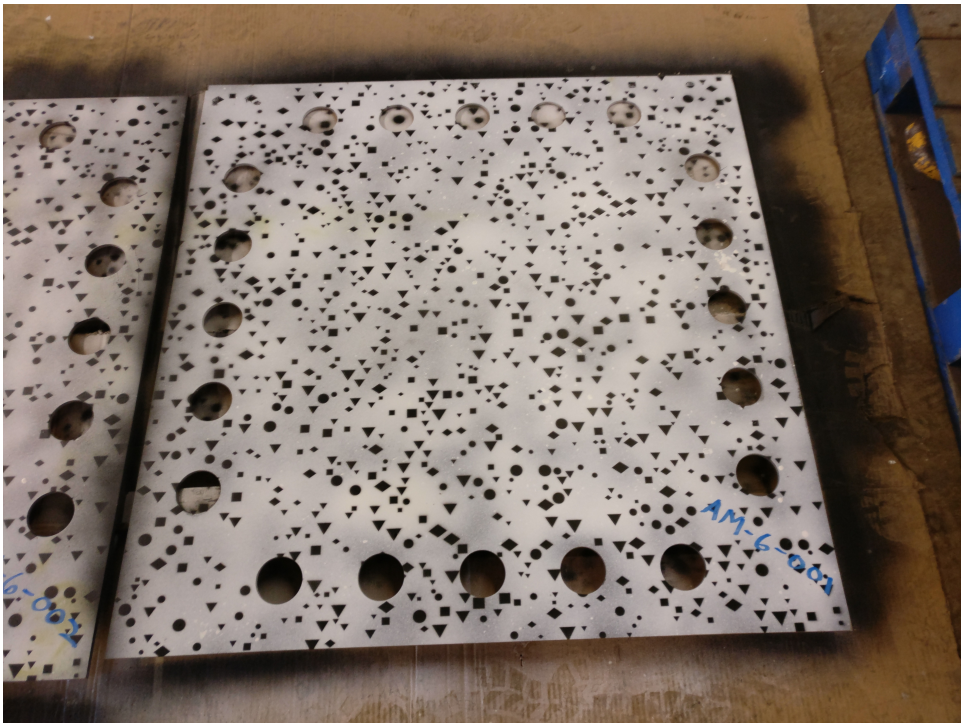

Figure 3.21: Example of target with speckle pattern before firing

3.6 Chapter summary and test program

Existing literature and previous work at the University of Sheffield was used to define the requirements and develop the concept for a new testing apparatus. The authors own engineering calculations, engineering experience and an in-depth understanding of the research aims was used to perform the detailed design, produce the engineering drawings, sub-contract component machining and personally construct and fabricate the testing apparatus in-situ.

The experimental approach was developed based on the aims of the research; i.e. to investigate whether knowledge of the distribution of impulse from a buried blast event can be used to predict target deformation without any FE modelling of the target or any numerical modelling of the blast event. For different target spans, thickness, materials and total impulse values. As such the 3 different charge sizes were used (giving different total impulses), 4 different thicknesses of Armox 440T were tested, all for the same burial depth and aspect ratio of the charge. As will be detailed in Section 4, using the charge sizes based around previous work allowed the loading for each test to be calculated individually. Table 4.1 details the full list of the tests presented in this thesis.

Chapter 4

Results and analysis

4.1 Overview of results

Twenty-one test results are presented in this thesis. These are all the tests using a single layer of Armox 440T steel; 3 Armox 440T tests were omitted from the results because the plates exhibited gross failure as a result of overloading. These failures occurred when the charge weight assessments were being conducted at the start of the series to determine what charge sizes would produce reasonable deformations. Figure 4.1 is an example of a post test target.

Figure 4.1: Example of target deformation on impact face after firing

Overall more than 70 tests have been completed to date for other materials and layered systems than Armox 440T. Only the results from Armox 440T are presented here because the author does not have permission to publish any of the other results.

Table 4.1 provides the basic information about the initial conditions for each of the 21 tests presented, as well as the basic test results, in tabular form.

Test	Thickness (mm)	Weight (grams)	Dynamic (mm)	Residual(mm)
1	6.27	800	134	102.3
2	6.22	400	67	50.1
3	6.45	600	95	78
4	8.41	800	79	71.2
5	8.47	800	84	72.9
6	8.36	800	102	73.8
7	8.45	1000	112	92.5
8	8.43	1000	111	85.8
9	8.4	1000	122	94.1
10	10.13	800	73	56.8
11	10.21	800	85	56.9
12	10.23	800	85	57.7
13	10.55	1000	101	74.1
14	10.3	1000	112	71.8
15	10.31	1000	99	72.2
16	12.31	800	79	49.4
17	12.41	800	66	50
18	12.38	800	75	48.9
19	12.3	1000	95	62.4
20	12.26	1000	95	63.8
21	12.36	1000	92	62.2

Table 4.1: Test results matrix with average target thickness, charge weight, central peak dynamic deflection, and central peak residual deflection

Figures 4.2 and 4.3 show how deflection changes with target thickness for different charge sizes, for both residual and dynamic deflection.

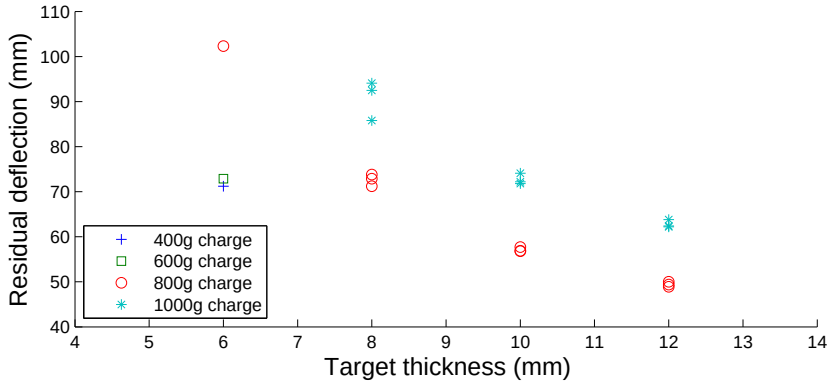

Figure 4.2: Target thickness plotted against peak central residual deflection for different charge sizes

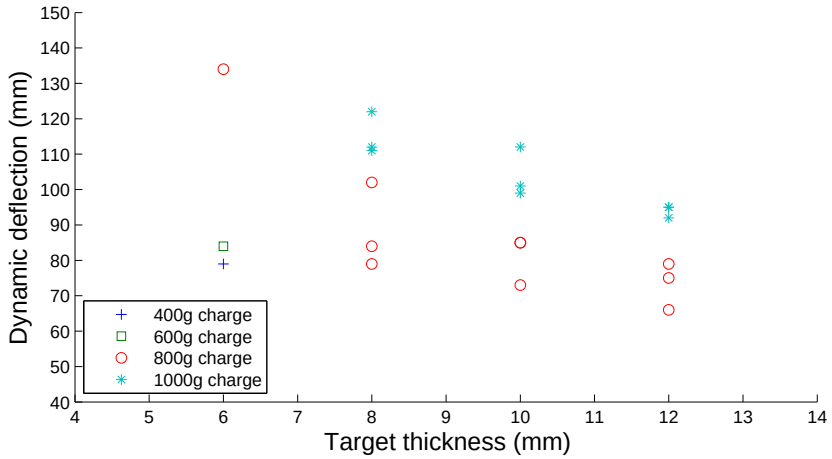

Figure 4.3: Target thickness plotted against peak central dynamic deflection for different charge sizes

Figure 4.4 is an example of the residual deformation profile plots produce for every tests from the photogrammetry data, the plots for the other tests can be found in Appendix A.

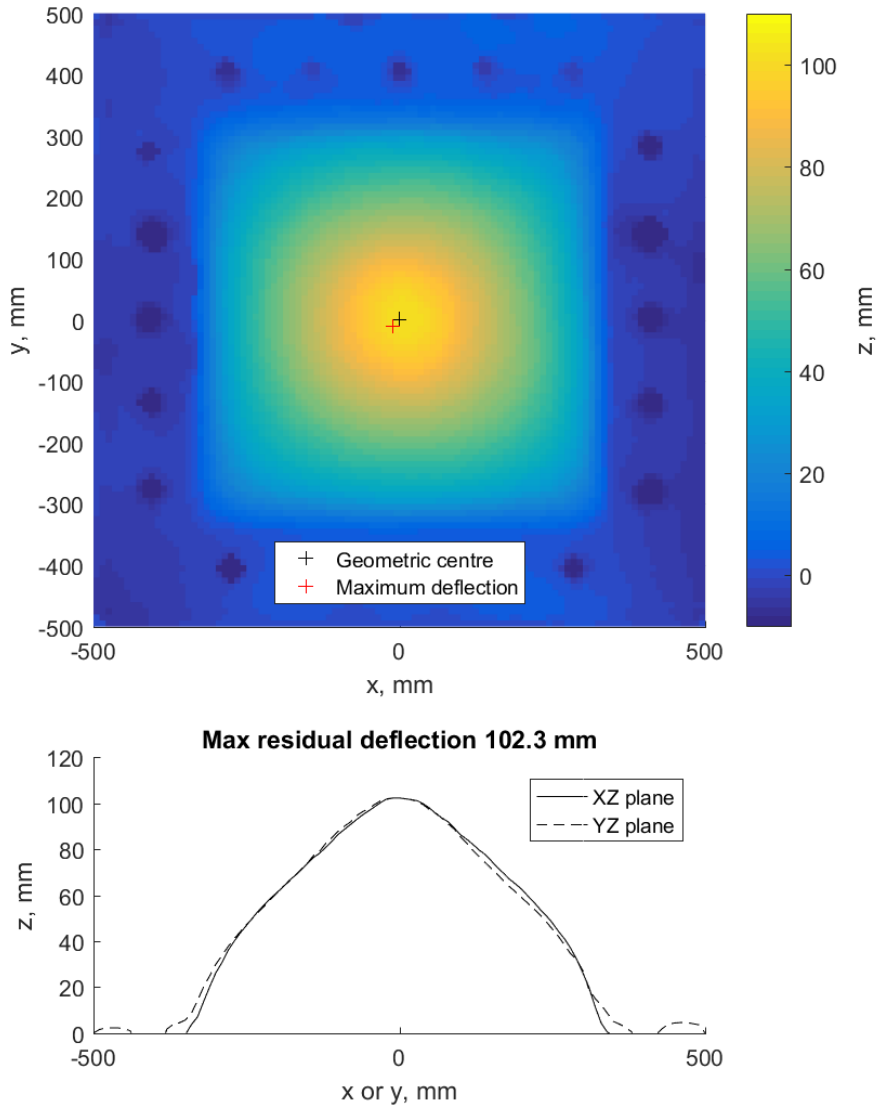

Figure 4.4: Deformation profile for Test 1, target no. AM-06-004, plan view (top) and central section views (bottom)

4.2 Introduction to analysis

The test series undertaken in this thesis was initially intended to serve solely as a benchmark data set by which to compare the performance of other materials and protective systems against a well characterised buried blast event. However, by incorporating information regarding the loading from the research published by the University of Sheffield, briefly described in Section 2.8, the results can be used to understand more about how the loading from buried blast events effects target deformation.

4.3 Loading

Combining Westine's model of scaled impulse against scaled distance with the experimental data produced by the University of Sheffield leads to a powerful resource for predicting the loading delivered to a target by a buried blast event. Given any soil condition for which the reflected pressure distribution test was performed, the distribution of impulse is known. The distribution can be used to calibrate the shape of Westine's model. The model can then be scaled to produce the correct total impulse, over the area of the target in consideration, according to the total impulse data produced by the tests with a vertical pendulum. In this way, for 5 different soil types, for the full range of probable moisture contents and densities, both the total impulse and distribution of impulse can be predicted with reasonable accuracy, especially between 1/4 and 1/2 scale STANAG 4569. Although the duration of loading is well characterised for the 1/4 scale tests from the pressure traces, the duration of the loading from the 1/2 scale tests was not directly measured.

Westine's model for scaled impulse against scaled distance, across the target face, is capable of representing the loading from a given buried blast event accurately; however, because the geotechnical conditions were not individually considered in his analysis and were not well controlled, the model describes a broad trend rather than the trend of one specific soil condition. The soil conditions used for the testing in this work have already been characterised in terms of total impulse at 1/2 scale STANAG 4569 NATO (2006) and in terms of the distribution of impulse at 1/4 scale. Using these load characterisations allows Westine's model to be calibrated to the specific soil conditions employed in the tests shown here. The process of load characterisation, beginning with the calibration of Westine's model, is shown in Figure 4.5.

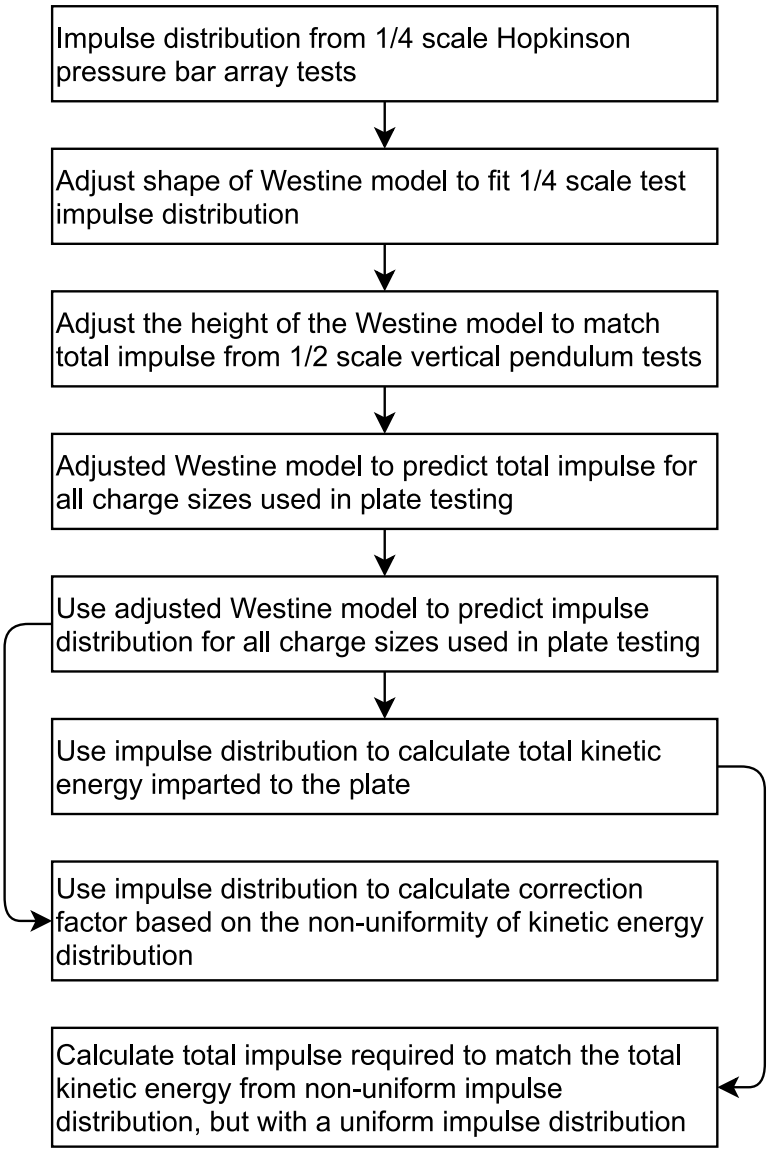

Figure 4.5: Flow chart of load prediction and analysis using University of Sheffield test data in combination with Westine's normalized load prediction model

In this way the total impulse, the distribution of impulse, the total kinetic energy and the distribution of kinetic energy imparted to the target in each test can be calculated.

As shown in Figure 4.6 the results from the 1/4 scale testing at the University of Sheffield define different curves for different soil conditions, which sit inside the Westine model space but offer a higher degree of correlation to the unique line they describe. Although the data points are not shown here, Westine's model only encompassed his data points if it was divided and multiplied by 1.8, and even then several of the results were still outside the bounds. In order to be able to predict the total impulse measured in the 1/2 scale experiments Westine's model needed to be further calibrated in terms of the vertical height of the curve. This is likely due to some differences in scaled target size vs instrumented area between the 1/4 scale and 1/2 scale testing. Once the Westine model was adjusted to match the available test data for the soil conditions used in this test series, the model was used to predict the loading for all the charge sizes and test arrangements in the series as shown in Table 4.2.

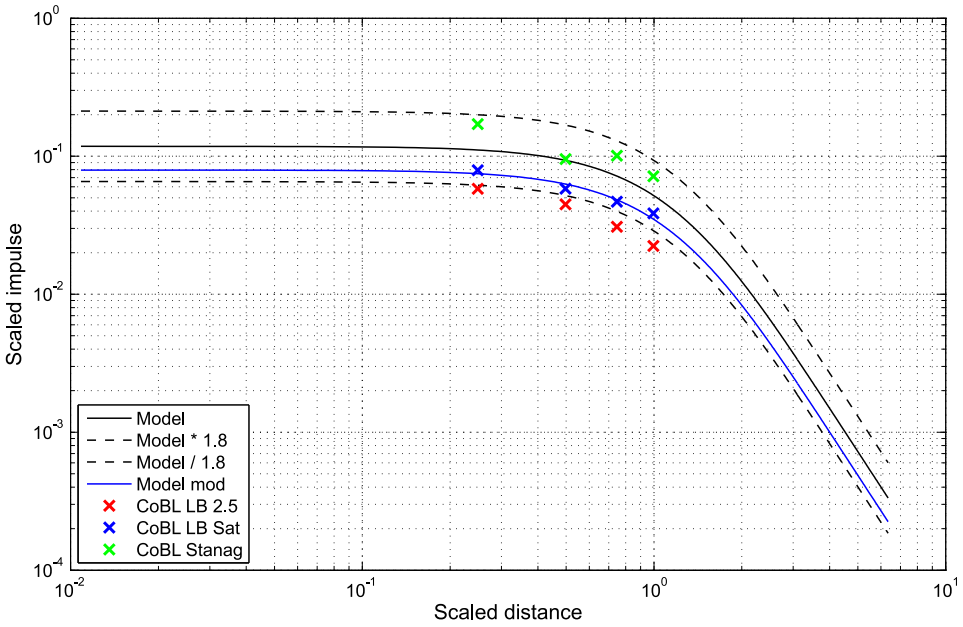

Figure 4.6: Westine normalized data and model with data from the University of Sheffield (CoBL LB 2.5, CoBL LB Sat, and CoBL Stanag; names of different soil conditions)

Test number	Charge weight (g)	Calculated impulse (Ns)	Kinetic energy (kJ)	Equivalent impulse (Ns)
1	800	3742	416	4411
2	400	2065	148	2632
3	600	2934	271	3564
4	800	3763	316	4437
5	800	3763	316	4437
6	800	3763	316	4437
7	1000	4526	438	5227
8	1000	4526	438	5227
9	1000	4526	438	5227
10	800	3784	255	4463
11	800	3784	255	4463
12	800	3784	255	4463
13	1000	4551	354	5257
14	1000	4551	354	5257
15	1000	4551	354	5257
16	800	3805	215	4490
17	800	3805	215	4490
18	800	3805	215	4490
19	1000	4576	299	5288
20	1000	4576	299	5288
21	1000	4576	299	5288

Table 4.2: Impulse values as calculated by adjusted Westine model with kinetic energy equivalent uniform impulse values

Table 4.2 details the kinetic energy applied to the deformable area of the target as well as the "equivalent impulse". Because the distribution of impulse delivered to the target is known, the distribution of kinetic energy applied to the target can be calculated as well by assuming that the loading is impulsive and using impulse to calculate initial velocity for any discrete area defined across the plate. The MATLAB script that was used to implement the Westine model takes advantage of the quarter symmetry of the targets and calculates the specific impulse for a discrete square grid over one quarter of the target. The square grid was 1000 × 1000 divisions. As such, for every discretized mass across the target the imparted impulse and kinetic energy was calculated. Integrating the kinetic energy over the whole area of the plate gives the total kinetic energy.

Because kinetic energy is proportional to the square of velocity, a non-uniform distribution of impulse will impart more total kinetic energy to a target than a uniform distribution of the same total impulse, as demonstrated by Tyas and Pope (2003). Figure 4.8 demonstrates this effect with an illustration and several example calculations (shown on the next page due to size). Using Test 1 as an example, if the impulse was assumed to be uniformly distributed the KE delivered to the deformable area of the target would be 288 kJ whereas the actual kinetic energy applied by the distributed impulse is 44% higher, at 416 kJ. The demonstration of the difference in kinetic energy for uniform and distributed impulses in shown here because the kinetic energy information is integral to the analysis in Section 4.5.

As early as 1989 Nurick was employing an analysis approach which used a normalised impulse and a normalised deflection to interpret central deflection data for air blast testing of thin targets Nurick and Martin (1989). In theory this approach would bring all the data from different tests using different target material, different total impulse values, and different plate thicknesses all onto one line which could be used to predict the central deflection of a target given a total impulse, as shown in Figure 4.7. As will be shown in the next section, Nurick's analysis was balancing the applied kinetic energy against the membrane strain energy developed in the targets.

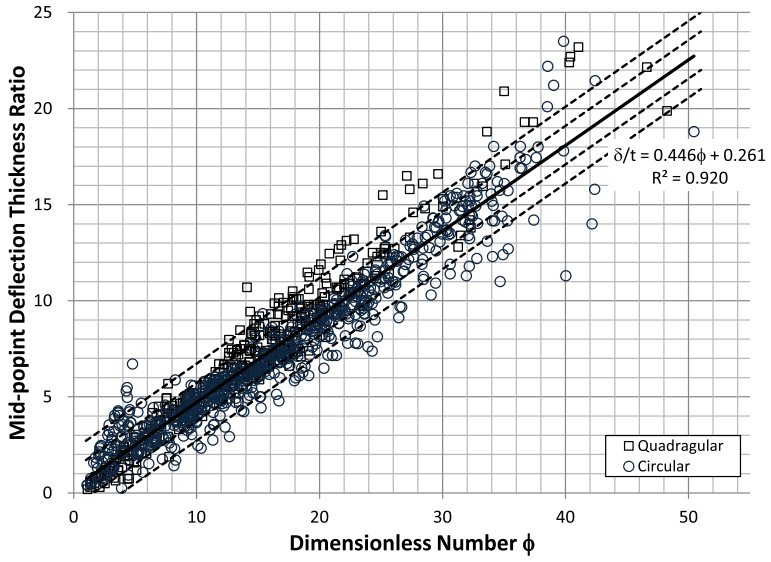

Figure 4.7: "Graph of displacement-thickness ratio versus non-dimensional impulse for the combined circular and quadrangular plate data, both pre-1989 and post 1989." Chung Kim Yuen et al. (2016) The "Dimensionless Number" used is the same as normalized impulse in this thesis

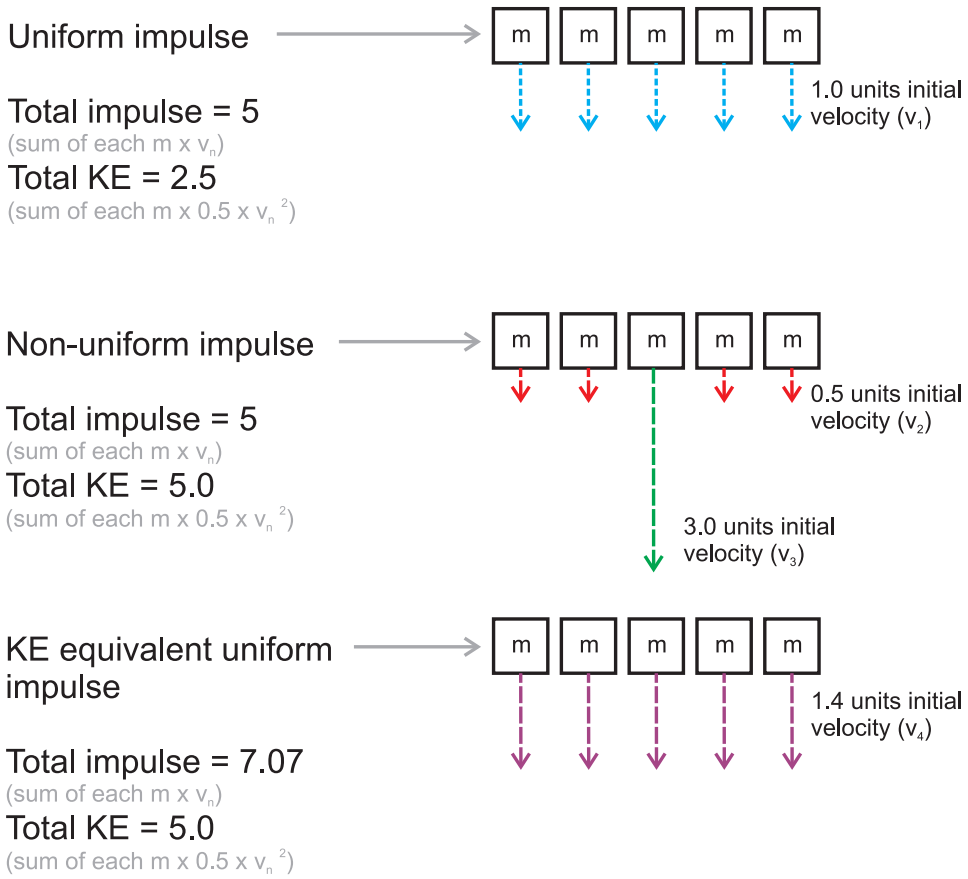

Figure 4.8: Example calculations demonstrating the difference in kinetic energy (KE) uptake, for impulsively loaded targets with different distributions of impulse; assuming discretely lumped masses (m)

4.4 Nurick Analysis

Nurick normalized the deflection by dividing by the plate thickness as in Equation 4.1 and the impulse was normalized according to Equation 4.2 where:

I_N = Normalized impulse
I = Total impulse
M_P = Mass of plate
t_p = Plate thickness
B_p = Plate breadth
L_p = Plate length
ρ = Material density
δ = Deflection
δ_N = Normalized deflection
σ = Material yield stress

$$\delta_N = \frac{\delta}{t_p} \tag{4.1}$$

$$I_N = \frac{I}{2t_p^2\sqrt{(B_P L_P \rho \sigma)}} \tag{4.2}$$

Nurick's normalized analysis approach relies on several assumptions; first, that the load is actually impulsive. Second, that the target is fully clamped at the perimeter, with no slippage to release deformation other than through membrane strain. Cloete and Nurick (2014) showed that apart from at very small deformations the contribution of bending resistance is negligible relative to the contribution of membrane resistance to resist deformation. Third, given that only the residual deformation of the target was being measured, the implication is that the percentage difference between the dynamic deformation and residual is very small. Given that Nurick's tests involved thin mild steel and aluminium plates which over relatively large spans would have very little elastic spring back, following large plastic deformation, this is an appropriate assumption. Initially the test data analysed with this approach was from experiments which applied a uniformly distributed impulse to the target. The equation of

the line for quadrangular plates in the normalized approach proposed by Nurick is given by Equation 4.3. This line was determined for plates with uniformly distributed loads.

$$\delta_N = (0.471 \times I_N) + 0.001 \tag{4.3}$$

Further testing by Nurick using concentrated loads showed that using the normalised analysis approach was effective for concentrated loads, still bringing results onto one straight line; however, the line had a different slope and a correction factor was used to bring the data onto the original line for uniform loading. Effectively, for the concentrated loading, the targets were less effective at resisting deformation for the same total impulse, i.e. the slope of the line was steeper (the same increase in I_N resulted in a larger increase in δ_N than for uniform loads). In the next section the results from the tests presented in this work are normalized in the same way.

4.5 Modifying and applying the Nurick Analysis

Figures 4.9 and 4.10 show the un-normalised and normalized results respectively, for the tests presented in this work in terms of deflection vs impulse .

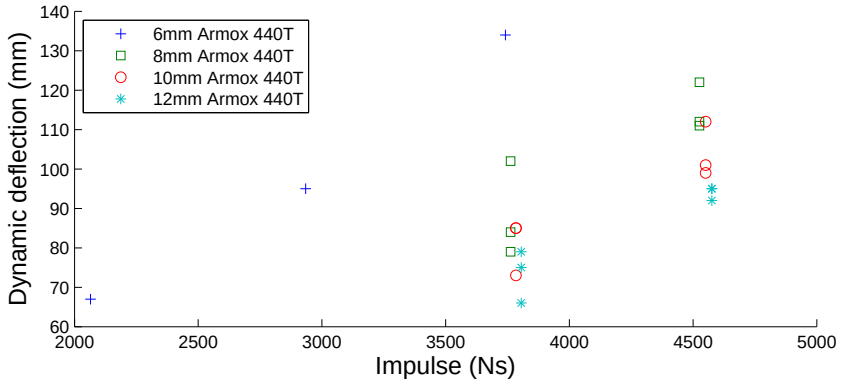

Figure 4.9: Peak dynamic central deflection against total impulse for different target thickness and charge sizes

The physical meaning of Nurick's normalization approach is not explicitly discussed in any of the publications using the approach; however, it can be shown that the approach is balancing the kinetic energy against the developing strain energy, as a function of deflection.

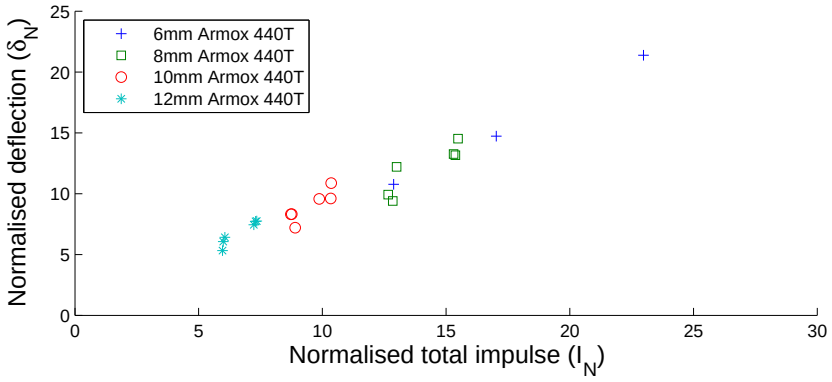

Figure 4.10: Normalized peak dynamic central deflection against total normalized impulse for different target thickness and charge sizes

Kinetic energy (E_k) can be defined for a target plate in terms of the total impulse and the mass of the plate (M_p), as defined by Equation 4.4.

$$E_k = \frac{I^2}{2M_p} \tag{4.4}$$

Ignoring the +0.001 Equation 4.3 can be written as:

$$\frac{\delta}{t_p} = 0.471 \times \frac{I}{2t_p^2\sqrt{(B_P L_P \rho \sigma)}} \tag{4.5}$$

Square rooting both sides of Equation 4.4 gives:

$$\sqrt{E_k} = \sqrt{\frac{I^2}{2B_p L_p \rho t_p}} \tag{4.6}$$

Equation 4.5 can be rewritten as:

$$\delta = 0.471 \times \sqrt{\frac{I^2}{2B_p L_p \rho t_p}} \times \frac{\sqrt{2}}{2\sqrt{\sigma t_p}} \tag{4.7}$$

Using Equation 4.6, Equation 4.7 can be rewritten as:

$$\delta = 0.471 \times \sqrt{E_k} \times \frac{\sqrt{2}}{2\sqrt{\sigma t_p)}} \tag{4.8}$$

Solving Equation 4.8 for E_k gives Equation 4.9 where kinetic energy is defined by something related to membrane resistance (σt_p), deflection (δ^2) and a constant (9.02). Membrane resistance per unit le is given by σt_p, but in Equation

4.9 this quantity is multiplied by δ^2 and a constant, indicating that the strain energy developed in the plate is defined within the Nurick analysis as a function of δ alone. That is, σ and t_p can change as the material or plate thickness changes for any given test, but with respect to any individual test and Equation 4.9, kinetic energy is a function of deflection. The units of the right side of Equation 4.9 are given by Equation 4.10.

$$E_k = 9.02 \times (\sigma t_p) \times \delta^2 \tag{4.9}$$

$$E_k = \frac{\text{Newtons} \times \text{meters} \times \text{meters} \times \text{meters}}{\text{meters} \times \text{meters}} = \text{Newtons} \times \text{meters} \tag{4.10}$$

Essentially, Equation 4.9 defines the efficiency with which quadrangular plates mobilize strain energy with increasing deflection. Because the difference between dynamic deflections and residual deflections was significant for the tests presented in this work and given that in Nurick's normalization kinetic energy is being balanced by strain energy, which is given by $\sigma \times t_p \times \delta \times \delta$ and reaches its maximum at maximum deflection, it is necessary to use dynamic deflection instead of residual deflection when implementing Nurick's approach. Figure 4.11 shows the normalized data with a line of best fit as well as the Nurick line described by Equation 4.3. Because the loading in these tests was not uniform the slope of the line for the normalised results in Figure 4.11 does not match the Nurick line developed from uniform loads (Equation 4.3). As demonstrated in Section 4.2 concentrated loads actually impart more kinetic energy for the same total impulse as compared to uniform loads.

Using the equivalent impulse detailed in Section 4.2 to account for the extra kinetic energy reduces the slope of the line and brings it closer to the Nurick line as shown by Figure 4.13 (blue line and data), but the difference in total kinetic energy does not account for all of the discrepancy; there is still a large difference between the slopes of the lines. The reason that adjusting for the additional kinetic energy does not fully account for the difference between the slopes is because deformed shape is also affected by the distribution of the loading; as discussed in Section 2.7. If the deformed shape is different, then the constant in Equation 4.9 will have a different value, which means that for the same δ less strain energy will be mobilized to balance the imparted kinetic energy. Equation 4.11 shows the Equation for the line of best fit through the data in Figure 4.11.

$$\delta_N = (0.90 \times I_N) \tag{4.11}$$

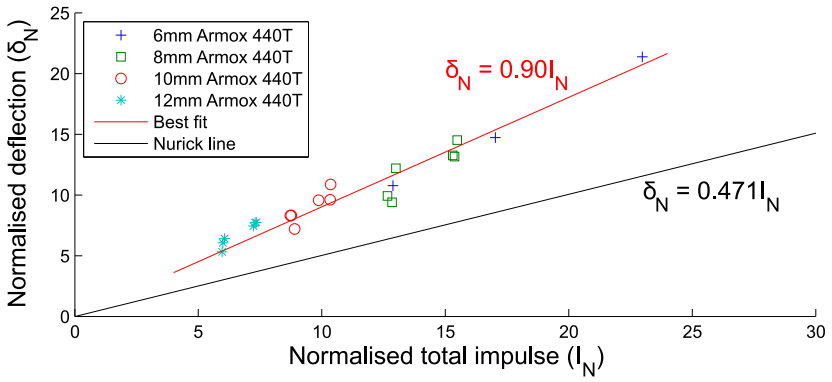

Figure 4.11: Normalized peak dynamic central deflection against total normalized impulse for different target thickness and charge sizes with line of best fit and Nurick line

Equation 4.9 re-calculated using the slope of Equation 4.11 gives:

$$E_k = 2.47 \times (\sigma t_p) \times \delta^2 \tag{4.12}$$

The efficiency with which these quadrangular plates mobilize strain energy with increasing deflection is less than in Equation 4.9, i.e constant of 2.47 vs 9.02. This is consistent with the discussion in Section 2.7 where in Figure 2.7 the deformation profile of the 0 mm burial depth plate shows a central deflection 2 times larger than the 70 mm burial depth plate despite the fact that the measured impulse for the 0 mm burial depth plate was half that of the 70 mm burial depth plate. The shape of the deformation profile is what gave rise to this inconsistency. The 0 mm burial depth plate exhibits deformation that is concentrated in the centre, i.e. the strain energy density is greater in the the central portion of the target. As shown by Figure 4.12 the deformation profiles of the targets presented in the results section have a shape with two different slopes as detailed in Example 3 of Figure 2.8 in the literature review section.

There is a correlation between the distribution of the loading and the slope of the line in Nurick's analysis; concentrated loads can cause concentrated deformation which leads to a steeper slope for the normalized trend line. Moreover, a linear trend will only emerge if all the test data being used is from tests with the same distribution of loading.

The question is, can the slope of the line in a normalized analysis be predicted such that deflection can be calculated for any distribution of impulse? The key is to be able to predict the factor required to bring results onto the uniform impulse Nurick line, for any given distribution of impulse.

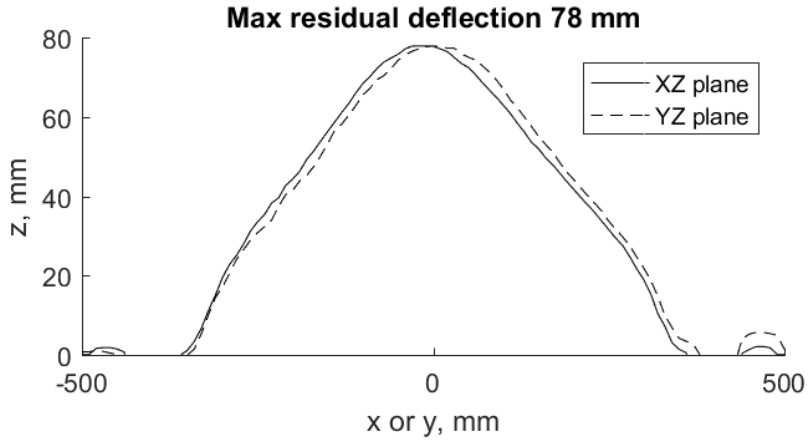

Figure 4.12: Example deformation profile from Test 3, target number AM-06-002

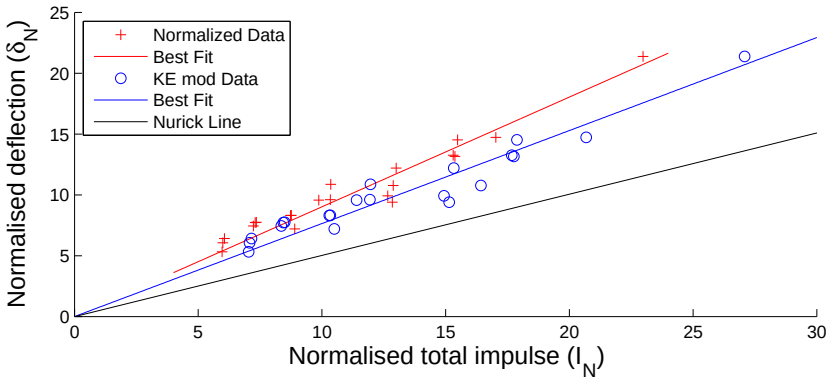

Figure 4.13: Normalized deflection against total normalized impulse with kinetic energy modified data and Nurick Line

Figure 4.14 shows how for a target loaded with a non-uniform distribution of impulse, the upper-bound assumption is that the impulse is delivered fast enough to ensure all the impulse (I_D) applied to any discrete area/mass (M_D) will result in an kinetic energy (E_{kd}) uptake of $\frac{I_D^2}{2M_D}$. Figure 4.14 also shows the upper-bound assumption for target strain response to the upper-bound kinetic energy uptake; that is, the strain distribution is proportional to the kinetic energy distribution. In short, it shows that the kinetic energy imparted to any discrete mass can only be balanced by the strain developed with an adjacent mass; which will only be possible if the adjacent mass is travelling more slowly and can provide some inertial restraint. The lower-bound assumption of strain distribution shown in Figure 4.14 (next page due to size) is that it will be uni-

form across the target even if the kinetic energy imparted across the plate is non-uniform.

If the deformed profile of targets exhibited the same basic shape of deformation regardless of the distribution of the load, no correction factor would be required; however, as demonstrated by Figure 2.7 targets are not always capable of evenly distributing strain energy.

Figures 4.15 and 4.16 (forward two pages due to size) explain how a factor to adjust normalized results based on knowledge of the loading is calculated. The idea is that target response can be quickly predicted for any known distribution of impulse using the normalized relationship established by Nurick if there is a correction factor to account for the difference in slope due to the non-uniform load. Section 4.2 showed how the deformable area of the targets used in this study were discretized and the distribution of kinetic energy was calculated from the distribution of impulse provided by the modified Westine model. As indicated by Figure 4.15 the central line of discretized squares from the support to the centre of the plate was used in the calculation of the correction factor.

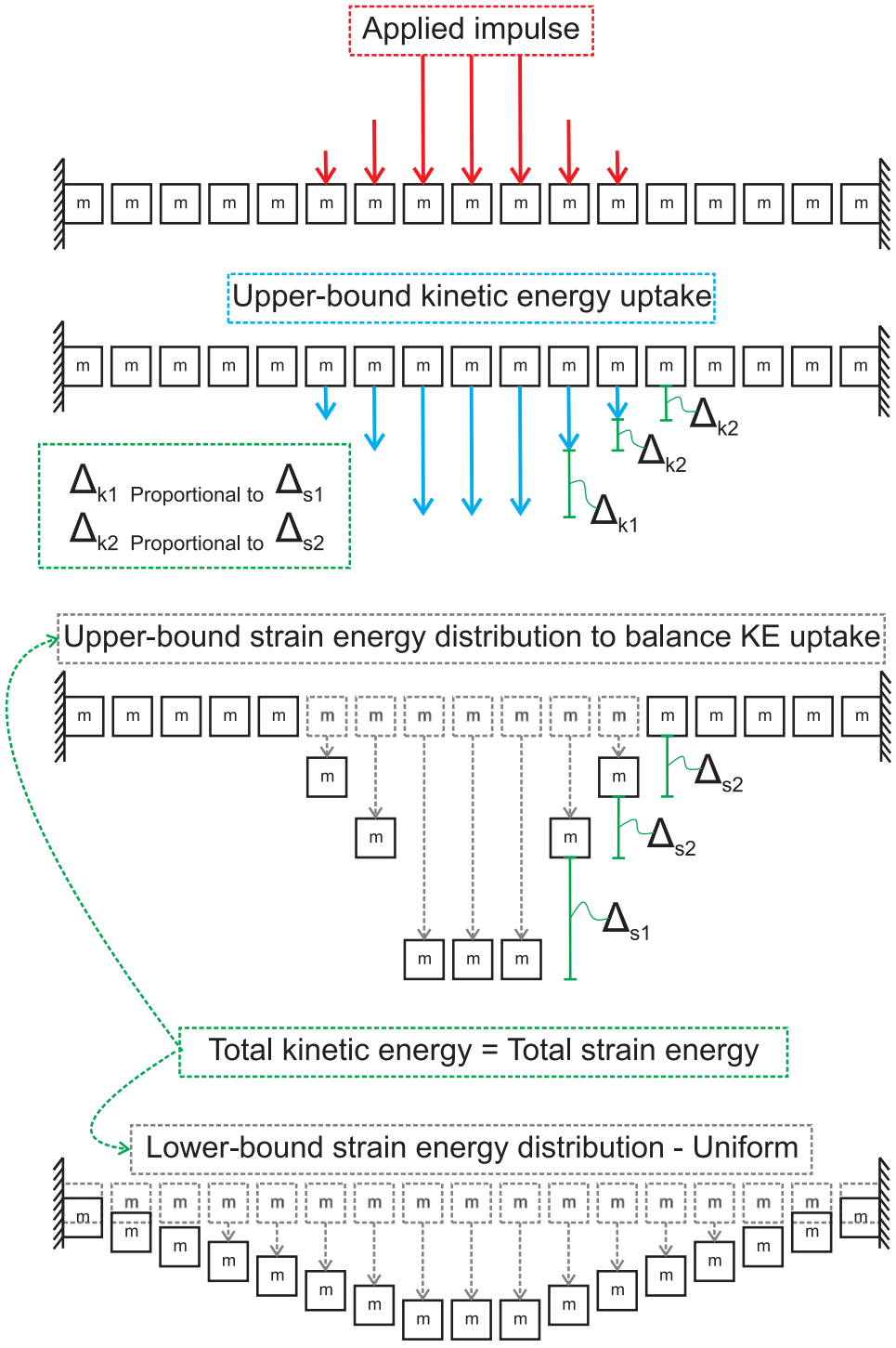

Figure 4.14: Diagram of theoretical upper-bound and lower-bound strain energy distribution response to the upper-bound kinetic energy uptake for a target loaded with a non-uniform impulse distribution

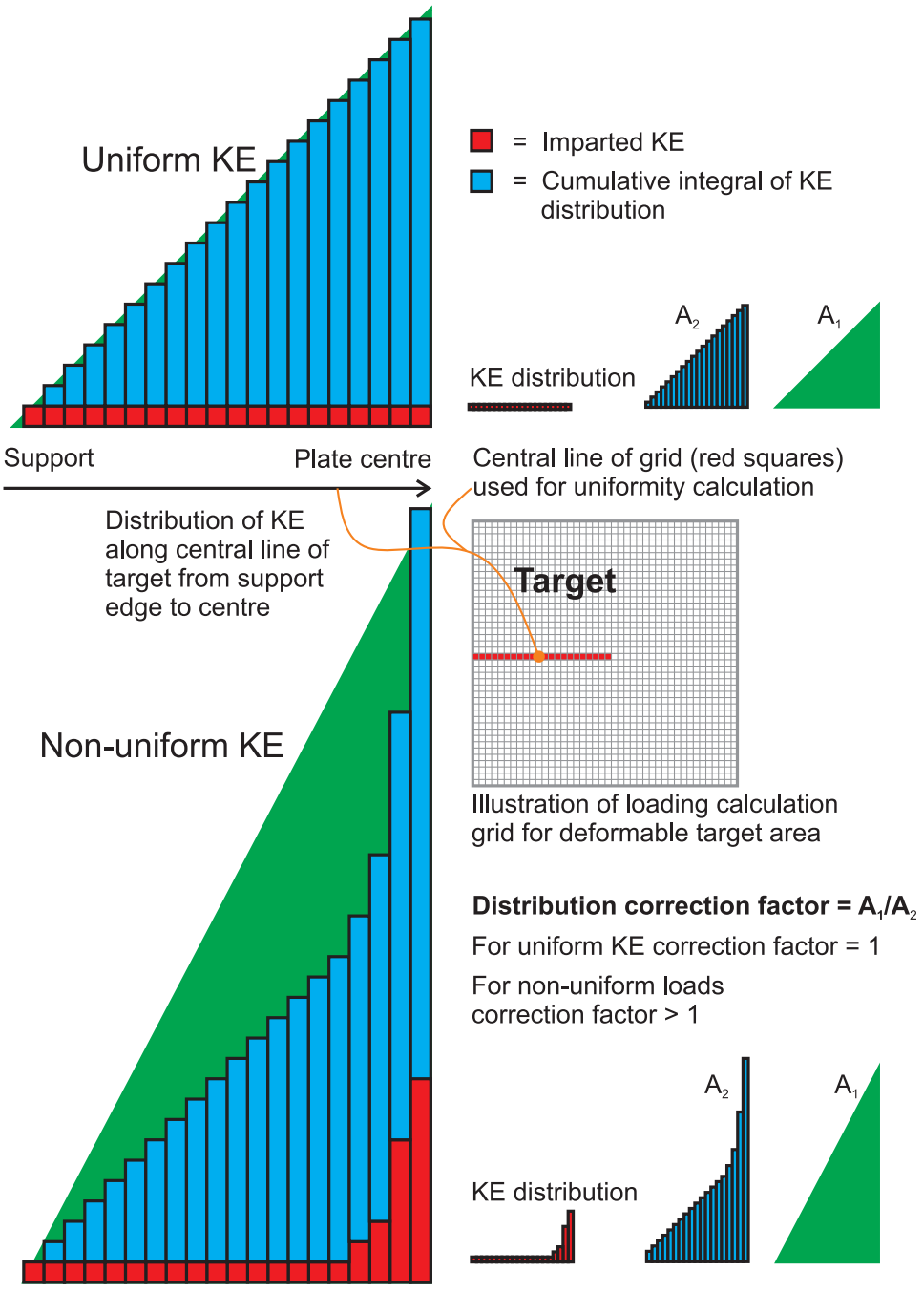

Figure 4.15: Details of kinetic energy correction factor

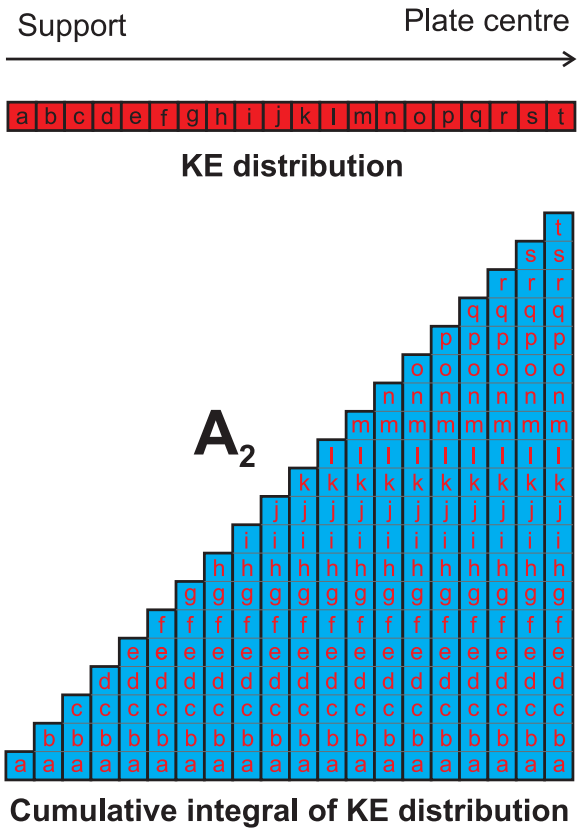

Figure 4.16: Cumulative integral of KE distribution explained

The line of reasoning for the correction factor is as follows:

a) Assume the applied impulse results in the upper-bound uptake of kinetic energy as in Figure 4.14

b) Assume the deformed profile is proportional to the profile of the upper-bound kinetic energy uptake as in Figure 4.14

c) Assume that the ratio of the area under a cumulative non-uniform kinetic energy distribution graph to the area required to produce that same total cumulative kinetic energy in the centre of the target, but with a uniform distribution, is equal to the ratio when considering the area under the deformation profile in the same way. Hence, if deflection distribution is proportional to the kinetic energy uptake profile, then the associated ratios described above will be the same.

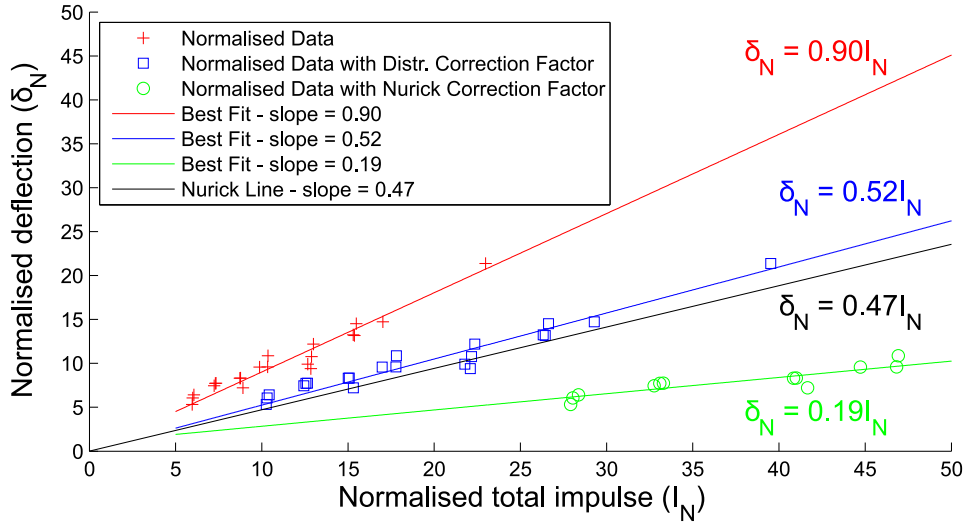

Figure 4.17: Normalized deflection against total normalized impulse data, normalised data with distribution based correction factor, normalised data with Nurick correction factor, and Nurick Line

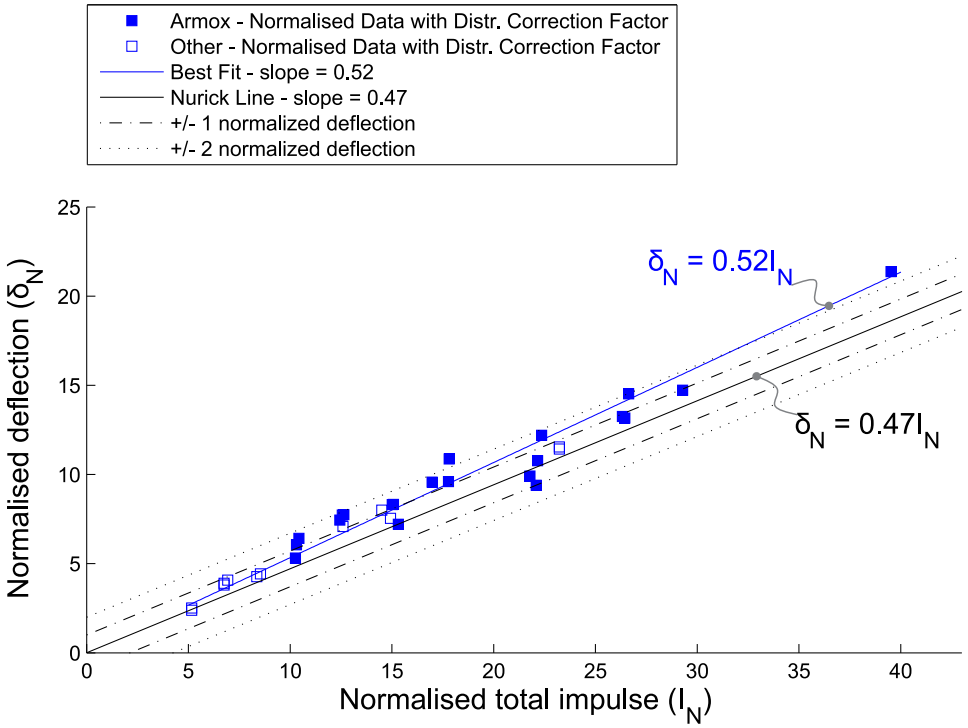

Figure 4.18: Normalised data with distribution based correction factor vs Nurick Line

The distribution of loading calculated by using the modified Westine model defines a correction factor of 1.72. Dividing through the normalized data by this value produces the corrected blue line in Figures 4.17 and 4.18. For this series of tests the correlation between the data with the applied correction factor and Nurick's line is high (Figure 4.18). Especially when considering the origin of Nurick's line and the spread of data associated as seen in Figure 4.7. Figure 4.18 shows Nurick's line with the same ± 1 & ±2 normalised deflection lines as Figure 4.7 and the data from this thesis with the applied correction factor, which sits almost inside the upper and lower bounds.

Figure 4.18 also shows 12 additional data points which represent 5 other material types other than Armox 440T, all the test data presented up to this point has been Armox 440T. The additional 12 targets were tested using either 800 gram or 1000 gram charges and all the other test parameters were identical to the tests performed on Armox 440T. No further information can be given here regarding the additional tests due to the security classification of the tests. The additional data points support the hypothesis that regardless of material type, target thickness, material strength or material density the normalization approach presented here, can be used to accurately characterize the deflection response.

As described in Chung Kim Yuen et al. (2016), a correction factor for non-uniform loads was suggested by Nurick; however, the correction is more of an empirical formulae than a correction factor based on the difference in loading distribution. Moreover, it was informed by free-air blast testing, not buried blast. As such, it is not an accurate correction factor for the tests conducted in this study as shown by the green line in Figure 4.17.

4.6 Chapter summary

The analysis chapter in this thesis has detailed the way in which the loading applied to the targets in this study can be calculated. As well as, how this loading along with the measured central plate deflections can be normalised according to an existing approach defined by Nurick and Martin (1989). Lastly this chapter explains the rationale behind and the method of modifying Nurick's analysis; improving the understanding of the approach and broadening its range of application. Some conclusions that can be drawn from this chapter are:

- The distributed impulse from a buried blast event can be calculated using Westine's model when it is calibrated to the specific soil conditions of the testing.
- Using the normalized approach developed by Nurick collapses the otherwise scattered data from all the tests in the series presented in this thesis onto one straight line.
- The slope of the line produced by the tests in this thesis is steeper than Nurick's line because the loading is not uniform.
- Non-uniform distributions of impulse impart more total kinetic energy to a target than uniformly distributed impulses of the same total value.
- Accounting for the increase in kinetic energy alone does not bring the test data from this thesis onto Nurick's line, because a concentration of impulse can result in a concentration of strain as well.
- A correction factor based solely on the upper-bound distribution of kinetic energy across the plate produces results that match well with Nurick's line from uniformly loaded targets.
- Being able to predict the calibration factor to bring the data onto the uniform load line defined by Nurick is the starting point for a fast running engineering model for plate deflection from impulsive loading, including non-uniform loads.

Chapter 5

Conclusions

The work presented in this thesis aims to detail an investigation into shallow buried blast events and their effect on protective materials. Shallow buried blast events are an intricate series of physical processes that interact with and effect each other from the initial detonation of the high explosive to the end of the loading on the target. Four main objectives were outline in the introduction; the four concluding paragraphs that follow address those objectives.

1. The literature review in Chapter 2 is robust in its appraisal of previous work and how each publication should be viewed in light of all the work that has been done to date. The lack of high quality experimental studies to inform an understanding of the physical mechanisms of buried blast loading affects all of the work published in the field. Most modeling approaches have not been validated against relevant experimental data. Because the loading is not well understood in terms of spacial or temporal distribution existing load deflection data can seem inconsistent and results in a misunderstanding of how soil conditions will affect target response.

2. Based on the findings of the literature review and some commercial requirements, Chapter 3 defines the methodology development process for the experimental work carried out. Essentially this experimental arrangement ensures consistent loading that can be calculated with a modified Westine model to understand the distribution of impulse across the target in every test. The apparatus and test protocol were carefully designed after examining the large body of buried blast testing that had already been done at the University of Sheffield. The modified apparatus and test protocol improved the ease with which shots could be set up accurately.

3. As was demonstrated by the analysis of the work presented by Pickering et al. (2012), an understanding of the distribution and the duration of

the loading is essential for an accurate prediction of target performance; total impulse alone is simply insufficient information to predict behaviour with confidence. This conclusion was also supported by the explanation of target response in different hypothetical scenarios, demonstrating that non-uniform distributions of the same total impulse value will deliver different amount of kinetic energy to the target.

4. The analysis chapter pulls together ideas initially developed as part of the literature review and uses them to further develop an analysis approach from other existing literature, making use of the loading information that can be calculated because of the particular experimental setup developed for this work. For any given combination of soil condition, burial depth and charge shape only a few tests are needed to characterize the loading distribution. Once the loading distribution is known, Nurick's approach of normalizing impulse and deflection can be modified to accurately predict deformations for non-uniform buried blast for a range of total impulse values, target thicknesses and materials. These findings can also be applied to free-air blasts or any other short duration loading where the shape of the impulse distribution is known. The experimental results presented here can be used as a benchmark by which to measure the performance of materials other than Armox 440T against a well characterised buried blast event. Given that the loading can be calculated for the event as well, the results could be used to validate numerical modelling of the blast event. Finally, the analysis of the results presented in this thesis shows that a fast running engineering model to predict plate deformations for known impulsive load distributions is possible.

Chapter 6

Synopsis by chapter and future work

The important points from this thesis are summarised in bullet point form below for the convenience of the reader, roughly in the order which the appear in the document and divided by chapter:

Literature review

- Some of the most useful work in the field is also some of the earliest where Westine et al. (1985) measured the impulse from buried blast events at discrete locations across a rigid target using impulse plugs

- Since Westine's work there has been little agreement regarding the relative contributions of air blast, detonation products and soil impact to the loading experienced by the target. Nor has there been any experimental approaches that have been able to unpick these factors from each other

- Much work has been done regarding the effect of various soil conditions on the total impulse imparted to a target from a shallow buried blast and many models have been able to predict the correct total impulse for the experimental work they were configured around; however, very little work crosses multiple data sets in terms of model validation and very little work has been done to determine how to predict the correct parameters for a soil model without doing blast tests and calibrating

- Almost no modelling approaches have been validated against reflected pressure-time histories or distributed impulse

- Many studies have shown that has a soil reaches saturation the total impulse delivered to a target increases dramatically

- Recent experimental work at the University of Sheffield has shown that very repeatable buried blast tests are possible both in terms of total impulse and distributed impulse if the geotechnical conditions are tightly controlled

- Experimental work to gain an understanding of the detonation of the explosive with it's expanding detonation products and how this process interacts with the soil overburden and air gap, before eventually loading a target, is crucial to improving prediction and modelling capability

- A review of Pickering et al. (2012) shows that an understanding of the distribution of impulse and the delivery time of that impulse is crucial for understanding plate deformations

Methodology

- Existing literature and previous work at the University of Sheffield was used by the author to define the requirements and develop the concept for a new testing apparatus

- The authors own engineering calculations, engineering experience and an in-depth understanding of the research aims was used to perform the detailed design, produce the engineering drawings, sub-contract component machining and personally construct and fabricate the testing apparatus in-situ

- The test program was developed based on the aims of the research; i.e. to investigate whether knowledge of the distribution of impulse from a buried blast event can be used to predict target deformation without any FE modelling of the target or any numerical modelling of the blast event

- Three different charge sizes were used (giving different total impulses), 4 different thicknesses of Armox 440T were tested, all for the same burial depth and aspect ratio of the charge. Five other material types were also tested but are only presented at the end of the analysis section in normalized form due to security classification.

- Using the charge sizes based around previous work allowed the loading for each test to be calculated individually

Results and analysis

- Twenty-one test results are presented in this thesis. These are all the tests using a single layer of Armox 440T steel; 3 Armox 440T tests were omitted from the results because the plates exhibited gross failure as a result of overloading. These failures occurred when the charge weight assessments were being conducted at the start of the series to determine what charge sizes would produce reasonable deformations
- Overall more than 70 tests have been completed to date for other materials and layered systems than Armox 440T. But as already mentioned, all the tests cannot be presented directly because of security classification.
- The distributed impulse from a buried blast event can be calculated using Westine's model when it is calibrated to the specific soil conditions of the testing
- Using the normalize approach developed by Nurick brings all the tests from the series presented in this thesis onto one straight line
- The slope of the line produced by the tests in this thesis is steeper than Nurick's line because the loading is not uniform
- Non-uniform distributions of impulse impart more total kinetic energy to a target than uniformly distributed impulses of the the same total value
- Accounting for the increase in kinetic energy alone does not bring the test data from this thesis onto Nurick's line, because a concentration of impulse can result in a concentration of strain as well.
- A correction factor based solely on the upper-bound distribution of kinetic energy across the plate produces results that match well with Nurick's line from uniformly loaded targets
- Being able to predict the adjustment factor to bring the data onto the uniform load line defined by Nurick is the starting point for a fast running engineering model for plate deflection from impulsive loading, especially including non-uniform loads

6.1 Future Work

This section is intended to give brief details of how the investigation presented in the thesis should be expanded and improved going forward. As well as, what further work is needed to improve the understanding of buried blast, specifically with respect to the areas where knowledge is lacking as highlighted by the literature review.

The first area of further work would be to investigate whether or not the proposed correction factor based on the distribution of loading is accurate for other distributions of loading. The approach needs to validated against other experimental data where the distribution of loading and the peak dynamic deflection are known. Another approach would be to use a numerical model for plate response which has been validated against several experimental tests where the distribution of the load was measured, to populate an artificial data set of load distributions and plate responses to test the correction factor against.

The most significant problem for the field of shallow buried blast as a whole is the lack of understanding of the physical processes actually taking place in the region directly in contact and above the buried charge. There is very little information about how changes in geotechnical conditions effect the physical mechanisms developing between explosive detonation and loading of a target. As a result there is no consensus in the field regarding the relative contributions of soil impact, air shock and detonation products to the loading imparted to a target. The first step in addressing the lack of knowledge would be to devise an experimental approach that would be able measure side-on over-pressures and reflected over-pressures for a buried blast event. This would allow the soil impact contribution to be separated from the air-shock and detonation product contribution to the loading. Performing such experiments and investigating the parameter space presented by changing various geotechnical parameters would inform the "what" of the loading, but it would not answer the "why". "Why" does changing one soil condition fundamentally change the behaviour of the event and the resulting loading experienced by the target. An experimental approach which is able to provide information about what is happening in the soil layer just above the charge so as to be able to describe the physical mechanisms taking place and how they change with different soil conditions is essential for improving modelling routines. The physics that needs to be modelled, needs to be understood qualitatively before robust modelling approaches can be developed. It may be that the physics can be represented well by a simplified model, but until the actual events are better understood, it will be difficult to know if

the assumptions of a simplified model are valid for the full parameter space of shallow buried blast events.

Bibliography

Anderson, C. E., Behner, T. and Weiss, C. E. (2011), 'Mine blast loading experiments', *International Journal of Impact Engineering* **38**(8-9), 697–706.

Barr, A. and Fuller, B. (2018), 'Bt-256 appliqué', *Technical Report issued to DSTL, Porton Down* .

Bergeron, D. and Tremblay, J. (2000), Canadian Research to Characterize Mine Blast Output, *in* 'Military Aspects of Blast and Shock 16', Oxford, pp. 501–511.

Bergeron, D., Walker, R. and Coffey, C. (1998), Detonation of 100-gram antipersonell mine surrogate charges in sand - a test case for computer code validation, Technical report, Defence Research Establishment, Suffield, Canada.

Borvik, T., Olovsson, L., Hanssen, A., Dharmasena, K., Hansson, H. and Wadley, H. (2011), 'A discrete particle approach to simulate the combined effect of blast and sand impact loading of steel plates', *Journal of the Mechanics and Physics of Solids* **59**, 940–958.

Chung Kim Yuen, S., Nurick, G. N., Langdon, G. S. and Iyer, Y. (2016), 'Deformation of thin plates subjected to impulsive load : Part III an update 25 years on', *International Journal of Impact Engineering* **107**.

Clarke, S. D., Fay, S. D., Tyas, A., Warren, J., Rigby, S., Elgy, I. and Livesey, R. (2014), Repeatability of Buried Charge Testing, *in* 'Military Aspects of Blast and Shock 23', Oxford, UK.

Clarke, S. D., Fay, S. D., Warren, J. A., Tyas, A., Rigby, S. E. and Elgy, I. (2015a), 'A large scale experimental approach to the measurement of spatially and temporally localised loading from the detonation of shallow-buried explosives', *Measurement Science and Technology* **26**, 015001.

Clarke, S. D., Fay, S. D., Warren, J. A., Tyas, A., Rigby, S. E., Reay, J. J., Livesey, R. and Elgy, I. (2015b), 'Geotechnical causes for variations in output measured from shallow buried charges', *International Journal of Impact Engineering* **86**, 274–283.

Clarke, S. D., Fay, S. D., Warren, J. A., Tyas, A., Rigby, S. E., Reay, J. J., Livesey, R. and Elgy, I. (2017), 'Predicting the role of geotechnical parameters on the output from shallow buried explosives', *International Journal of Impact Engineering* **102**, 117–128.

Clarke, S. D., Rigby, S. E., Fay, S. D., Tyas, A. and Elgy, I. (2018), 'Characterisation of Blast Loading', *In preparation for submission to International Journal of Impact Engineering* .

Clarke, S. D., Warren, J. A., Fay, S., Rigby, S. E. and Tyas, A. (2012), The Role of Geotechnical Parameters on the Impulse Generated by Buried Charges, *in* 'Military Aspects of Blast and Shock 22', Bourges, France.

Clarke, S., Warren, J. and Tyas, A. (2011), The influence of soil density and moisture content on the impulse from shallow buried explosive charges, *in* '14th International Symposium on the Interaction of the Effects of Munitions with Structures (ISIEMS)', Seattle, WA, USA, pp. 19–23.

Cloete, T. J. and Nurick, G. N. (2014), 'On the influence of radial displacements and bending strains on the large deflections of impulsively loaded circular plates', *International Journal of Mechanical Sciences* **82**.

Deshpande, V., McMeeking, R., Wadley, H. and Evans, A. (2009), 'Constitutive model for predicting dynamic interactions between soil ejecta and structural panels', *Journal of the Mechanics and Physics of Solids* **57**(8), 1139–1164.

Ehrgott, J. Q., Akers, S. A., Windham, J. E., Rickman, D. D. and Danielson, K. T. (2011b), 'The Influence of Soil Parameters on the Impulse and Airblast Overpressure Loading The in fl uence of soil parameters on the impulse and airblast overpressure loading above surface-laid and shallow-buried explosives', *Shock and Vibration* **18**, 857–874.

Ehrgott, J. Q., Rhett, R. G., Akers, S. A. and Rickman, D. D. (2011a), 'Design and Fabrication of an impulse measurement device to quantify the blast environment from a near-surface detonation', *Experimental Techniques* **35**(3), 51–62.

Fourney, W. L., Leiste, H. U., Hauch, A. and Jung, D. (2010), Distribution of Specific Impulse on Vehicles Subjected to IEDs, *in* 'Proceedings of the IMPLAST 2010 Conference', Providence, Rhode Island, USA.

Fourney, W., Leiste, U., Bonenberger, R. and Goodings, D. (2005), 'Mechanism of loading on plates due to explosive detonation', *Fragblast* **9**(4), 205–217.

Fox, D., Akers, S., Leiste, U., Fourney, W., Windham, J., Lee, J., Ehrgott, J. and Taylor, L. (2014), 'The effects of air filled voids and water content on the momentum transferred from a shallow buried explosive to a rigid target', *Intl J of Impact Eng* **69**(0), 182–193.

Fox, D. M., Huang, X., Jung, D., Fourney, W. L., Leiste, U. and Lee, J. S. (2011), 'The response of small scale rigid targets to shallow buried explosive detonations', *International Journal of Impact Engineering* **38**(11), 882–891.

Grujicic, M. and Pandurangan, B. (2008), 'A combined multi-material euler/lagrange computational analysis of blast loading resulting from detonation of buried landmines', *Multidiscipline Modeling in Materials and Structures* **4**(2), 105–124.

Grujicic, M., Pandurangan, B. and Cheeseman, B. a. (2006a), 'The effect of degree of saturation of sand on detonation phenomena associated with shallow-buried and ground-laid mines', *Shock and Vibration* **12**, 1–21.

Grujicic, M., Pandurangan, B. and Cheeseman, B. a. (2006b), 'A Computational Analysis of Detonation of Buried Mines', *Multidiscipline Modeling in Materials and Structures* **2**(4), 363–388.

Grujicic, M., Pandurangan, B., Cheeseman, B. A. and Roy, W. N. (2007a), 'Application of the modified compaction material model to the analysis of landmine detonation in soil with various degrees of water saturation', *Shock and Vibration* **14**(1), 1–15.

Grujicic, M., Pandurangan, B. and Hariharan, A. (2011), 'Comparative Discrete-Particle Versus Continuum-Based Computational Investigation of Soil Response to Impulse Loading', *Journal of Materials Engineering and Performance* **20**(9), 1520–1535.

Grujicic, M., Pandurangan, B., Huang, Y., Cheeseman, B. A., Roy, W. N. and Skaggs, R. R. (2007b), 'Impulse loading resulting from shallow buried explosives in water-saturated sand', *Proceedings of the Institution of Mechanical Engineers, Part L: Journal of Materials: Design and Applications* **221**(1), 21–35.

Grujicic, M., Pandurangan, B., Qiao, R., Cheeseman, B. A., Roy, W. N., Skaggs, R. R. and Gupta, R. (2008), 'Parameterization of the porous-material model

for sand with different levels of water saturation', *Soil Dynamics and Earthquake Engineering* **28**(1), 20–35.

Heider, N. and Klomfass, A. (2005), Numerical and experimental analysis of the detonation of sand-buried mine, *in* 'Proc. 22nd Int. Symp. Ballistics'.

Hlady, S. (2004), Effect of soil parameters on landmine blast, *in* 'Military Aspects of Blast and Shock 18'.

Jacob, N., Yuen, S. C. K., Nurick, G. N., Bonorchis, D., Desai, S. A. and Tait, D. (2004), 'Scaling aspects of quadrangular plates subjected to localised blast loads - experiments and predictions', **30**, 1179–1208.

Kincheloe, W. L. (1962), Reduction of Blast Effects, Technical report, Cleveland Army Tank Automotive Plant, Allison Division of General Motors.

Leiste, B. H. U., Fourney, W. L. and Duff, T. (2013), 'Experimental Studies to Investigate Pressure Loading on Target Plates', *Blasting and Fragmentation* **7**(2), 99–126.

Milne, A. M., Floyd, E., Longbottom, A. W. and Taylor, P. (2014), 'Dynamic fragmentation of powders in spherical geometry', *Shock Waves* **24**(5), 501–513.

NATO (2006), 'Procedures for evaluating the protection level of logistic and light armoured vehicles', *Allied Eng. Publication (AEP) 55* **Vol.2 (for Mine Threat)**.

Neuberger, A., Peles, S. and Rittel, D. (2007), 'Scaling the response of circular plates subjected to large and close-range spherical explosions. Part II: Buried charges', *International Journal of Impact Engineering* **34**(5), 874–882.

Nurick, G. N. and Martin, J. B. (1989), 'Deformation of thin plates subjected to impulsive loading - a review. Part I: Theoretical considerations', *International Journal of Impact Engineering* **8**(2), 159–170.

Pickering, E., Chung Kim Yuen, S., Nurick, G. and Haw, P. (2012), 'The response of quadrangular plates to buried charges', *International Journal of Impact Engineering* **49**, 103–114.

Rigby, S. E., Fay, S. D., Tyas, A., Clarke, S. D., Reay, J. J., Warren, J. A., Gant, M. and Elgy, I. (2018), 'Influence of particle size distribution on the blast pressure profile from explosives buried in saturated soils', *Shock Waves* **28**(3), 613–626.

Rigby, S. E., Tyas, A., Clarke, S. D., Fay, S. D., Reay, J. J., Warren, J. a., Gant, M. and Elgy, I. (2015), 'Observations from Preliminary Experiments on Spatial and Temporal Pressure Measurements from Near-Field Free Air Explosions', *International Journal of Protective Structures* **6**(2), 175–190.

Rigby, S. E., Tyas, A., Fay, S. D., Clarke, S. D., Warren, J. A., Elgy, I. and Gant, M. (2014), Testing Apparatus for the Spatial and Temporal Pressure Measurements from Near-Field Free Air Explosions, *in* '6th International Conference on Protection of Structures Against Hazards', Tianjin, China.

Rigby, S., Fay, S., Clarke, S., Tyas, A., Reay, J., Warren, J., Gant, M. and Elgy, I. (2016), 'Measuring spatial pressure distribution from explosives buried in dry leighton buzzard sand', *International Journal of Impact Engineering* **96**, 89 – 104.

Taylor, L. C., Fourney, W. L. and Leiste, H. U. (2010), Pressures on Targets From Buried Explosions, *in* 'IMPLAST 2010 Conference'.

Tyas, A. and Pope, D. J. (2003), The energy take-up of panels subjected to near-field blast loading, *in* 'International Conference on the Response of Structures to Extreme Loading', Toronto.

Wenzel, A. B. and Esparza, E. D. (1972), Measurements of Pressure and Impulses at Close Distances From Explosive Charges Buried and In Air, Technical report, Southwest Research Institute.

Westine, P. S. (1972), 'The Impulse Imparted to Targets by the detonation of land mines', *The Shock and Vibration Bulletin* pp. 97–107.

Westine, P. S., Morris, B. L., Cox, P. A. and Polch, E. (1985), 'Development of computer program for floor plate response from landmine explosions', *Contract Report No. 1345, for US Army TACOM Research and Development Center* .

Appendix A

Deflection figures

Note: The "z" axis on the section view deflections does not have the same scale for every test. This is because the size of the plot was kept the same to be able to readily compare relative shape more easily. These figures can be found in Barr and Fuller (2018).

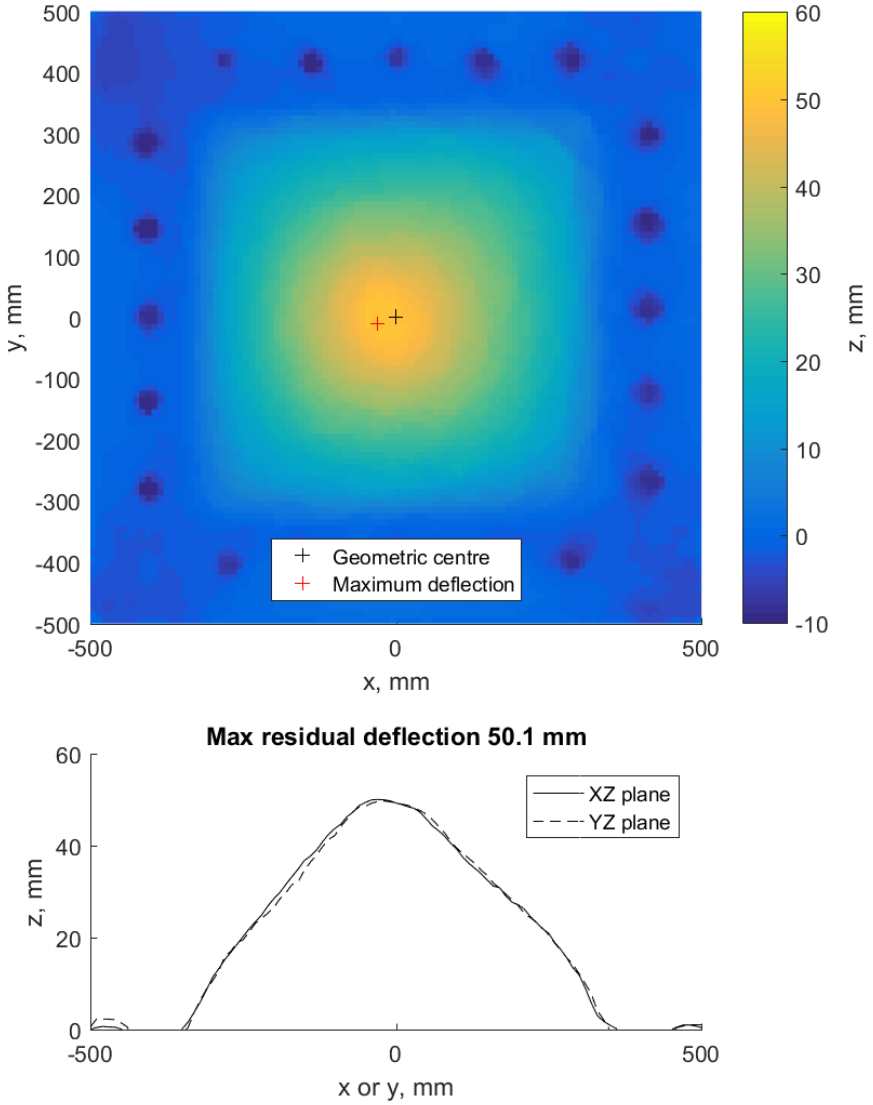

Figure A.1: Deformation profile for Test 2, target no. AM-06-001, plan view (top) and central section views (bottom)

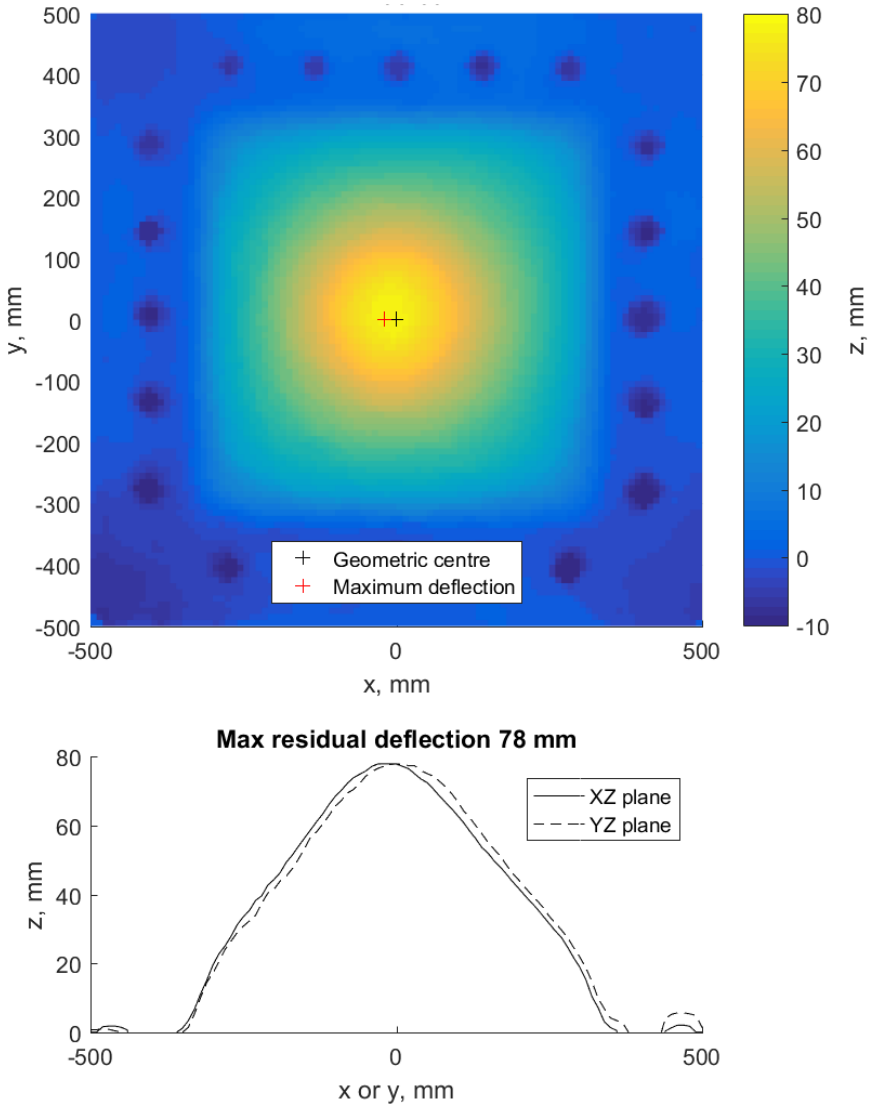

Figure A.2: Deformation profile for Test 3, target no. AM-06-002, plan view (top) and central section views (bottom)

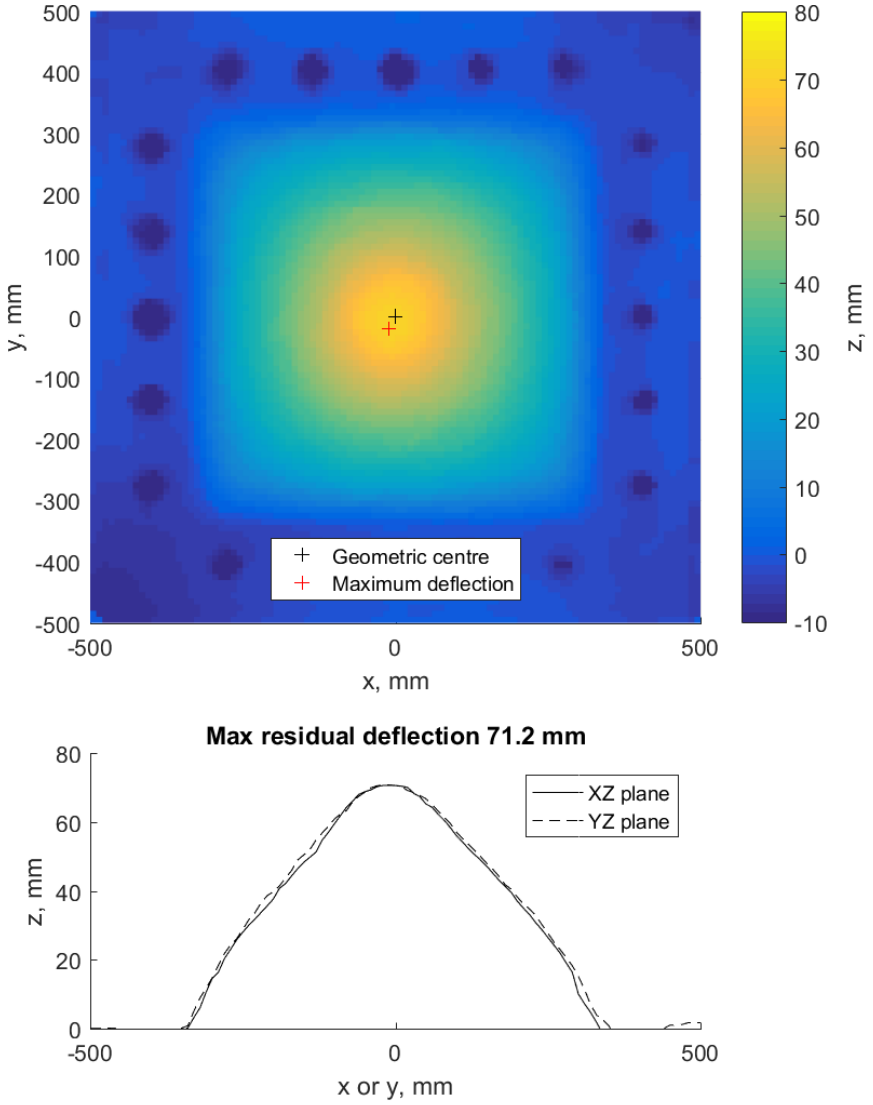

Figure A.3: Deformation profile for Test 4, target no. AM-08-001, plan view (top) and central section views (bottom)

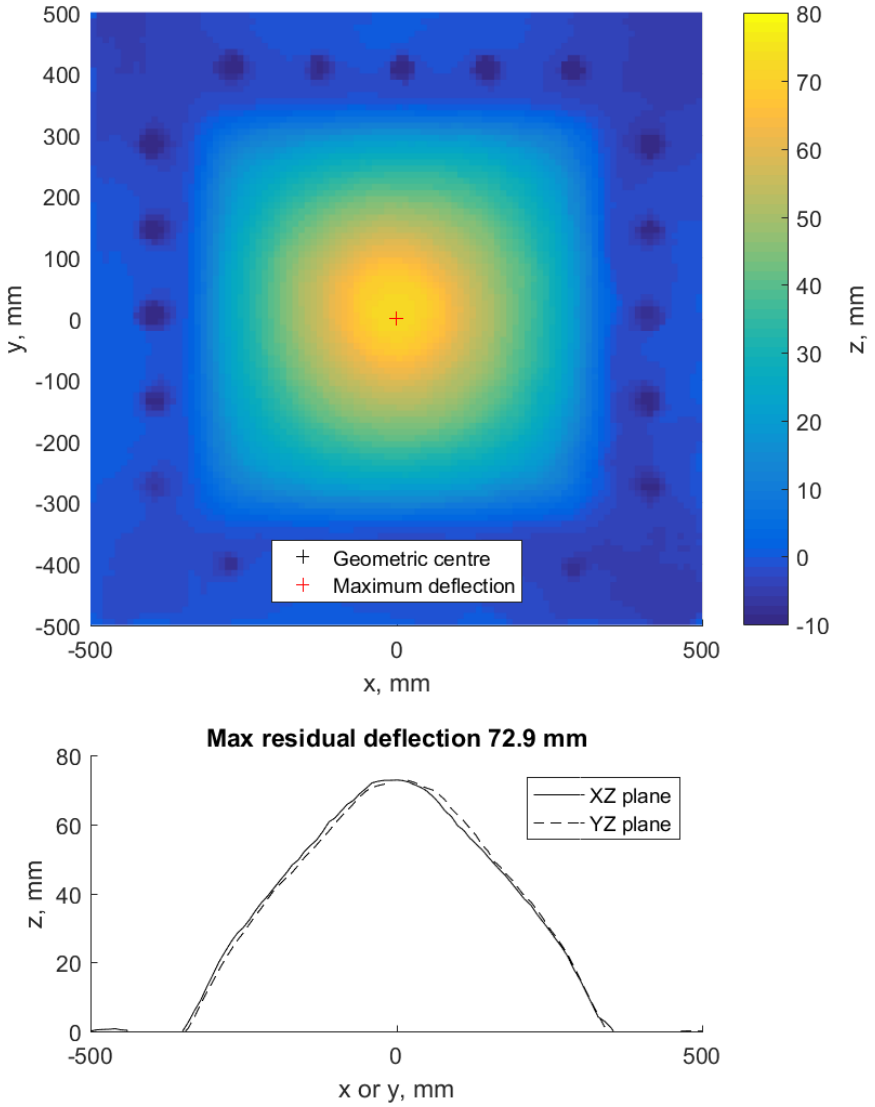

Figure A.4: Deformation profile for Test 5, target no. AM-08-002, plan view (top) and central section views (bottom)

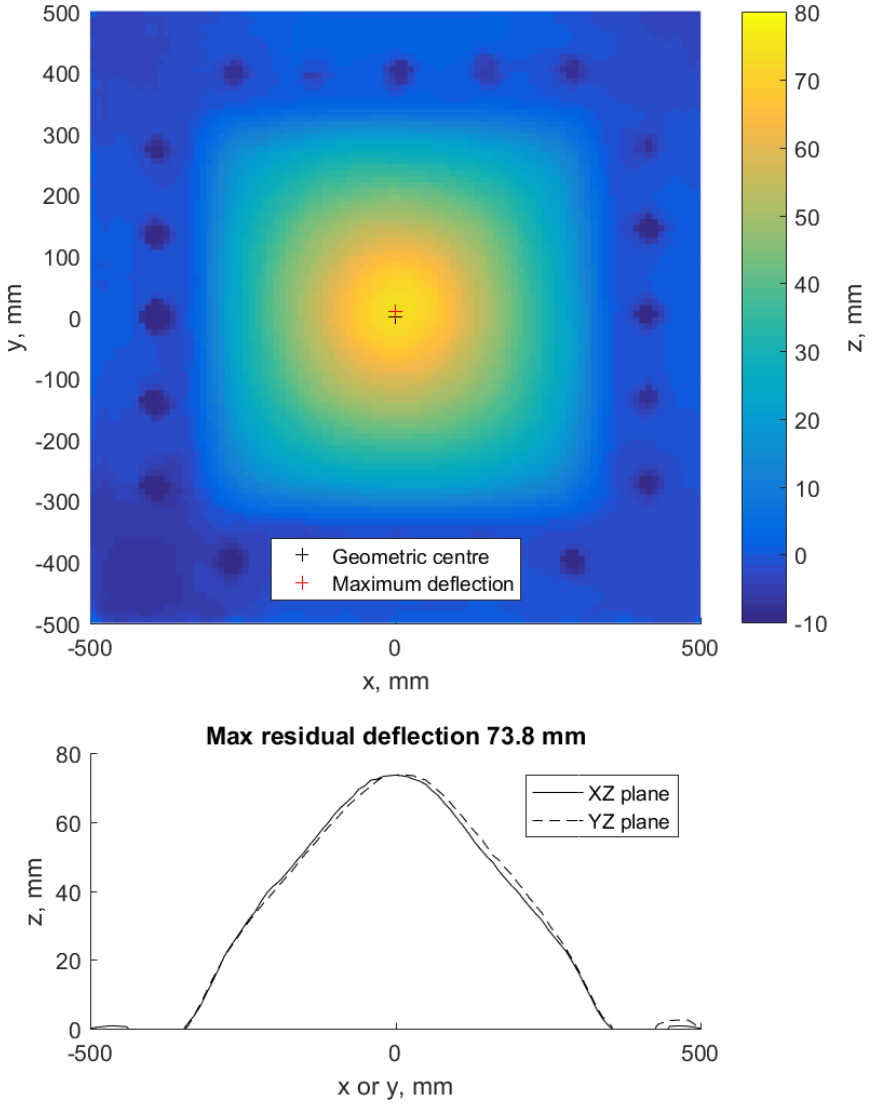

Figure A.5: Deformation profile for Test 6, target no. AM-08-003, plan view (top) and central section views (bottom)

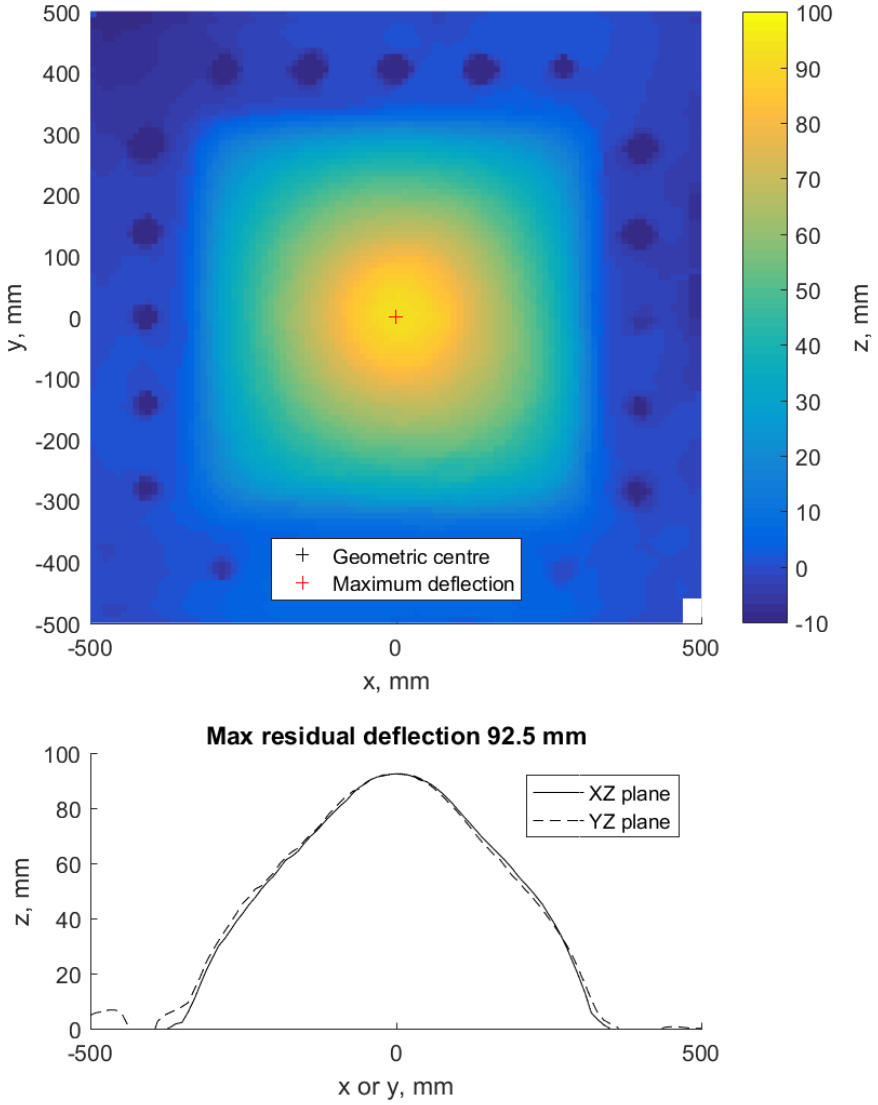

Figure A.6: Deformation profile for Test 7, target no. AM-08-004, plan view (top) and central section views (bottom)

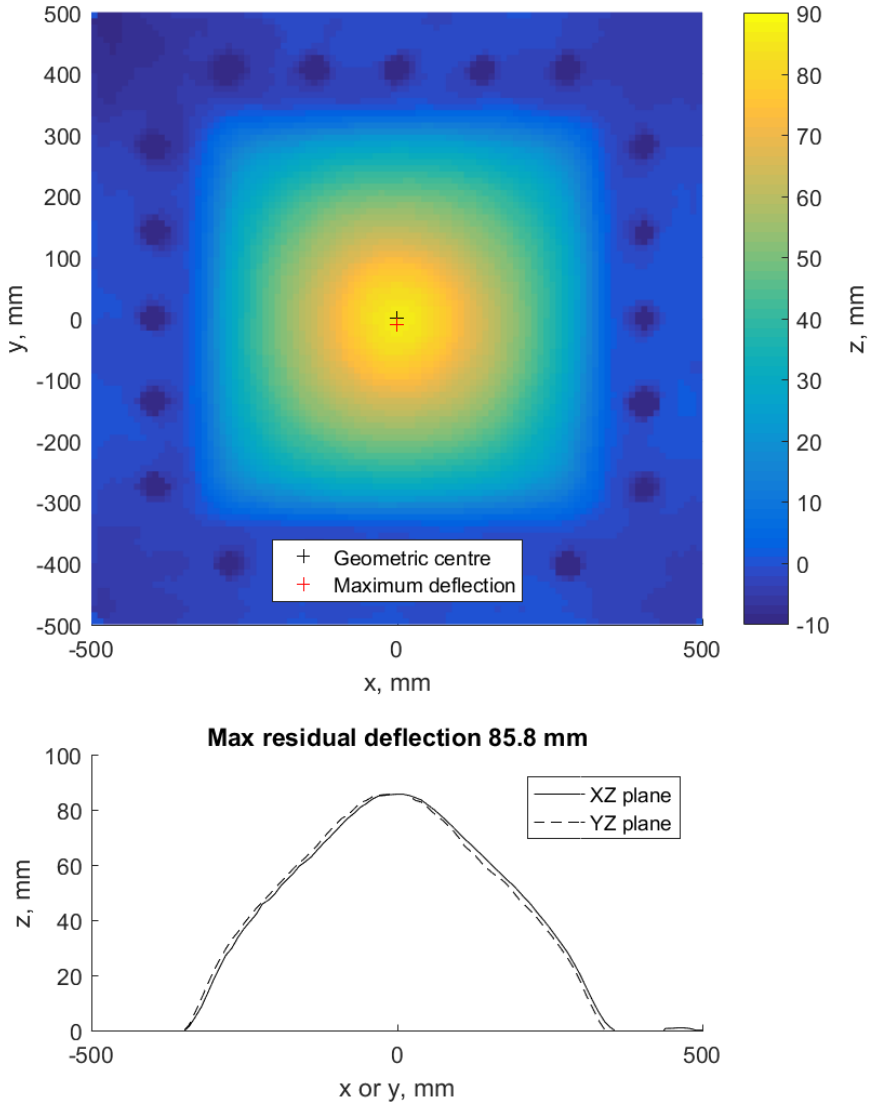

Figure A.7: Deformation profile for Test 8, target no. AM-08-005, plan view (top) and central section views (bottom)

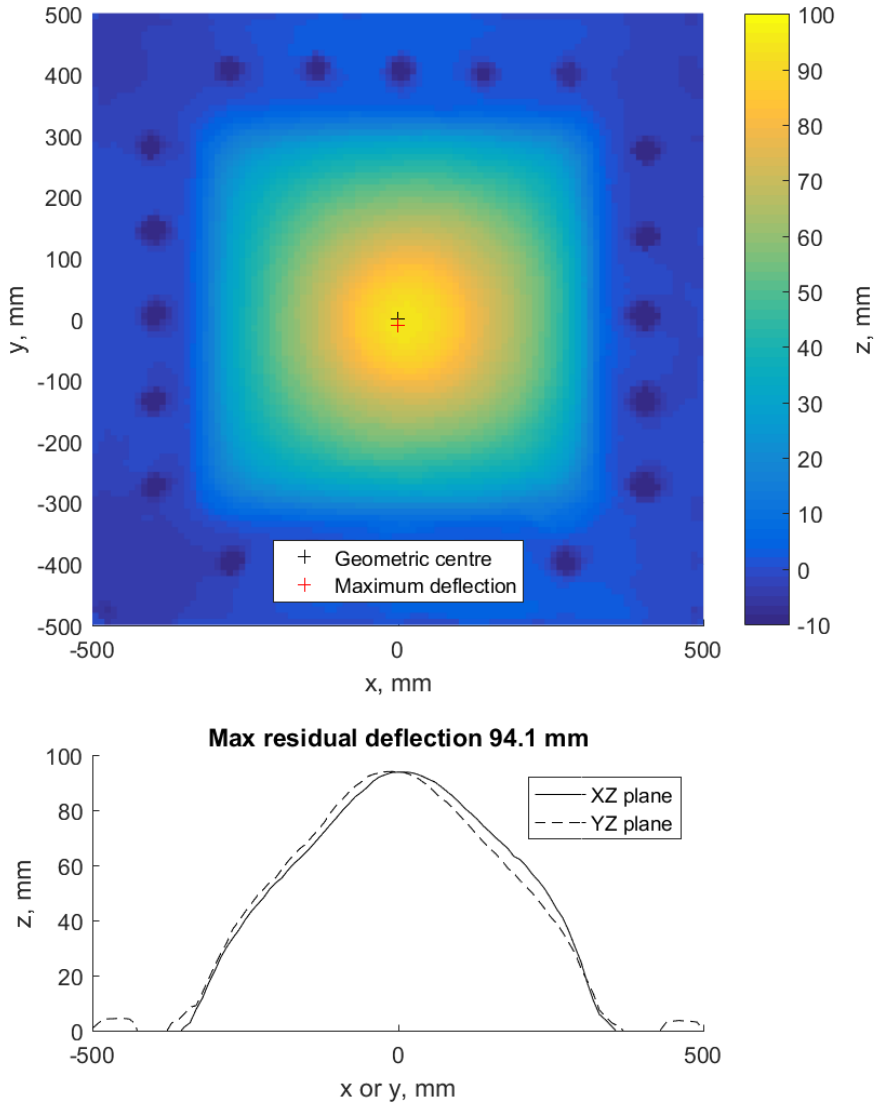

Figure A.8: Deformation profile for Test 9, target no. AM-08-006, plan view (top) and central section views (bottom)

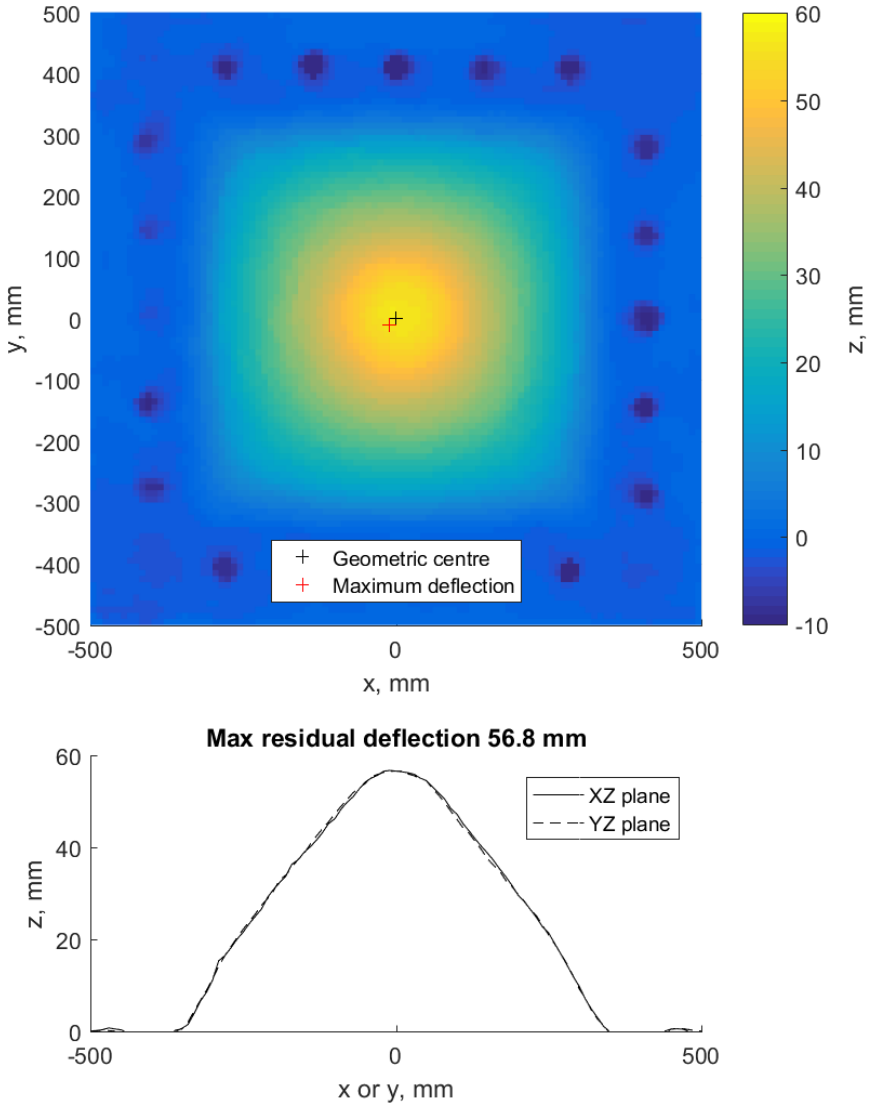

Figure A.9: Deformation profile for Test 10, target no. AM-10-001, plan view (top) and central section views (bottom)

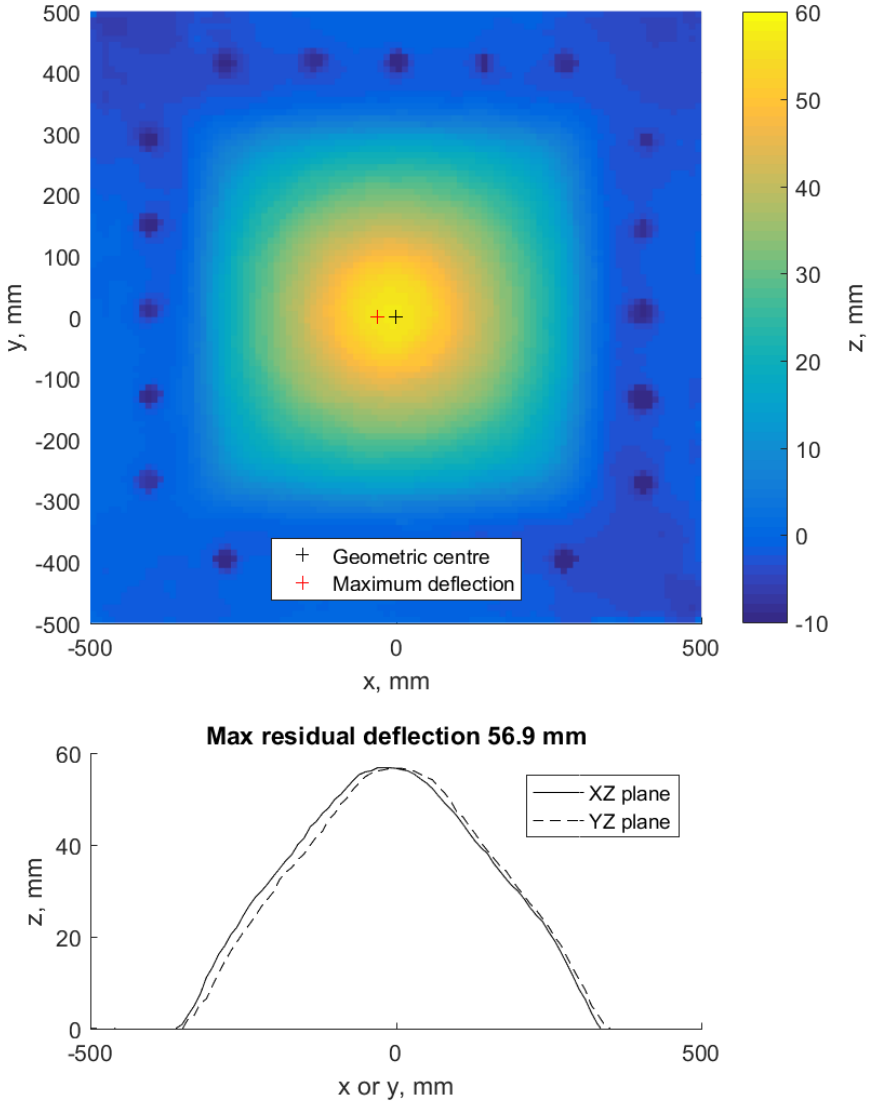

Figure A.10: Deformation profile for Test 11, target no. AM-10-002, plan view (top) and central section views (bottom)

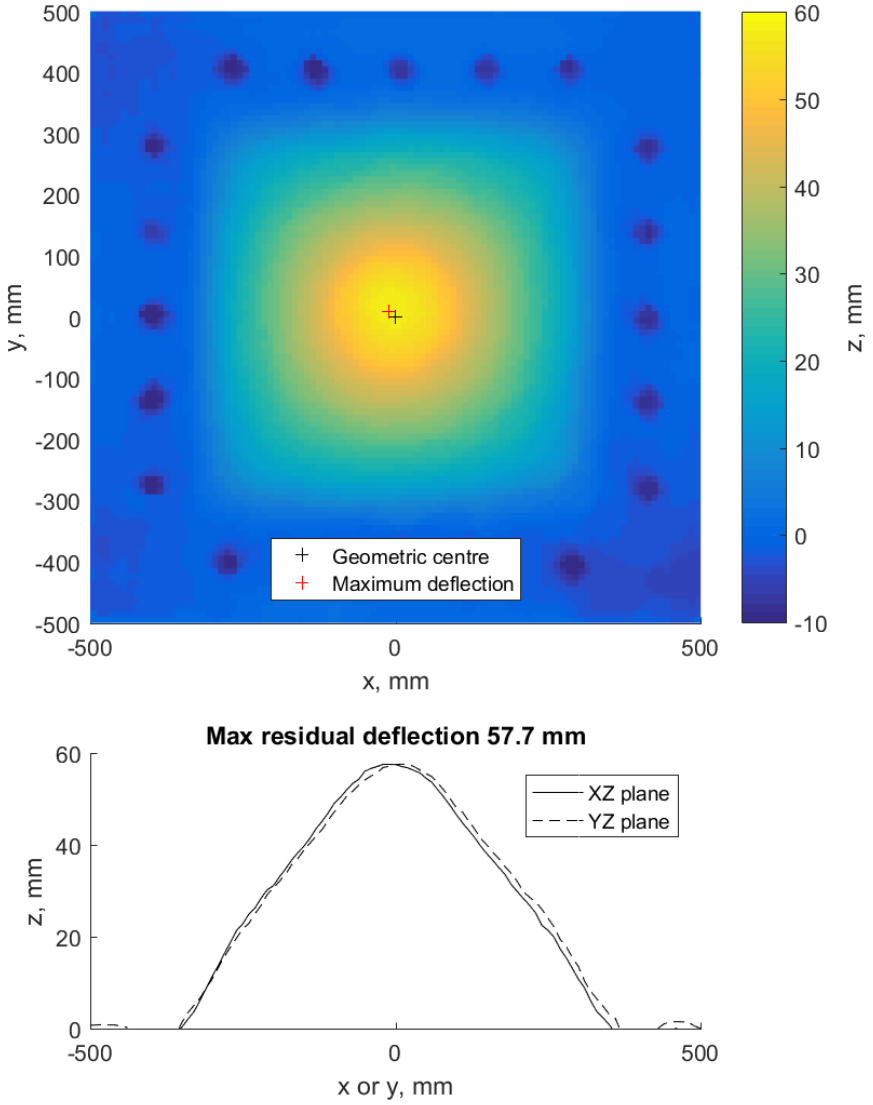

Figure A.11: Deformation profile for Test 12, target no. AM-10-003, plan view (top) and central section views (bottom)

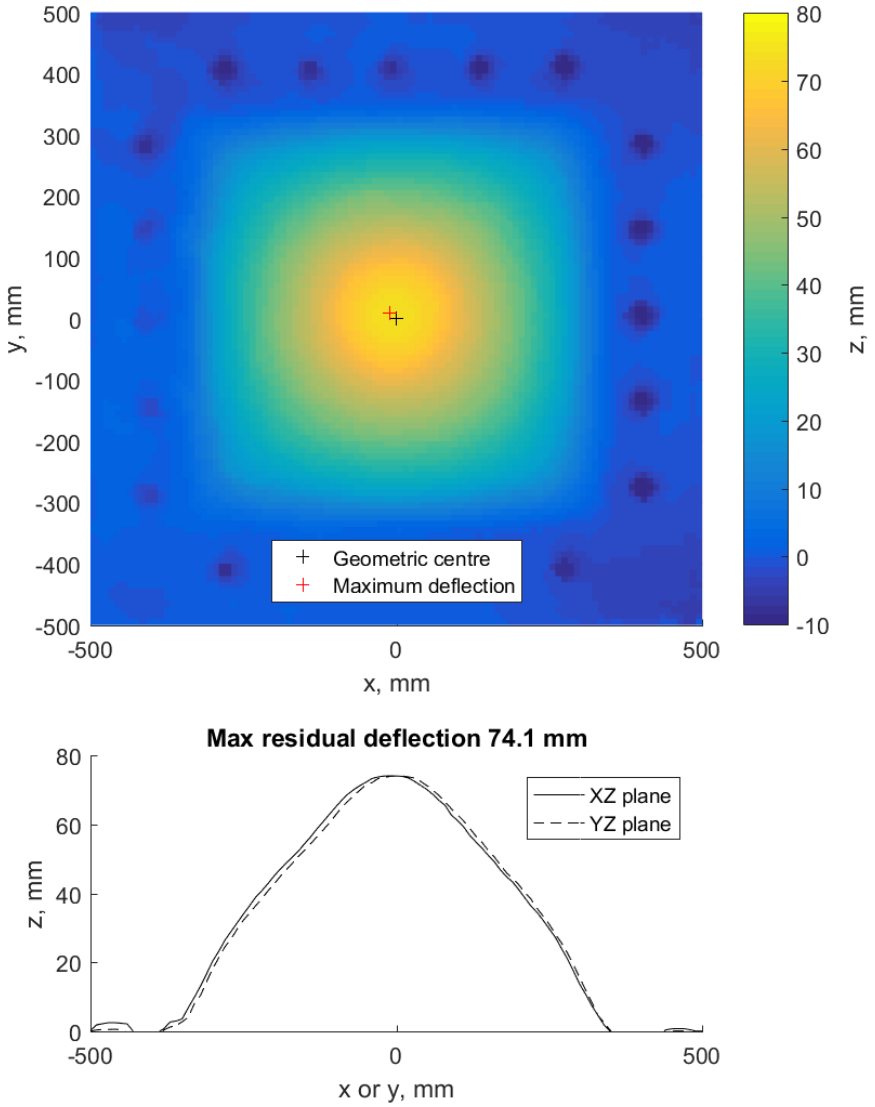

Figure A.12: Deformation profile for Test 13, target no. AM-10-004, plan view (top) and central section views (bottom)

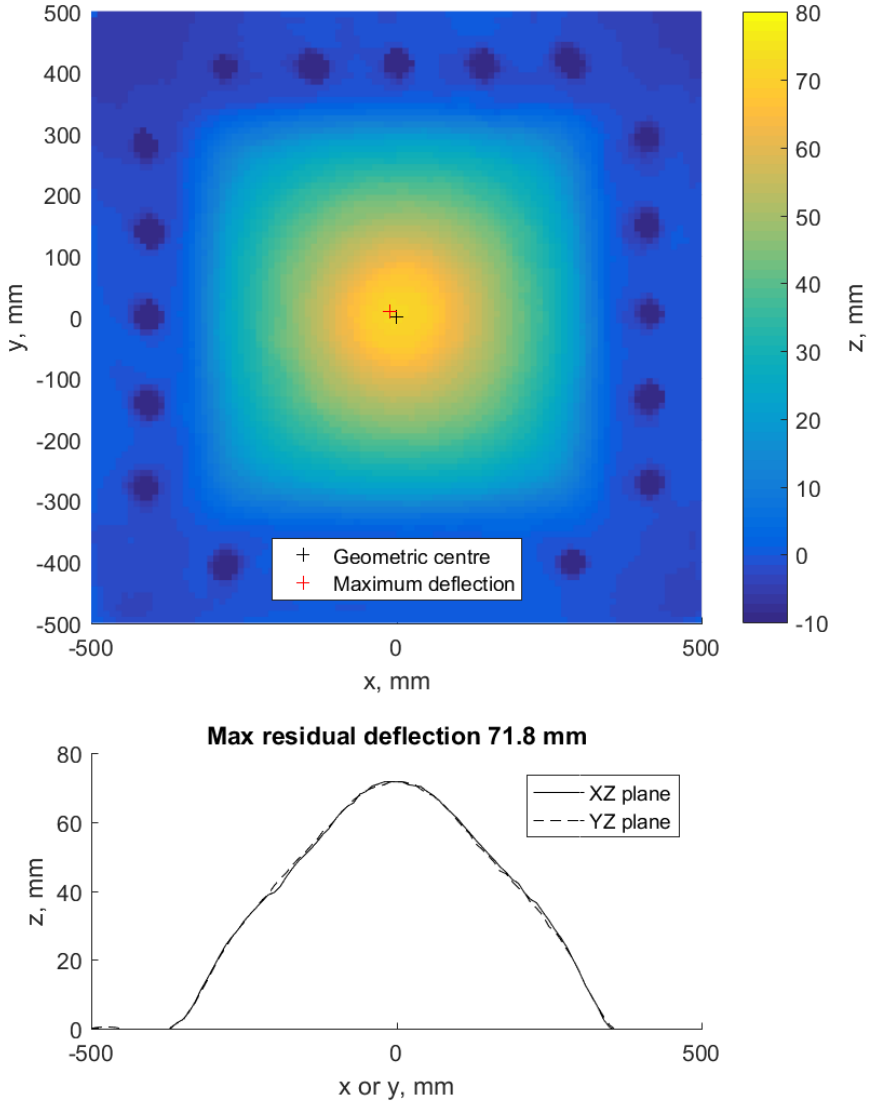

Figure A.13: Deformation profile for Test 14, target no. AM-10-005, plan view (top) and central section views (bottom)

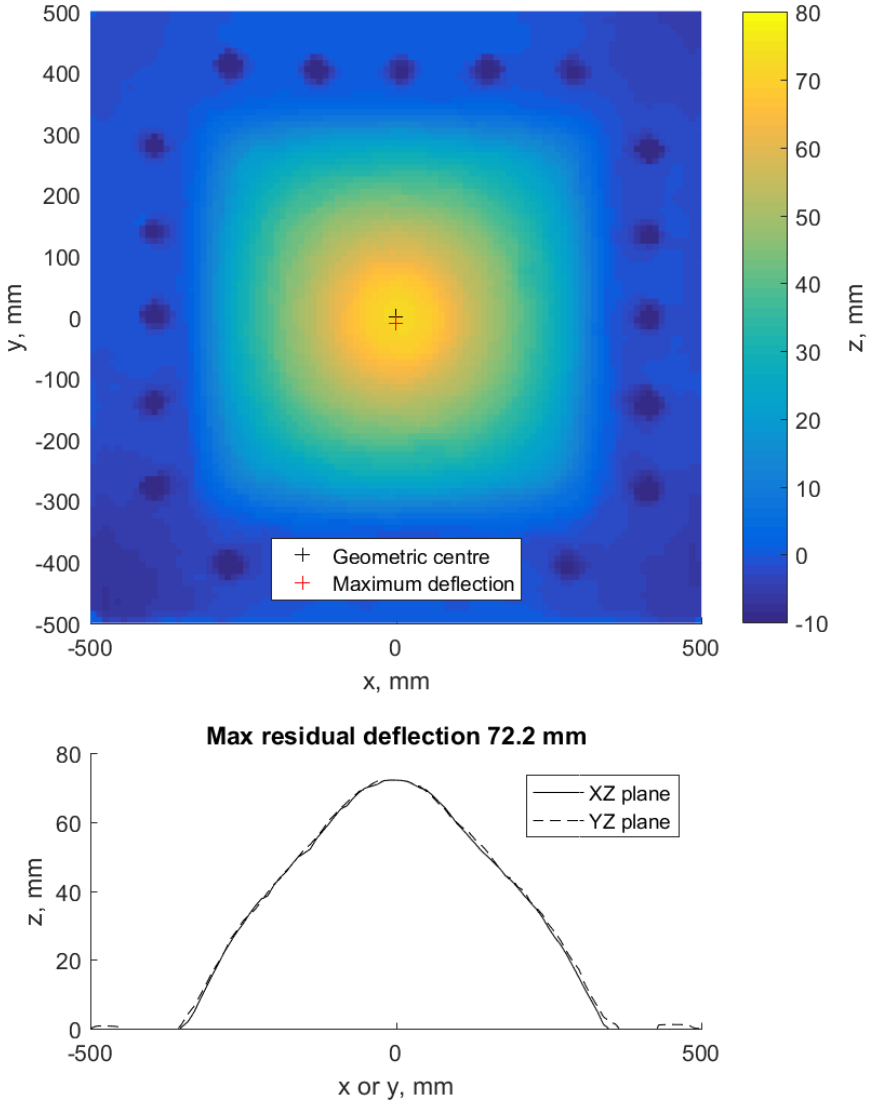

Figure A.14: Deformation profile for Test 15, target no. AM-10-006, plan view (top) and central section views (bottom)

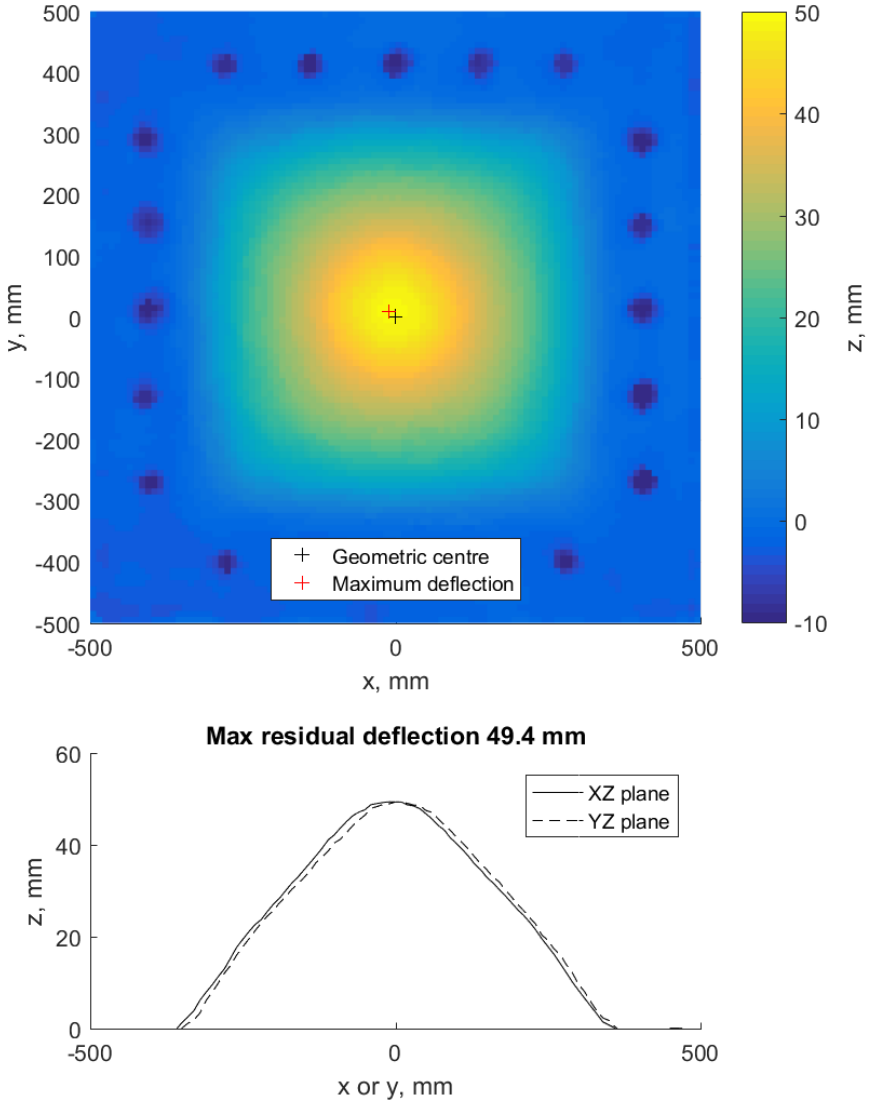

Figure A.15: Deformation profile for Test 16, target no. AM-12-003, plan view (top) and central section views (bottom)

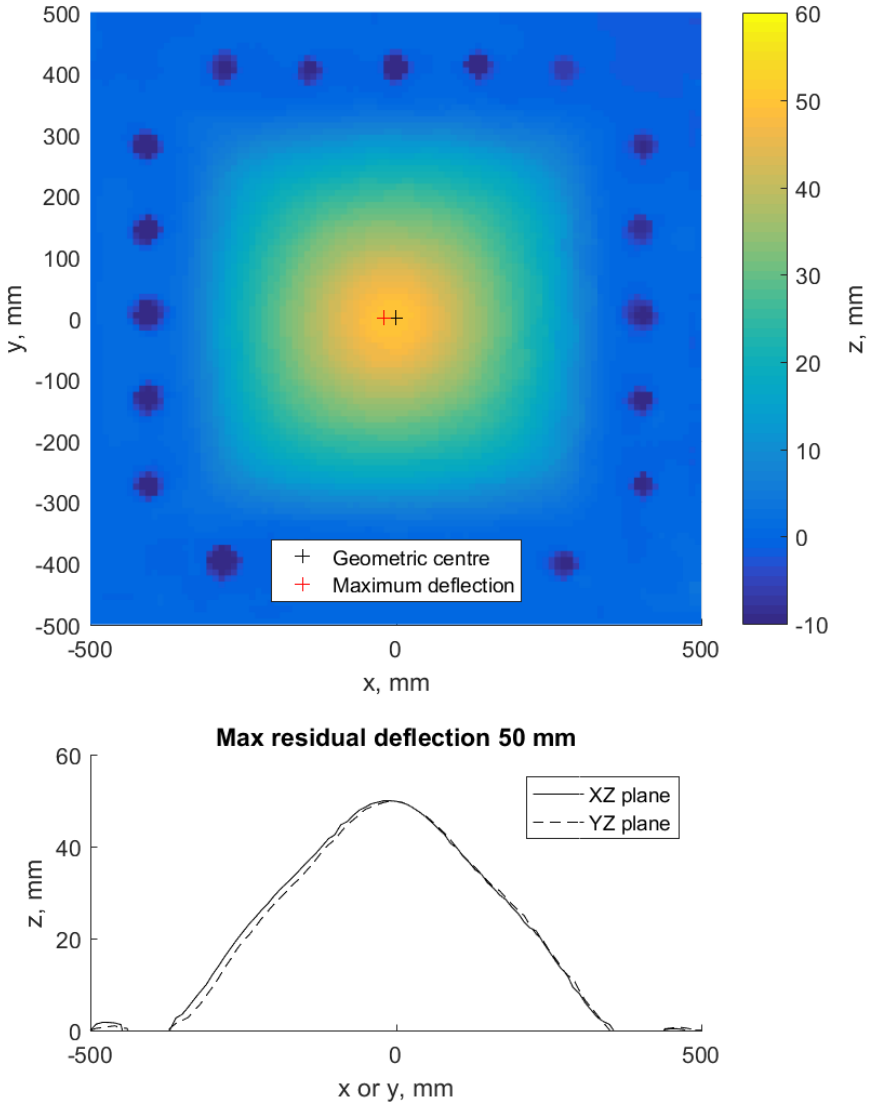

Figure A.16: Deformation profile for Test 17, target no. AM-12-001, plan view (top) and central section views (bottom)

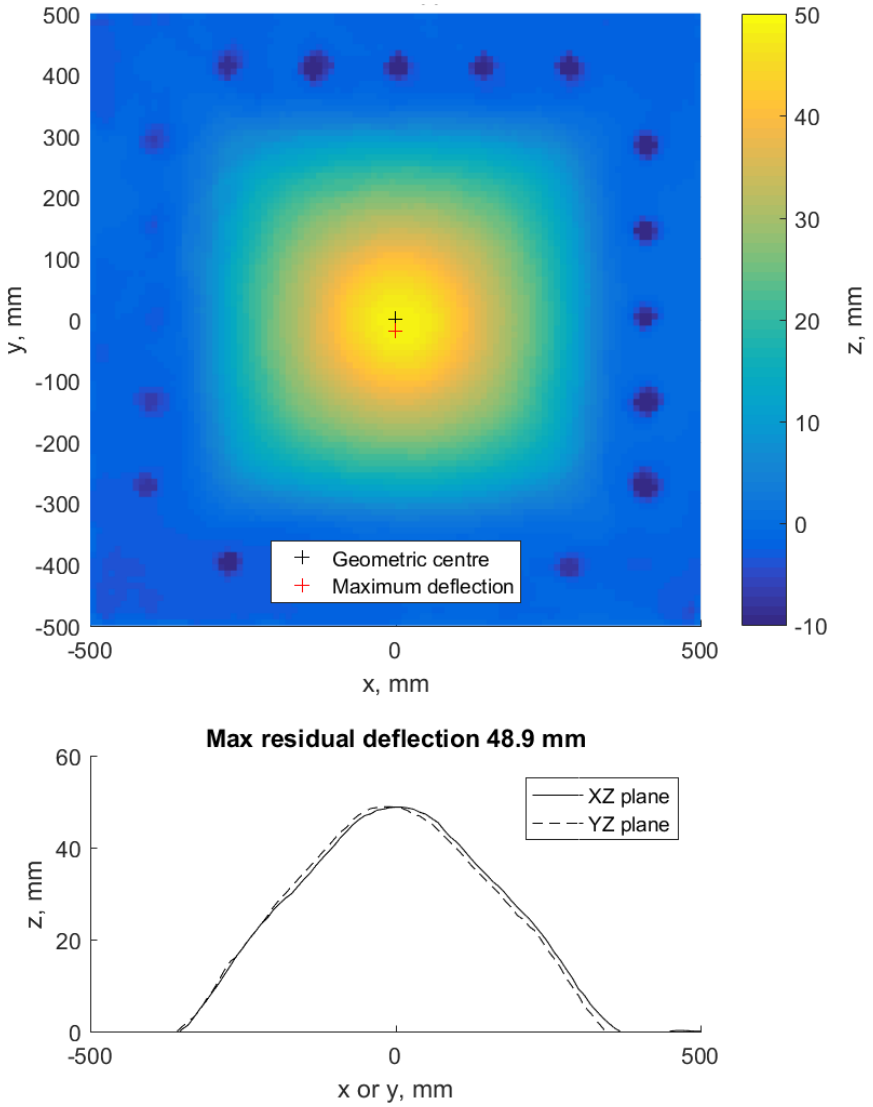

Figure A.17: Deformation profile for Test 18, target no. AM-12-002, plan view (top) and central section views (bottom)

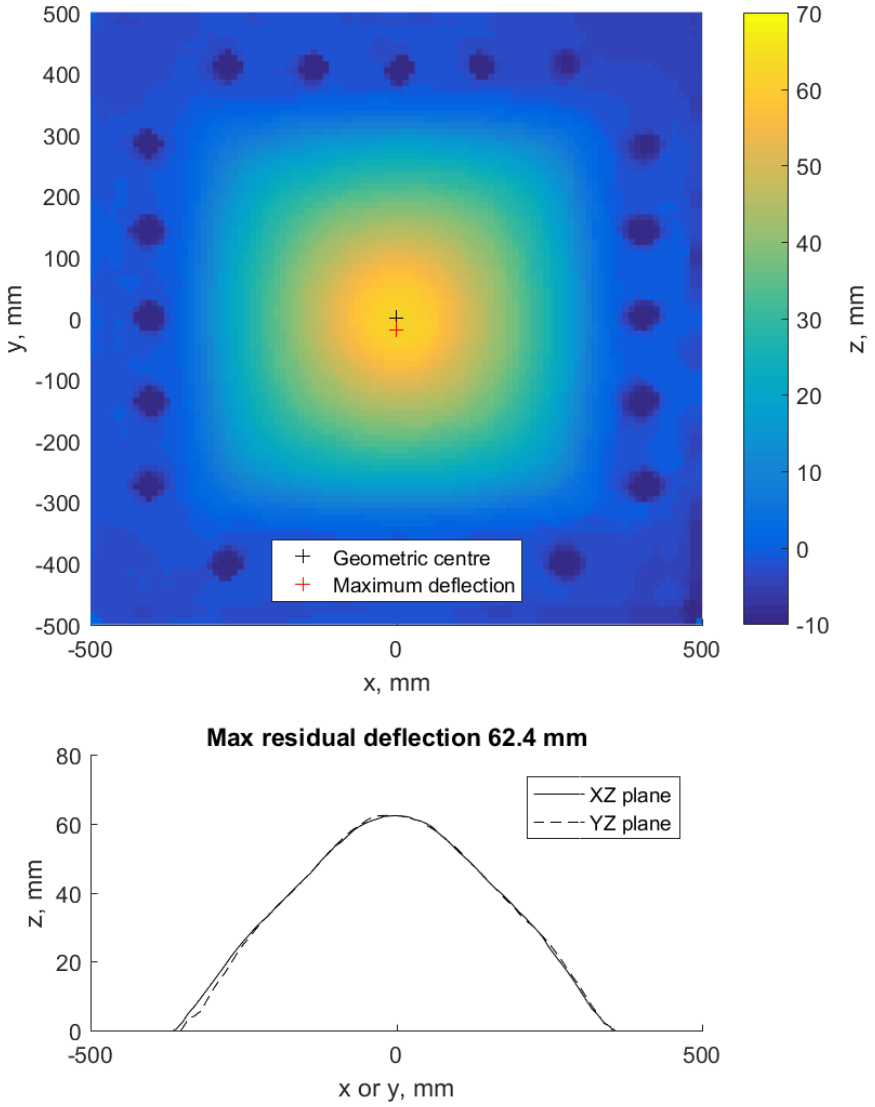

Figure A.18: Deformation profile for Test 19, target no. AM-12-004, plan view (top) and central section views (bottom)

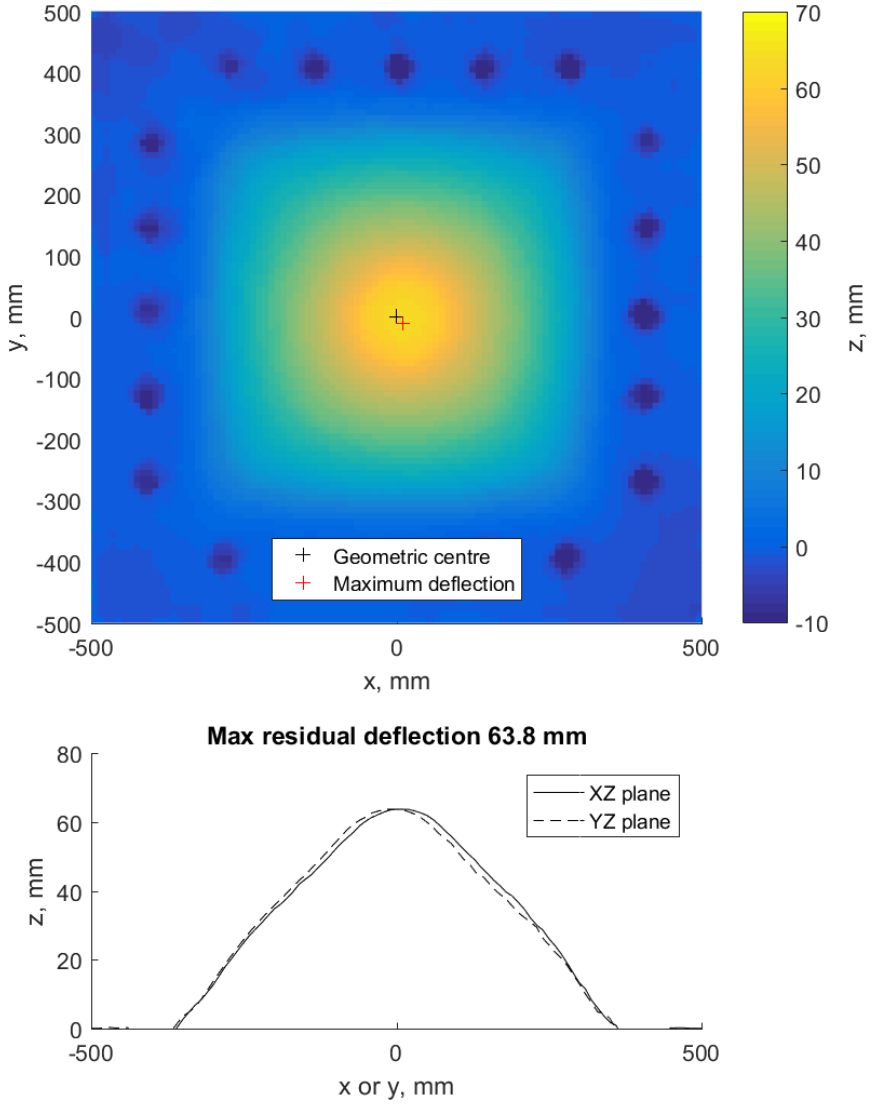

Figure A.19: Deformation profile for Test 20, target no. AM-12-005, plan view (top) and central section views (bottom)

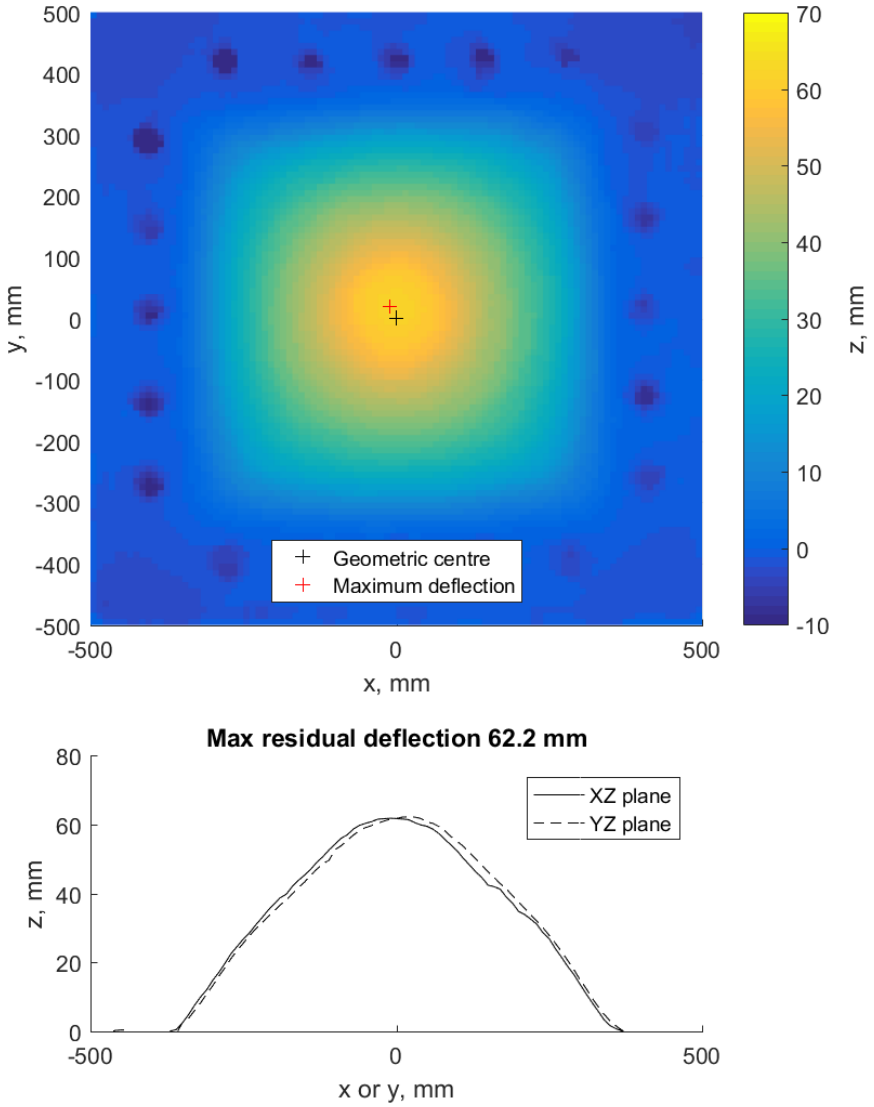

Figure A.20: Deformation profile for Test 21, target no. AM-12-006, plan view (top) and central section views (bottom)

Appendix B

MATLAB for random speckle pattern

```
clear;
clc;
clf;

tic

NWANT=1500;  % the  number of circles to be generated, if ...
    this is set to high relative to the R1t(i) controls ...
    NWANT will not be reached in a reasonable timescale ...
    (seconds) and/or the number of attempts defined by "N" ...
    may not be sufficient to achieve the desired number of ...
    circles.  As the number of circles found increases, ...
    the likelyhood of randonmly finding another circle ...
    which does not intersect any other circle decreases ...
    (obviously).

N=NWANT^1.2;  %number of attempts

A=1000;  %cooridnate magnitude amplifier (adjusted to ...
    account range of axis to cover) (unitless)

Cx(1)=A*rand;  %first x coord in pool
Cy(1)=A*rand;  %first y coord in pool

R1(1)=((7*rand)+3);  %length of first circle radius in ...
    pool (+3 sets minimum, max < (3+7)

R2(1) = (R1(1)^2) ;  %used to control the size of the ...
    "markers" in the scatter plot based on the size of the ...
    circle  generated (trial and error adjustment) The ...
    problem is that the scaling of the the marker required ...
    depends on the physical size of the plot generated.  ...
```

```
   This value works when you maximize the screen of the ...
   plot and then export.

count = 1;  %first attempt is already generated
flag = 0 ;  %at loop start no new circles have been found
flagm = 1 ; %used to scroll through 4 "marker" types in ...
   scatter

for i=2:N
if count < NWANT
    Cxt(i)=A*rand;  %x coord attempt
    Cyt(i)=A*rand;  %y coord attempt

    R1t(i)=((7*rand)+3);  %radius associated with x-y ...
       corrordinate attempt

        for j=1:size(R1,2);  %needs to check against all ...
           circles already found

            if (R1t(i)+R1(j)) < ...
               sqrt((Cxt(i)-Cx(j))^2+(Cyt(i)-Cy(j))^2);  ...
               %condition for radius of attempt not to ...
               touch circle being checked against

                flag = 1;  %circle passes

            else

                flag = 0;  %circle fails

            end;

            if flag == 0

                break  %try a new circle

            end
        end;

        if flag == 1;  %if circle passes

            count = count + flag;  %number of cirlce in ...
               pool increases by one

            Cx(count)=Cxt(i);       %add x-coord to pool
            Cy(count)=Cyt(i);       %add y-coord to pool
            R1(count)=R1t(i);       %add radius to pool
            R2(count)=(R1t(i)^2);  %add marker scaling ...
               factor to pool
```

```
            if flagm == 1;  %which marker symbol is in use
                shape = "o";
            elseif flagm == 2;
                shape = "d";
            elseif flagm == 3 ;
                shape = "s";
            elseif flagm == 4 ;
                shape = "<";
            end




            s = R2(count);  %used to control the size of ...
               the "markers" in the scatter plot based on ...
               the size of the circle generated (trial ...
               and error adjustment)

            scatter(Cxt(i),Cyt(i),s,shape)
            hold on

            if flagm <= 4  ;  %advance marker symbol flag
                flagm = flagm + 1;
            else flagm = 1;
            end;
        else;
        end;
else;
end;
end;

Attempts = size(Cxt,2)

axis square  %adjusts window

h = gcf

set(h,"Position",[100 100 1000 1000])
toc
```